

Symmetry and topological classification of Floquet non-Hermitian systems

Chun-Hui Liu,^{1,2,*} Haiping Hu,^{1,†} and Shu Chen^{1,2,3,‡}

¹*Beijing National Laboratory for Condensed Matter Physics,
Institute of Physics, Chinese Academy of Sciences, Beijing 100190, China*

²*School of Physical Sciences, University of Chinese Academy of Sciences, Beijing 100049, China*

³*Yangtze River Delta Physics Research Center, Liyang, Jiangsu 213300, China*

Recent experimental advances in Floquet engineering and controlling dissipation in open systems have brought about unprecedented flexibility in tailoring novel phenomena without any static and Hermitian analogues. It can be epitomized by the various Floquet and non-Hermitian topological phases. Topological classifications of either static/Floquet Hermitian or static non-Hermitian systems based on the underlying symmetries have been well established in the past several years. However, a coherent understanding and classification of Floquet non-Hermitian (FNH) topological phases have not been achieved yet. Here we systematically classify FNH topological bands for 54-fold generalized Bernard-LeClair (GBL) symmetry classes and arbitrary spatial dimensions using K -theory. The classification distinguishes two different scenarios of the Floquet operator's spectrum gaps [dubbed as Floquet operator (FO) angle-gapped and FO angle-gapless]. The results culminate into two periodic tables, each containing 54-fold GBL symmetry classes. Our scheme reveals FNH topological phases without any static/Floquet Hermitian and static non-Hermitian counterparts. And our results naturally produce the periodic tables of Floquet Hermitian topological insulators and Floquet unitaries. The framework can also be applied to characterize the topological phases of bosonic systems. We provide concrete examples of one and two-dimensional fermionic/bosonic systems. And we elucidate the meaning of the topological invariants and their physical consequences. Our paper lays the foundation for a comprehensive exploration of FNH topological bands. And it opens a broad avenue toward uncovering unique phenomena and functionalities emerging from the synthesis of periodic driving, non-Hermiticity, and band topology.

I. INTRODUCTION

Over the past decades, topological phase of matter [1–5] has become one of the major research fields in the interdisciplinary areas of condensed matter physics, photonics, cold-atom physics, electrical circuits, acoustics, etc. In topological matter, symmetry plays a central role: the topological matter can be categorized into distinct classes based on its underlying symmetries, and the appearance of gapless surface states is protected against symmetry-preserving perturbations. Quite recently, the topological phases well-studied in isolated quantum systems described by Hermitian Hamiltonians have been extended to the non-Hermitian regime [6–14], partially fueled by the explosive research advancements in a diverse set of, e.g. atomic, molecular and optical platforms [15–21]. Non-Hermitian Hamiltonian emerges as an effective description of a variety of quantum and classical systems, ranging from condensed matter materials with finite-lifetime quasiparticles [22–30], bosonic particles governed by Bogoliubov-de Gennes (BdG) equations [31–46], open quantum systems dictated by quantum master equation [47–50], to photonic setups with gain and loss [9, 51–66]. Compared to the Hermitian case, non-Hermitian Hamiltonians generally have complex eigenenergies, giving rise to a plethora of intriguing phenomena without any Her-

mitian analogues [66–89].

Floquet engineering is the control of a system through the periodic drive, which has been widely utilized in photonic systems and ultracold atoms [90–97] and provides a powerful tool for tailoring topologically nontrivial band structures. In Floquet systems, the Hamiltonian is periodic in time $H(t + \tau) = H(t)$, with τ the driving period [98–101], and $\omega = 2\pi/\tau$ the driving frequency. The topological phases in static Hermitian systems have also been generalized to the Floquet Hermitian systems [102–105]. Stroboscopically, the time evolution over one period is effectively described by the so-called Floquet Hamiltonian (FH), with its spectra called quasienergies. The quasienergies are only well-defined up to integer multiples of the driving frequency ω . Due to such periodicity of the quasienergy, the topological properties of Floquet systems turn out to be much richer than static cases. Typical examples include the anomalous Floquet topological phases [106–113], with the appearance of boundary states even when the bulk quasienergy bands are trivial. The anomalous Floquet phases are intrinsically dynamical without static counterparts, and their topological characterization requires a scrutinization of the time-evolution operator inside the whole driving period [106].

For a comprehensive understanding of the various topological phases and their associated unique features, a coherent topological classification according to basic symmetry classes is the key step. The topological classifications for either the static (time-independent) Hermitian or Floquet Hermitian systems have previously been obtained. For the static case, taking into account the three fundamental internal symmetries: time-reversal,

* liuchunhui@iphy.ac.cn

† hhu@iphy.ac.cn

‡ schen@iphy.ac.cn

particle-hole, and chiral symmetry, yields the famous Altland-Zirnbauer (AZ) tenfold way [114–120]. For example, the Chern insulator and quantum spin Hall insulator belong respectively to class A and class AII. They are described by the \mathbb{Z} and \mathbb{Z}_2 invariants, respectively. For the FH real gapped Floquet case, the dynamics of the system are dictated by its unitary time-evolution operator $U(\mathbf{k}, t)$. From a homotopic point of view, the unitary operator $U(\mathbf{k}, t)$ can be decomposed into a unitary loop operator followed by a constant evolution of the effective Floquet Hamiltonian. A complete understanding of the bulk topology involves the analysis of the effective Floquet Hamiltonian and the classification of the loop unitary through K -theory. The results are listed in the Floquet AZ periodic table [103, 104].

The extension of the AZ tenfold way of the Hermitian Hamiltonians to the undriven non-Hermitian systems accomplished during the past several years is highly nontrivial. First, the complex eigenenergies of a generic non-Hermitian Hamiltonian bring more possibilities for the energy gap. Generally speaking, the non-Hermitian Hamiltonians feature either point-like or line-like gaps, as sketched in Fig. 1 or separable bands without any band singularities [121]. Second, the non-Hermiticity ramifies the celebrated AZ symmetry classes to the Bernard-LeClair (BL) symmetry classes [122, 123] due to the nonequivalence between complex conjugation and transposition for non-Hermitian operators. For separable band structures without any symmetries, a purely homotopical classification [124–126] by taking into account the band braidings is carried out. Further refining to spectra to possess point-like or line-line gaps, the 38 fold BL classifications and 54 fold generalized BL (GBL) classifications have been obtained, respectively [14, 127–131]. The last quarter of the whole classification map—the Floquet non-Hermitian (FNH) system, is not yet touched upon. The theoretical explorations of the richness of FNH topological phases are still in their early stages. A complete topological classification of FNH systems based on their underlying symmetries is not only of fundamental significance but also experimentally relevant. A periodically driven non-Hermitian system features non-unitary quantum dynamics. And it describes a variety of physical settings, e.g., photonic systems with gain and loss or nonreciprocal effects under Floquet driving [132–141], ultracold atoms with dissipation interacting with an external electromagnetic field [27, 142–146], and non-unitary quantum walks [58, 62, 63, 88, 147].

In this paper, we develop a systematic topological classification of FNH systems according to the internal symmetries based on K -theory. We demonstrate that there exist 54-fold distinct GBL classes for time-dependent non-Hermitian systems. In contrast to the previous classification frameworks of static point gap non-Hermitian Hamiltonians [14, 127–131], a more natural spectrum gap is defined directly through the Floquet operator (FO) $U(\mathbf{k}, \tau)$. We distinguish two different scenarios of the spectra of $U(\mathbf{k}, \tau)$ on the complex plane and dub them

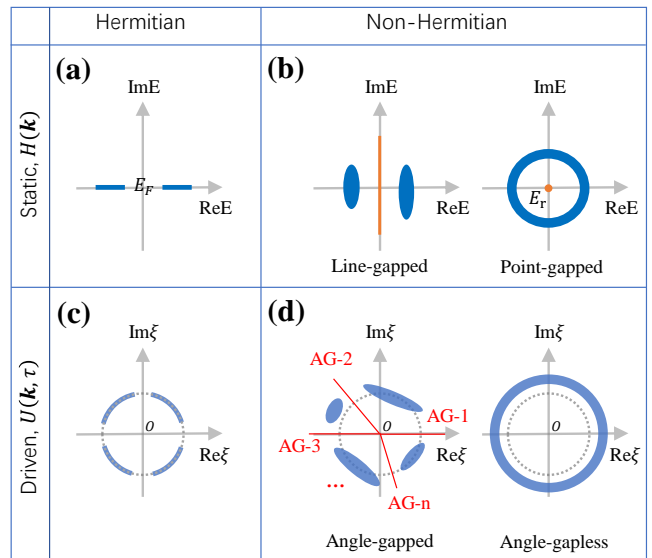


FIG. 1. Schematics of the spectrum gaps for the four different types (static Hermitian/non-Hermitian and Floquet driven Hermitian/non-Hermitian) of systems. (a) The energy gap of a static Hermitian Hamiltonian. A topological transition happens through band touching at the Fermi energy E_F accompanied by gap closing. (b) Energy gaps for a static non-Hermitian Hamiltonian. As the eigenenergies are complex, the band gaps can be line-like (left panel) or point-like (right panel). The line gap (orange line) separates the bands (blue) into two distinct regions. For the point-gap case, the complex bands (blue) do not touch a reference point E_r (orange, here set to be at zero). (c) The spectrum gaps of the Floquet operator $U(\mathbf{k}, \tau)$ for a Floquet driven Hermitian system. The spectra (blue) lie on the unit circle (dotted gray) as the Floquet operator is unitary. (d) The spectra (blue) of the Floquet operator for a Floquet driven non-Hermitian system. Left panel is the FO angle-gapped case. The spectra are split into several disjoint pieces around the origin by the radial lines (red), with the FO angle gaps denoted as AG-1, AG-2, ..., AG-n. Unlike the Floquet Hermitian system, the spectra of $U(\mathbf{k}, \tau)$ do not necessarily lie on the unit circle as the Floquet operator is non-unitary. Right panel is the FO angle-gapless case. The Floquet operator spectra encircle the origin without any FO angle gaps.

FO angle-gapped and FO angle-gapless, respectively. As depicted in the left panel Fig. 1(d), the FO angle-gapped spectra manifest as the appearance of angle gaps in the spectra of Floquet operator. From a well-defined loop operator and a well-defined static Hamiltonian, we obtain the periodic table containing each symmetry class and its associated topological invariants, summarized in Table I. For the FO angle-gapless case, the spectra of $U(\mathbf{k}, \tau)$ enclose the origin, leaving no additional constraints on the Floquet Hamiltonian. The topological classification is to find all the nonequivalent homotopy classes of the Floquet operator, culminating in the second periodic table summarized in Table II. A part of our classification reproduces/consists of Roy and Harper’s periodic table of Floquet Hermitian topological insulators [103–105]

and Higashikawa, Nakagawa, and Ueda's periodic table of Floquet unitaries [148]. Our frameworks can be directly applied to characterize the Floquet dynamics of bosonic systems. We consider concrete examples in one and two-dimensional fermionic/bosonic systems and elucidate the meaning of the topological invariants and their physical consequences.

The remainder of this paper is organized as follows. Sec. II illustrates the classification scheme of generic time-dependent non-Hermitian systems, which contains three subsections. Sec. IIA explores all the symmetry classes of time-dependent non-Hermitian systems. Consider time-reversal symmetry, chiral symmetry, and particle-hole symmetry as primary symmetries, the combinations of these primary symmetries produce all the 54 non-Hermitian GBL classes. Sec. IIB deals with the gap conditions of the non-unitary Floquet operator, whose spectra on the complex plane can be either FO angle-gapped or FO angle-gapless. Sec. IIC introduces the composition of the time-evolution operator and the concepts of homotopy and homeomorphic. These concepts are widely used in identifying topologically equivalent operators or spaces for later discussions. In Sec. III, we provide a complete classification of FNH systems for all the 54 GBL classes based on K -theory. We explicitly work out the extension problem of Clifford algebra in each symmetry class. Then we obtain periodic Table I and Table II corresponding to the FO angle-gapped and FO angle-gapless cases, respectively. In Sec. IV, we illustrate the FNH topology in fermionic systems through two simple examples, corresponding to the FO angle-gapped and FO angle-gapless cases, respectively. And we explain the physical meanings of the topological invariants. Sec. V applies the classification scheme developed in Sec. III and Sec. IV to the bosonic systems. Instead of the Hamiltonian itself, the dynamics of bosonic systems are governed by the M matrix. We conclude in Sec. VI and leave the technical details of derivations/calculations in the Appendices.

II. NON-UNITARY TIME-EVOLUTION AND SYMMETRY CLASSES

In this section, we provide the classification scheme for generic FNH systems. The classification involves two basic ingredients, i.e., to find out all the possible symmetry classes and to identify the spectrum gaps of the Floquet operator. We start by considering a time-dependent non-Hermitian system with Hamiltonian $H(t)$. In general, $H(t) \neq H^\dagger(t)$. The dynamics of the system is governed by the Schrödinger equation:

$$i \frac{d}{dt} |\Psi(t)\rangle = H(t) |\Psi(t)\rangle, \quad (1)$$

with $|\Psi(t)\rangle$ the time-dependent wave function. Suppose the initial state at $t = t_i$ is $|\Psi(t_i)\rangle$ and the time-evolved state at $t = t_f$ ($t_f > t_i$) is $|\Psi(t_f)\rangle$. The time-evolution

can be formally represented as $|\Psi(t_f)\rangle = U(t_f, t_i) |\Psi(t_i)\rangle$, where

$$U(t_f, t_i) := \mathcal{T} \exp[-i \int_{t_i}^{t_f} dt H(t)] \quad (2)$$

is the time-evolution operator. Here \mathcal{T} takes the time-ordering product. For $t_b > t_a$, we define $U(t_a, t_b) := U^{-1}(t_b, t_a)$. We denote $U(t) := U(t, 0)$ for brevity. As the Hamiltonian is non-Hermitian, the time-evolution operator $U(t)$ is non-unitary.

A. Symmetry classes

In this subsection, we build all the internal (non-spatial) symmetry classes of the time-dependent non-Hermitian systems. We begin with the primary symmetries that relate the dynamics at time t and $-t$:

$$U_{T_1} H^*(-t) U_{T_1}^{-1} = H(t), \quad U_{T_1} U_{T_1}^* = \pm \mathbb{I}, \quad (3)$$

$$U_{T_2} H(-t) U_{T_2}^{-1} = -H(t), \quad U_{T_2}^2 = \mathbb{I}, \quad (4)$$

For $t = 0$, Eq. (3) and Eq. (4) reduce to the time-reversal symmetry and chiral symmetry of Hermitian Hamiltonian, respectively. Here in the time-dependent settings, we dub them time-reversal symmetry (TRS) and chiral symmetry (CS), respectively. The TRS and CS keep the Schrödinger equation Eq. (1) unchanged under the transformation $t \rightarrow -t$. Besides the TRS and CS, we need to consider the particle-hole symmetry (PHS) as another primary symmetry. The PHS does not flip time and is preserved if the system has superconducting pairing or is described by a BdG-type Hamiltonian. The symmetry reads:

$$U_P H^T(t) U_P^{-1} = -H(t), \quad U_P U_P^* = \pm \mathbb{I}. \quad (5)$$

Starting from the above three primary symmetries, we can generate all the possible symmetry classes. For example, the combination of TRS and CS produces a K -type symmetry $H(t) = -k H^*(t) k^{-1}$; the combination of CS and PHS produces a C -type symmetry $H(t) = c H^T(-t) c^{-1}$ in the GBL class. All the possible symmetries generated from TRS, CS, and PHS are listed below:

$$H(t) = \epsilon_k k H^*(-\epsilon_k t) k^{-1}, \quad k k^* = \eta_k \mathbb{I}, \quad K \text{ sym.} \quad (6)$$

$$H(t) = \epsilon_q q H^\dagger(\epsilon_q t) q^{-1}, \quad q^2 = \mathbb{I}, \quad Q \text{ sym.} \quad (7)$$

$$H(t) = \epsilon_c c H^T(-\epsilon_c t) c^{-1}, \quad c c^* = \eta_c \mathbb{I}, \quad C \text{ sym.} \quad (8)$$

$$-H(t) = p H(-t) p^{-1}, \quad p^2 = \mathbb{I}, \quad P \text{ sym.} \quad (9)$$

Fourier transforms Eqs. (6)-(9) into momentum space, we get that,

$$H(\mathbf{k}, t) = \epsilon_k k H^*(-\mathbf{k}, -\epsilon_k t) k^{-1}, \quad k k^* = \eta_k \mathbb{I}, \quad K \text{ sym.} \quad (10)$$

$$H(\mathbf{k}, t) = \epsilon_q q H^\dagger(\mathbf{k}, \epsilon_q t) q^{-1}, \quad q^2 = \mathbb{I}, \quad Q \text{ sym.} \quad (11)$$

$$H(\mathbf{k}, t) = \epsilon_c c H^\mathbf{T}(-\mathbf{k}, -\epsilon_c t) c^{-1}, \quad c c^* = \eta_c \mathbb{I}, \quad C \text{ sym.} \quad (12)$$

$$-H(\mathbf{k}, t) = p H(\mathbf{k}, -t) p^{-1}, \quad p^2 = \mathbb{I}, \quad P \text{ sym.} \quad (13)$$

where $\eta_k, \eta_c, \epsilon_k, \epsilon_q, \epsilon_c = \pm 1$. k, q, c, p are four unitary matrices, satisfying

$$c = \epsilon_{pc} p c p^\mathbf{T}, \quad k = \epsilon_{pk} p k p^\mathbf{T}, \quad c = \epsilon_{qc} q c q^\mathbf{T}, \quad p = \epsilon_{pq} q p q^\dagger, \quad (14)$$

with $\epsilon_{pc}, \epsilon_{pk}, \epsilon_{qc}, \epsilon_{pq} = \pm 1$. By a full counting of the four types of symmetries P, Q, C, K , the signs of time flipping $\epsilon_k, \epsilon_q, \epsilon_c$, the signs of symmetry-operator involution η_k, η_c , and the signs in the commutation relations $\epsilon_{pc}, \epsilon_{pk}, \epsilon_{qc}, \epsilon_{pq}$, we obtain 54-fold nonequivalent symmetry classes (Details in Appendix A). Each class is specified by a definite choice of the symmetries and signs. To avoid confusion, we stress that these symmetries are for time-dependent Hamiltonians. Yet we still utilize the convention for static line gap non-Hermitian Hamiltonians and call the 54-fold classes the GBL classes [130]. They are labeled as [130] Non, P, Qa-b, K1-2a-b, C1-4, PQ1-2, PK1-2, PK3a-b, PC1-4, QC1-8a-b, PQC1-8, PQC9-12a-b in Table I and Table II.

The 54-fold GBL classes were first constructed in Ref. [130] to get a consistent description of line gap static non-Hermitian systems. And in the Appendix E of Ref. [14], there is a detailed review of the 54-fold GBL classes. However, Ref. [14] still call it Bernard-LeClair class. The derivation of 38-fold Bernard-LeClair (BL) classes needs to use the $H \rightarrow iH$ as an equivalent transformation, and the transformation needs to relate two symmetry classes for some cases.

For static point gap non-Hermitian topology, we set the point gap at 0. $H \rightarrow iH$ transformation didn't change the gap, and we can regard it as an equivalent transformation. And $H \rightarrow iH$ transformation relate two static GBL symmetries, for example $H = k H^* k^{-1}$ ($k k^* = \mathbb{I}$) and $H = -k H^* k^{-1}$ ($k k^* = \mathbb{I}$). Thus, part of 54-fold GBL classes can be regarded as equivalent if we only consider point gap topology. By subtracting the redundant equivalence classes, we get 38-fold BL classes. However, static point gap non-Hermitian topology also can be described by 54-fold GBL classes. It is due to the redundant equivalence classes didn't lead to any inconsistent conclusion.

We consider static line gap non-Hermitian topology, $H \rightarrow iH$ transformation changes the gap, and we can't regard it as an equivalent transformation. Thus, static line gap non-Hermitian topology is described by 54-fold GBL classes. If we use the 38-fold BL classes to describe the static line gap non-Hermitian topology, it leads to

inconsistent conclusions. For example, a non-Hermitian system with $H = k H^* k^{-1}$ ($k k^* = \mathbb{I}$) symmetry and a non-Hermitian system with $H = -k H^* k^{-1}$ ($k k^* = \mathbb{I}$) symmetry belong to the same class in the 38-fold BL classes description (BL class). For a 1-dimensional real line gap system with $H = k H^* k^{-1}$ ($k k^* = \mathbb{I}$) symmetry, the topological classification is 0 [128, 130]. For a 1-dimensional real line gap system with $H = -k H^* k^{-1}$ ($k k^* = \mathbb{I}$) symmetry, the topological classification is \mathbb{Z}_2 [128, 130]. These conclusions contradict the uniqueness of the topological classification in a certain dimension and symmetry class.

For time-dependent non-Hermitian systems, two different GBL symmetry classes didn't relate to each other by the $H \rightarrow iH$ transformation. For example, type-K symmetry takes the form of Eq. (6) in the time-dependent system. The $H \rightarrow iH$ transformation didn't transform type-K symmetry with $\epsilon_k = 1$ and $\eta_k = 1$ into type-K symmetry with $\epsilon_k = -1$ and $\eta_k = 1$. However, the $H \rightarrow iH$ transformation did transform type-K symmetry with $\epsilon_k = 1$ and $\eta_k = 1$ into type-K symmetry with $\epsilon_k = -1$ and $\eta_k = 1$ in static limit (hint: let $t = 0$).

54 is the total number of group structures generated by Eqs. (6)-(9). Thus, there is no inconsistent conclusion if we use 54-fold GBL classes to describe the general non-Hermitian system. If we use 38-fold BL classes to describe non-Hermitian systems, sometimes, it leads to inconsistent conclusions.

The four types of symmetries of Eqs. (10)-(13) on $H(\mathbf{k}, t)$ induce the symmetries on the time-evolution operator $U(\mathbf{k}, t)$ as follows:

$$U^*(-\mathbf{k}, -t) = k^{-1} U(\mathbf{k}, \epsilon_k t) k, \quad k k^* = \eta_k \mathbb{I}, \quad K \text{ sym.} \quad (15)$$

$$[U^\dagger(\mathbf{k}, t)]^{-1} = q^{-1} U(\mathbf{k}, \epsilon_q t) q, \quad q^2 = \mathbb{I}, \quad Q \text{ sym.} \quad (16)$$

$$[U^\mathbf{T}(-\mathbf{k}, t)]^{-1} = c^{-1} U(\mathbf{k}, -\epsilon_c t) c, \quad c c^* = \eta_c \mathbb{I}, \quad C \text{ sym.} \quad (17)$$

$$U(\mathbf{k}, -t) = p^{-1} U(\mathbf{k}, t) p, \quad p^2 = \mathbb{I}. \quad P \text{ sym.} \quad (18)$$

The derivation of Eqs. (15)-(18) is given in Appendix B. The above discussions in this section are for generic time-dependent systems. Now we restrict to the Floquet system with a time-periodic Hamiltonian

$$H(\mathbf{k}, t + \tau) = H(\mathbf{k}, t), \quad (19)$$

where τ is the driving period. The Floquet operator is defined as the time-evolution operator over one period. From now on, we concisely denote the Floquet operator as $U(\mathbf{k}) := U(\mathbf{k}, \tau)$. Starting from Eqs. (15)-(18), we can obtain the symmetry operations on the Floquet operator:

$$[U^*(-\mathbf{k})]^{-\epsilon_k} = k^{-1} U(\mathbf{k}) k, \quad k k^* = \eta_k \mathbb{I}, \quad K \text{ sym.} \quad (20)$$

$$[U^\dagger(\mathbf{k})]^{-\epsilon_q} = q^{-1} U(\mathbf{k}) q, \quad q^2 = \mathbb{I}, \quad Q \text{ sym.} \quad (21)$$

$$[U^\mathbf{T}(-\mathbf{k})]^{\epsilon_c} = c^{-1} U(\mathbf{k}) c, \quad c c^* = \eta_c \mathbb{I}, \quad C \text{ sym.} \quad (22)$$

$$[U(\mathbf{k})]^{-1} = p^{-1} U(\mathbf{k}) p, \quad p^2 = \mathbb{I}. \quad P \text{ sym.} \quad (23)$$

The derivation of Eqs. (20)-(23) is given in Appendix C.

B. Gap condition of the Floquet operator

The gap condition is an essential ingredient in the classification theory. A spectrum gap means a region without any spectrum. Two Hamiltonian operators (or time-evolution operators in the driven case) are equivalent if they can continuously transform into each other while keeping the gap open and preserving their corresponding symmetries. Topological transition happens accompanied by gap closings. Here we compare the spectrum gaps for the four different cases: static Hermitian/non-Hermitian Hamiltonian and Floquet Hermitian/non-Hermitian Hamiltonian. For a static Hermitian Hamiltonian, all eigenvalues are real, and the spectrum gap is defined on the real-energy axis when the energy bands do not touch the Fermi energy E_F , as depicted in Fig. 1(a). For a static non-Hermitian Hamiltonian, its eigenvalues are complex. As shown in Fig. 1(b), the spectrum gap can be either a line-like region or a point-like region on the complex-energy plane [128–130]. Correspondingly, the spectrum of the non-Hermitian Hamiltonian possesses a line-like gap or point-like gap.

For Floquet Hermitian/non-Hermitian systems, we consider the spectra of the Floquet operator (FO) $U(\mathbf{k})$. We denote the spectra of FO as $\xi_n(\mathbf{k})$, and n is the band index. A *FO angle gap at θ* ($\theta \in R$) is defined as $\forall \rho > 0, \forall n$ s.t. $\xi_n(\mathbf{k}) \neq \rho e^{-i\theta}$. If a Floquet Hermitian/non-Hermitian system has a FO angle gap, we call such system *FO angle-gapped*. If a Floquet Hermitian/non-Hermitian system doesn't have any FO angle gap, we call such system *FO angle-gapless*.

We can define a widely used concept—the Floquet Hamiltonian (FH) as:

$$H_F := \frac{i}{\tau} \ln(H(\mathbf{k})). \quad (24)$$

The Floquet Hamiltonian's definition Eq. (24) is the same as previous articles. We denote the spectra of FH as $\varepsilon_n(\mathbf{k})$. $\varepsilon_n(\mathbf{k})$ usually be called quasienergies. The quasienergies are only well-defined up to integer multiples of the driving frequency $\omega = 2\pi/\tau$ since $\ln()$ is a multivalued function. A *FH real gap at E_0* ($E_0 \in R$) defined as: $\forall j \in \mathbb{Z}, \forall n$ s.t. $\text{Re}(\varepsilon_n(\mathbf{k})) \neq E_0 + 2\pi j/\tau$. Here, $\text{Re}(\varepsilon_n(\mathbf{k}))$ takes the real part of $\varepsilon_n(\mathbf{k})$.

It is worth stressing that: A Floquet system has a FO angle gap at θ ($\theta \in R$) is equivalent to the Floquet system has an FH real gap at θ/τ . For the Floquet Hermitian system, $U(\mathbf{k})$ is unitary, giving rise to real quasienergies. The spectra of $U(\mathbf{k})$ lie on the unit circle. Fig. 1(c) is the schematic diagram of the spectrum of a Floquet Hermitian system, and it is FO angle-gapped. We can directly extend this scenario to the driven non-Hermitian systems. Note that the Floquet operator $U(\mathbf{k})$ is non-unitary in FNH systems, and its spectra do not necessarily lie on the unit circle. Fig. 1(d) is the schematic

diagram of the spectrum of an FNH system, Fig. 1(d) (left panel) is FO angle-gapped, and Fig. 1(d) (right panel) is FO angle-gapless.

C. Composition of evolution operators, homotopy and homeomorphic

For the classification problem, a widely used concept is the composition of two time-evolution operators [104]. Given that U_1 is the time-evolution operator generated by Hamiltonian $H_1(t)$ and U_2 is the time-evolution operator generated by Hamiltonian $H_2(t)$, we define the composition of U_1 and U_2 as $U_1 * U_2$, which is the time-evolution generated by the following Hamiltonian:

$$H(t) = \begin{cases} H_2(\mathbf{k}, 2t) & 0 \leq t \leq \tau/4; \\ H_1(\mathbf{k}, 2t - \tau/2) & \tau/4 < t < 3\tau/4; \\ H_2(\mathbf{k}, 2t - \tau) & 3\tau/4 \leq t \leq \tau. \end{cases} \quad (25)$$

The above operator composition is consistent with all the GBL symmetries. In fact, we have:

Lemma 1. *If $H_1(t)$ and $H_2(t)$ belong to the same GBL class defined in Eqs. (10)-(13) and the first two columns of Table I, then the composed Hamiltonian $H(t)$ belongs to the same GBL class of $H_1(t)$ and $H_2(t)$.*

The proof of Lemma 1 is provided in Appendix D. Besides the operator composition, another two widely used mathematical concepts in the topological classification of Floquet systems are homotopy and homeomorphic [104]. They are defined below: (1) *Homotopy*: Suppose that the two operators g and h satisfy the same symmetry condition and constraint, and the operator g is homotopic to h if and only if there exists a continuous operator function f_t ($t \in [0, 1]$) with $f_0 = g$ and $f_1 = h$. And f_t satisfies the same symmetry condition and constraint as g or h . (2) *Homeomorphic*: Space A is homeomorphic to space B , if and only if there exists a continuous function $F : A \rightarrow B$. F is a one-to-one, onto function and has a continuous inverse. The mapping F preserves all the topological properties of a given space. Two homeomorphic spaces are the same from a topological point of view.

III. TOPOLOGICAL CLASSIFICATION OF FLOQUET NON-HERMITIAN SYSTEMS

This section is devoted to a complete classification of the FNH band topology, which contains both the FO angle-gapped and FO angle-gapless cases. We have demonstrated that for the FO angle-gapped case, there exists FH real gap. Thus, we also call the FO angle-gapped topological classification as FH real gapped topological classification. For the FO angle-gapless case, two time-evolution operators are considered topologically equivalent if they can be continuously transformed to

each other while preserving the FO angle gaps and corresponding symmetries. It turns out the band topology of a FO angle-gapped system is not fully encoded in the Floquet Hamiltonian itself [103, 104, 106–113] due to the periodicity of the quasienergy zone. In fact, a FO angle gap naturally defines the branch cut of the Floquet Hamiltonian. To complete the topological classification, both the branch-cut-dependent Floquet Hamiltonian and its associated loop operator should be taken into account. While for the FO angle-gapless system, there is no additional spectrum restriction on the quasienergies. And the Floquet Hamiltonian is not always continuous in the Brillouin zone (BZ) for any chosen branch cut in the absence of the FO angle gap. For the FO angle-gapless systems, the band topology is only extracted from the Floquet operator [101, 148, 149]. Thus, we also call the FO angle-gapless topological classification as the Floquet operator's topological classification.

To proceed, we expand the Floquet operator $U(\mathbf{k})$ according to its eigenenergy spectra:

$$U(\mathbf{k}) = \sum_n \xi_n(\mathbf{k}) |\psi_{n,R}\rangle \langle \psi_{n,L}|. \quad (26)$$

Here n is the band index. As $U(\mathbf{k})$ is non-unitary, the expansion involves both the left and right eigenvectors [150], which are defined as $U(\mathbf{k})|\psi_{n,R}\rangle = \xi_n(\mathbf{k})|\psi_{n,R}\rangle$, and $U^\dagger(\mathbf{k})|\psi_{n,L}\rangle = \xi_n^*(\mathbf{k})|\psi_{n,L}\rangle$. We further define the logarithm function \ln_α as:

$$e^{\ln_\alpha(z)} := z, \text{ and } \alpha < \text{Im}[\ln_\alpha(z)] < \alpha + 2\pi. \quad (27)$$

Here, $\text{Im}(z)$ takes the imaginary part of z . We have set the branch cut of the logarithm \ln_α at α , and it is a single-valued function. For example, let us suppose $\phi_1, \phi_2 \in R$ (R is real number field) and $\alpha < \phi_1 < \alpha + 2\pi$. According to our definition, $\ln_\alpha[e^{i(\phi_1 + 2\pi N_1) + \phi_2}] = i\phi_1 + \phi_2$, for any $N_1 \in \mathbb{Z}$. Using the above logarithm function with a definite branch cut α , we define the effective Floquet Hamiltonian at a branch cut θ as follows:

$$H_{F,\theta} := \frac{i}{\tau} \ln_{-\theta}[U(\mathbf{k})] = \sum_n \frac{i}{\tau} \ln_{-\theta}(\xi_n) |\psi_{n,R}\rangle \langle \psi_{n,L}|. \quad (28)$$

The Floquet Hamiltonian defined above explicitly depends on the branch cut θ . A suitable choice of the branch cut is important when we consider the topological equivalence in the following discussions. According to Eqs. (27) and (28), the definition of $H_{F,\theta}$ requires a FO angle gap at θ . And $H_{F,\theta}$ is a continuous function in BZ. With a bit of abuse of notation, we still call the spectrum of $H_{F,\theta}$ as the quasienergy spectrum. From Eqs. (27) and (28), it is easy to see the real part of the quasienergy spectrum of $H_{F,\theta}$ lies inside $((\theta - 2\pi)/\tau, \theta/\tau)$.

Correspondingly, from $H_{F,\theta}$ and the time-evolution operator $U(\mathbf{k}, t)$ (Note that in general, $U(\mathbf{k}, t) \neq U(\mathbf{k}, t + \tau)$), we can define a time-periodic evolution operator

$$U_{l,\theta}(\mathbf{k}, t) := U(\mathbf{k}, t) * e^{iH_{F,\pi}(\mathbf{k})t}. \quad (29)$$

$U_{l,\theta}(\mathbf{k}, t)$ satisfies $U_{l,\theta}(\mathbf{k}, t + \tau) = U_{l,\theta}(\mathbf{k}, t)$ and is usually called as the *loop operator* [103–105]. The definition of $H_{F,\theta}$ and $U_{l,\theta}(\mathbf{k}, t)$ both require a FO angle gap at θ . And $U_{l,\theta}(\mathbf{k}, t)$ is a continuous function of (\mathbf{k}, t) . For generic settings of the time evolution (It may not have a FO angle gap), we can't define $H_{F,\theta}$ which is a well-defined single-value continuous function in BZ.

It is worth stressing that: A Floquet system have n FO angle gaps at $\tilde{\theta}_1, \tilde{\theta}_2, \dots, \tilde{\theta}_n$ ($\tilde{\theta}_j \in [\tilde{\theta}_1 - 2\pi, \tilde{\theta}_1]$, $j = 1, 2, \dots, n$) is equivalent to the Floquet system have n FH real gaps at $\tilde{\theta}_1/\tau, \tilde{\theta}_2/\tau, \dots, \tilde{\theta}_n/\tau$. It is also equivalent to the $H_{F,\tilde{\theta}_1}$ of this system have $n - 1$ real gaps at $\tilde{\theta}_2/\tau, \tilde{\theta}_3/\tau, \dots, \tilde{\theta}_n/\tau$. The $\tilde{\theta}_1$ is chosen as the branch cut and doesn't contribute to a $H_{F,\tilde{\theta}_1}$ real gap.

A. FO angle-gapped case

In this subsection, we consider the topological classification for the FO angle-gapped FNH systems. We first elaborate on the simplest case with only a FO angle gap at $\theta_0 = \pi$ in the Floquet operator spectra and explicitly work out the Clifford algebra's extension problem for all the symmetry classes. The discussions are then extended to the generic cases with more real gaps allowed by their underlying symmetries. The results are listed in the topological classification Table I for all the FO angle-gapped FNH topological phases.

1. Only one FO angle gap at $\theta_0 = \pi$

For the simple case, when the quasienergy spectra possess one FO angle gap at $\theta_0 = \pi$, we have

Lemma 2. *The loop operator $U_{l,\pi}(\mathbf{k}, t)$ and time-evolution operator $U(\mathbf{k}, t)$ have the same symmetries. The Floquet Hamiltonian $H_{F,\pi}$ and the initial Hamiltonian $H(\mathbf{k}, t = 0)$ also have the same symmetries.*

The proof of Lemma 2 is provided in Appendix E for mathematical rigorousness. Following Lemma 2, we can decompose the time-evolution operator $U(\mathbf{k}, t)$ into two separate parts, which is described below

Theorem 1. *The time-evolution operator $U(\mathbf{k}, t)$ with FO angle gap at π can be continuously transformed to $U_f(\mathbf{k}, t) = L * C$, where L is a loop operator satisfying $L(t) = L(t + \tau)$ and C is a constant evolution generated by a time-independent Hamiltonian. Here L and C are unique up to homotopy. The loop operator can be chosen as $L = U_{l,\pi}(\mathbf{k}, t)$. Correspondingly, C is the constant evolution of Hamiltonian $H_{F,\pi}$. The continuous transformation preserves all the GBL symmetries.*

Theorem 1 can be regarded as a non-unitary and GBL symmetries generalization of the Theorem III. 1 in Ref. [104]. The detailed proof of Theorem 1 is provided in Appendix F. Theorem 1 indicates that the topological

classification for FNH systems with FO angle gap at π reduces to the topological classification of $U_{l,\pi}(\mathbf{k}, t)$ and $H_{F,\pi}$. The latter has been previously investigated for static non-Hermitian Hamiltonians [128–130]. For the simplest case with only a single FO angle gap at $\theta_0 = \pi$ (it is equivalent to only a single FH real gap at $E_0 = \pi/\tau$), the spectra of $H_{F,\pi}$ can be continuously contracted to a single point since there is no FH real gap that separates them. Therefore we only need to consider the topological classification of the loop operator $U_{l,\pi}$.

The topological classification of $U_{l,\pi}(\mathbf{k}, t)$ can be obtained through a ‘‘Hermitianization’’ procedure. We consider the following Hermitian operator:

$$\tilde{H}(\mathbf{k}, t) = \begin{bmatrix} 0 & U_{l,\pi}(\mathbf{k}, t) \\ U_{l,\pi}(\mathbf{k}, t)^\dagger & 0 \end{bmatrix}. \quad (30)$$

The mapping from $U_{l,\pi}(\mathbf{k}, t)$ to $\tilde{H}(\mathbf{k}, t)$ is homeomorphic since $\det(U_{l,\pi}(\mathbf{k}, t)) \neq 0$ implies $\det(\tilde{H}(\mathbf{k}, t)) \neq 0$. The Hermitianization procedure greatly simplifies the classification problem, e.g., we can continuously transform $\tilde{H}(\mathbf{k}, t)$ into a band-flattened Hamiltonian [i.e., $(\tilde{H}(\mathbf{k}, t))^2 = \mathbb{I}$] without altering any symmetries [119]. According to Lemma 2, $U_{l,\pi}(\mathbf{k}, t)$ and $U(\mathbf{k}, t)$ belong to the same GBL symmetry class. From the symmetries of the loop operator $U_{l,\pi}(\mathbf{k}, t)$ as described in Eqs. (15)–(18), we obtain the symmetries:

$$\tilde{H}(-\mathbf{k}, -\epsilon_k t) = \tilde{K} \tilde{H}(\mathbf{k}, t) \tilde{K}^{-1}, \quad k k^* = \eta_k \mathbb{I}, \quad K \text{ sym.} \quad (31)$$

$$\tilde{H}(\mathbf{k}, \epsilon_q t) = \tilde{Q} \tilde{H}(\mathbf{k}, t) \tilde{Q}^{-1}, \quad q^2 = \mathbb{I}, \quad Q \text{ sym.} \quad (32)$$

$$\tilde{H}(-\mathbf{k}, -\epsilon_c t) = \tilde{C} \tilde{H}(\mathbf{k}, t) \tilde{C}^{-1}, \quad c c^* = \eta_c \mathbb{I}, \quad C \text{ sym.} \quad (33)$$

$$\tilde{H}(\mathbf{k}, -t) = \tilde{P} \tilde{H}(\mathbf{k}, t) \tilde{P}^{-1}, \quad p^2 = \mathbb{I}, \quad P \text{ sym.} \quad (34)$$

satisfied by the Hamiltonian $\tilde{H}(\mathbf{k}, t)$. Here $\tilde{K} = \sigma_0 \otimes k\mathcal{K}$, $\tilde{Q} = \sigma_0 \otimes q$, $\tilde{P} = \sigma_0 \otimes p$ and $\tilde{C} = \sigma_0 \otimes c\mathcal{K}$. \mathcal{K} is the complex conjugate. The derivation of Eqs. (31)–(34) is given in Appendix G. Besides, the Hamiltonian $\tilde{H}(\mathbf{k}, t)$ has an additional chiral symmetry $\Sigma = \sigma_z \otimes \mathbb{I}$, with

$$\Sigma \tilde{H}(\mathbf{k}) = -\tilde{H}(\mathbf{k}) \Sigma. \quad (35)$$

We then utilize K -theory to deal with the topological classification of $\tilde{H}(\mathbf{k}, t)$ for each of the 54 GBL symmetry classes. According to the standard classification scheme in terms of Clifford algebra [117], we represent $\tilde{H}(\mathbf{k}, t)$ as

$$\tilde{H}(\mathbf{k}, t) = m\tilde{\gamma}_0 + k_1\tilde{\gamma}_1 + \dots + k_d\tilde{\gamma}_d + t\tilde{\gamma}_t. \quad (36)$$

Here, $\tilde{\gamma}_0, \tilde{\gamma}_i$ ($i = 1, \dots, d$) and $\tilde{\gamma}_t$ are the basis of the Clifford algebra. They anticommute with each other and square to the identity. $m\tilde{\gamma}_0$ is the mass term. From the commutation relations of the symmetry operators and Hamiltonian, we can construct the Clifford algebra’s extension for each symmetry class. The space of the mass

term is obtained through its correspondence with Clifford algebra’s extension. (See Table I and Table VI of Ref. [130]). Once the space of the mass term is obtained, we finalize the topological classification by calculating its 0th homotopy group. We illustrate the above procedure by an explicit example of the class Non in Table I. The generators of this class are $\{\tilde{\gamma}_0, \tilde{\gamma}_1, \dots, \tilde{\gamma}_d, \tilde{\gamma}_t, \Sigma\}$. The Clifford algebra’s extension of this class is $\{\tilde{\gamma}_1, \dots, \tilde{\gamma}_d, \tilde{\gamma}_t, \Sigma\} \rightarrow \{\tilde{\gamma}_0, \tilde{\gamma}_1, \dots, \tilde{\gamma}_d, \tilde{\gamma}_t, \Sigma\} = Cl_{d+2} \rightarrow Cl_{d+3}$. The space of the mass term follows as C_{d+2} , and the topological classification of the Non class is given by the homotopy group: $\pi_0(C_{d+2}) = \mathbb{Z}$ (0) for even (odd) d (d is the spatial dimension). The classifying space is equal to the space of mass term at $d = 0$. In a similar vein, we can construct the Clifford algebra’s extension for all the other GBL classes, as summarized in Table IV.

2. Complete classification for classes without P , Q ($\epsilon_q = -1$), C ($\epsilon_c = -1$) and K ($\epsilon_k = -1$) symmetry

In this part, we discuss the classification for classes without any of the P , Q ($\epsilon_q = -1$), C ($\epsilon_c = -1$), or K ($\epsilon_k = -1$) symmetry. For these classes, the FO angle gap could be along any radial line emitted from the origin, with the spectra satisfying the full symmetry of the system. Let us consider a FO angle gap at θ_0 and a constant Hamiltonian evolution $U_c(\mathbf{k}, t) = e^{-it\theta_c \mathbb{I}/\tau}$, with θ_c a real constant. The $U_c(\mathbf{k}, t)$ preserves the full symmetry of the system. The composition $\bar{U}(\mathbf{k}, t) = U(\mathbf{k}, t) * U_c(\mathbf{k}, t)$, which is homeomorphic to $U(\mathbf{k}, t)$. $\bar{U}(\mathbf{k}, t)$ preserves the full symmetry of $U(\mathbf{k}, t)$ and has a gap located at $\bar{\theta}_0 = \theta_0 + \theta_c$. In general, there may exist multiple FO angle gaps. For the Floquet spectra with n FO angle gaps, we can always continuously shift one of the FO angle gaps to π by adjusting θ_c without altering any symmetry of $\bar{U}(\mathbf{k}, t)$. Thus, we can focus on the case that $U(\mathbf{k})$ has a FO angle gap at π and $n - 1$ FO angle gaps at other angles. From Theorem 1, we conclude a complete topological classification of $U(\mathbf{k}, t)$ is equivalent to the topological classification of $H_{F,\pi}$ with $n - 1$ real gaps in $(-\pi/\tau, \pi/\tau)$ [128] plus the topological classification of loop operator $U_{l,\pi}$, as demonstrated in Sec. III A 1.

3. Complete classification for classes with P or Q ($\epsilon_q = -1$) or C ($\epsilon_c = -1$) or K ($\epsilon_k = -1$) symmetry

In this part, we demonstrate the complete classification for classes when any of the P or Q ($\epsilon_q = -1$) or C ($\epsilon_c = -1$) or K ($\epsilon_k = -1$) symmetry exists. For these classes, the FO angle gaps are pinned at $\theta_0 = 0$ or π or a pair of FO angle gaps located at $(\theta_i, -\theta_i)$ to make the spectra have the full symmetry of the system [128]. In the following, we elaborate on the different situations of the FO angle gap configurations.

S1: There is only one FO angle gap at π or 0. The topological classification for the former is given in Sec-

tion III A 1. For the latter, we can shift the FO angle gap at 0 to π through a homeomorphic mapping. As a representative example, we consider the class P with $p = \sigma_z$. The constant evolution $U_0(\mathbf{k}, t) = e^{-i\pi\sigma_x t/\tau}$ fulfills the P symmetry. The composition $\bar{U}(\mathbf{k}, t) = U_0(\mathbf{k}, t) * U(\mathbf{k}, t)$ is homeomorphic to $U(\mathbf{k}, t)$ and preserves the symmetry of $U(\mathbf{k}, t)$, while its associated Floquet spectra possess a FO angle gap at π . It follows that the system with only one FO angle gap at 0 has the same topological classification as that with only one FO angle gap at π . Similarly, we can shift the FO angle gap from 0 to π for all the other GBL classes.

S2: There are two FO angle gaps at 0 and π . According to Theorem 1, the topological classification is reduced to the topological classification of $H_{F,\pi}$ with a real gap at 0 [128] plus the topological classification of $U_{l,\pi}$, which is demonstrated in Sec. III A 1.

S3: There are one FO angle gap at π or 0 and n_q pairs of FO angle gaps at $(\theta_m, -\theta_m)$ ($m = 1, 2, \dots, n_q$). Here $0 < \theta_1 < \theta_2 < \dots < \theta_{n_q} < \pi$. Thus, there are one FH real gap at π/τ or 0 and n_q pairs of FH real gaps at $(\theta_m/\tau, -\theta_m/\tau)$ ($m = 1, 2, \dots, n_q$). For the former case, when one of the FO angle gaps is located at π and n_q pairs of FO angle gaps at $(\theta_m, -\theta_m)$ ($m = 1, 2, \dots, n_q$), $H_{F,\pi}$ possesses n_q pairs of real gap at $(\theta_m/\tau, -\theta_m/\tau)$, π is chosen as the branch cut and doesn't contribute to a $H_{F,\pi}$ real gap. $H_{F,\pi}$ is formally written as $H_{F,\pi} = \sum_j \mathcal{E}_j |\psi_j^R\rangle \langle \psi_j^L|$. According to Theorem 1, the topological classification is reduced to the classification of $H_{F,\pi}$ plus $U_{l,\pi}$. We rearrange the spectra of $H_{F,\pi}$ according to its real gaps and decompose $H_{F,\pi}$ into $n_q + 1$ sub-Hamiltonians $H_{F,\pi} = H_1 + H_2 + \dots + H_{n_q+1}$. Here $H_1 = \sum_j \mathcal{E}_j |\psi_j^R\rangle \langle \psi_j^L|$ with $-\theta_1/\tau < \text{Re}(\mathcal{E}_j) < \theta_1/\tau$, $H_{n_q+1} = \sum_j \mathcal{E}_j |\psi_j^R\rangle \langle \psi_j^L|$ with $\text{Re}(\mathcal{E}_j) \in (-\pi/\tau, -\theta_{n_q}/\tau) \cup (\theta_{n_q}/\tau, \pi/\tau)$, and $H_m = \sum_j \mathcal{E}_j |\psi_j^R\rangle \langle \psi_j^L|$ with $\text{Re}(\mathcal{E}_j) \in (-\theta_m/\tau, -\theta_{m-1}/\tau) \cup (\theta_{m-1}/\tau, \theta_m/\tau)$ for $1 < m < n_q + 1$. Each sub-Hamiltonian belongs to the same symmetry class as $H_{F,\pi}$. And H_n ($n = 1, 2, \dots, n_q + 1$) possesses a real gap at 0 except for H_1 . Thus H_1 is contractible to a trivial constant Hamiltonian. Combine the classification of H_n ($n = 2, 3, \dots, n_q + 1$) with a real gap at 0 [128] and the topological classification of loop operator $U_{l,\pi}$ in Sec. III A 1, we obtain the full classification of the system.

The discussion for the latter case when one of the FO angle gaps is located at 0 and n_q pairs of FO angle gaps at $(\theta_m, -\theta_m)$ ($m = 1, 2, \dots, n_q$) is similar to that in S1. We still take class P with $p = \sigma_z$ as an example. The homeomorphic mapping $\bar{U}(\mathbf{k}, t) = U_0(\mathbf{k}, t) * U(\mathbf{k}, t)$ does not alter any symmetry of $U(\mathbf{k}, t)$; while its associated Floquet spectra possess FO angle gap at π , $\theta_m - \pi$ and $\pi - \theta_m$ ($m = 1, 2, \dots, n_q$). It follows the topological classification is the same as the former case. Such a homeomorphic mapping works for all the other GBL classes.

S4: There are both FO angle gaps at 0 and π and n_q pairs of FO angle gaps at $(\theta_m, -\theta_m)$, where $m = 1, 2, \dots, n_q$ and $0 < \theta_1 < \theta_2 < \dots < \theta_{n_q} < \pi$. It is equivalent to there are both FH real gaps at 0 and π/τ and

n_q pairs of FH real gaps at $(\theta_m/\tau, -\theta_m/\tau)$, where $m = 1, 2, \dots, n_q$. According to Theorem 1, the topological classification is reduced to the classification of $H_{F,\pi}$ plus $U_{l,\pi}$. For this case, the $H_{F,\pi}$ has one real gap at 0, and n_q pairs of real gaps at $(\theta_m/\tau, -\theta_m/\tau)$, π is chosen as the branch cut and doesn't contribute to a real gap. We can decompose the Floquet Hamiltonian into $n_q + 1$ constant Hamiltonians according to quasienergy gaps: $H_{F,\pi} = H_1 + H_2 + \dots + H_m + \dots + H_{n_q+1}$. Here $H_1 = \sum_j \mathcal{E}_j |\psi_j^R\rangle \langle \psi_j^L|$ with $\text{Re}(\mathcal{E}_j) \in (-\theta_1/\tau, 0) \cup (0, \theta_1/\tau)$; $H_{n_q+1} = \sum_j \mathcal{E}_j |\psi_j^R\rangle \langle \psi_j^L|$ with $\text{Re}(\mathcal{E}_j) \in (-\pi/\tau, -\theta_{n_q}/\tau) \cup (\theta_{n_q}/\tau, \pi/\tau)$; and $H_m = \sum_j \mathcal{E}_j |\psi_j^R\rangle \langle \psi_j^L|$ with $\text{Re}(\mathcal{E}_j) \in (-\theta_m/\tau, -\theta_{m-1}/\tau) \cup (\theta_{m-1}/\tau, \theta_m/\tau)$ for $1 < m < n_q + 1$. All the sub-Hamiltonians H_m belong to the same symmetry class as $H_{F,\pi}$ and have a real gap located at 0. Combine the classification of H_n ($n = 1, 2, \dots, n_q + 1$) with a real gap at 0 [128] and the classification of $U_{l,\pi}$ in Sec. III A 1, we obtain a full topological classification for the system.

The discussions in Sec. III A 1-3 cover all the 54 GBL symmetry classes and the possible FO angle gap conditions of the Floquet spectra, culminating in a complete topological classification of all the FO angle-gapped FNH topological phases as summarized in the periodic Table I.

B. FO angle-gapless case

For the FO angle-gapless case, the spectra of the Floquet operator winds around the origin without any FO angle gaps [See Fig. 1(d)]. We remind that the FO angle gap is not allowed to be closed in the topological classification in the previous FO angle-gapped case. If there is a FO angle gap at θ , we can define $H_{F,\theta}$, which is a continuous function. In the FO angle-gapless case, there is no such spectrum restriction, and we can't define $H_{F,\theta}$. But Floquet operator $U(\mathbf{k})$ is a continuous function. To extract the band topology of the Floquet operator $U(\mathbf{k})$, we consider the following Hermitian operator:

$$\tilde{H}(\mathbf{k}) = \begin{bmatrix} 0 & U(\mathbf{k}) \\ U(\mathbf{k})^\dagger & 0 \end{bmatrix}. \quad (37)$$

As $\det(U(\mathbf{k})) \neq 0$ is equivalent to $\det(\tilde{H}(\mathbf{k})) \neq 0$, the mapping from $U(\mathbf{k})$ to $\tilde{H}(\mathbf{k})$ is homeomorphic, yielding that $U(\mathbf{k})$ has the same topology as $\tilde{H}(\mathbf{k})$. We can continuously transform the Hermitian operator $\tilde{H}(\mathbf{k})$ into a band-flattened Hamiltonian $\tilde{\tilde{H}}(\mathbf{k})$ [$(\tilde{\tilde{H}}(\mathbf{k}))^2 = \mathbb{I}$] without altering any symmetry [119]. When $U(\mathbf{k})$ satisfies the symmetries described by Eqs. (20)-(23), the corresponding symmetries satisfied by the band-flattened Hamiltonian $\tilde{\tilde{H}}(\mathbf{k})$ are:

$$\tilde{\tilde{H}}(-\mathbf{k}) = \bar{K} \tilde{\tilde{H}}(\mathbf{k}) \bar{K}^{-1}, \quad k k^* = \eta_k \mathbb{I}, \quad K \text{ sym.} \quad (38)$$

$$\tilde{\tilde{H}}(\mathbf{k}) = \bar{Q} \tilde{\tilde{H}}(\mathbf{k}) \bar{Q}^{-1}, \quad q^2 = \mathbb{I}, \quad Q \text{ sym.} \quad (39)$$

$$\tilde{\tilde{H}}(-\mathbf{k}) = \bar{C} \tilde{\tilde{H}}(\mathbf{k}) \bar{C}^{-1}, \quad c c^* = \eta_c \mathbb{I}, \quad C \text{ sym.} \quad (40)$$

$$\tilde{\tilde{H}}(\mathbf{k}) = \bar{P} \tilde{\tilde{H}}(\mathbf{k}) \bar{P}^{-1}. \quad p^2 = \mathbb{I}. \quad P \text{ sym.} \quad (41)$$

Here $\bar{K} = \sigma_x \otimes k\mathcal{K}$ if $\epsilon_k = 1$ and $\bar{K} = \sigma_0 \otimes k\mathcal{K}$ if $\epsilon_k = -1$; $\bar{Q} = \sigma_0 \otimes q$ if $\epsilon_q = 1$ and $\bar{Q} = \sigma_x \otimes q$ if $\epsilon_q = -1$; $\bar{P} = \sigma_x \otimes p$; $\bar{C} = \sigma_x \otimes c\mathcal{K}$ if $\epsilon_c = 1$ and $\bar{C} = \sigma_0 \otimes c\mathcal{K}$ if $\epsilon_c = -1$. The derivation of Eqs. (38)-(41) is given in Appendix H. Besides, the Hamiltonian $\tilde{H}(\mathbf{k})$ possesses an additional chiral symmetry ($\Sigma = \sigma_z$):

$$\Sigma \tilde{H}(\mathbf{k}) = -\tilde{H}(\mathbf{k})\Sigma. \quad (42)$$

We then use the K -theory to obtain the topological classification of $\tilde{H}(\mathbf{k})$ for each of the 54 GBL classes. Following the standard classification scheme [117] in terms of Clifford algebra, we represent $\tilde{H}(\mathbf{k})$ as

$$\tilde{H}(\mathbf{k}) = m\gamma_0 + k_1\gamma_1 + \dots + k_d\gamma_d. \quad (43)$$

Here, γ_0, γ_i ($i = 1, \dots, d$) anticommute with each other and square to identity. Using the commutation relations of the symmetry operators and $\tilde{H}(\mathbf{k})$, we construct the Clifford algebra's extension for each symmetry class. We can get the space of mass term from the Clifford algebra's extension. (See Table I and Table IV of Ref. [130]). By calculating the 0th homotopy group of the space of the mass term, we obtain the topological classification of the FO angle-gapless FNH topological phase for all the GBL classes. We still take the Non class as an example, with the generators of this class given by $\{\gamma_0, \gamma_1, \dots, \gamma_d, \Sigma\}$. The Clifford algebra's extension of this class is $\{\gamma_1, \dots, \gamma_d, \Sigma\} \rightarrow \{\gamma_0, \gamma_1, \dots, \gamma_d, \Sigma\} = Cl_{d+1} \rightarrow Cl_{d+2}$. The space of the mass term is C_{d+1} , and the classifying space is C_1 . The topological classification for the Non class is then $\pi_0(C_{d+1}) = 0$ (\mathbb{Z}) for even (odd) d . We note that it is different from the FO angle-gapped case (See Sec. III A 1), for example, the additional time dimension in FO angle-gapped case. We can similarly work out the Clifford algebra's extension for all the other GBL classes, as demonstrated in Table V of Appendix I. The topological classification for all the GBL classes in the FO angle-gapless case is summarized in Table II.

C. Relations with Floquet Hermitian topological phases

Our classification for the FNH topological phases fully covers the previous topological classifications of Floquet Hermitian topological phases [104, 148] as the special cases. In fact, the Hermitian constraint $H(\mathbf{k}, t) = H^\dagger(\mathbf{k}, t)$ can be represented by a type- Q ($\epsilon_q = 1$, $\eta_q = 1$, and $q = \mathbb{I}$) symmetry of the GBL classes in Eq. (11). Thus, the Hermitian A, AIII, AI, AII, C, D, CI, CII, BDI, and DIII classes of the AZ tenfold way correspond to the non-Hermitian Qa, PQ1, QC1a, QC3a, QC7a, QC5a, PQC9a, PQC5, PQC1, and PQC11a classes of the GBL 54-fold way, respectively.

Here we derive this conclusion. The Hermitian constraint is a type- η (pseudo-Hermitian) symmetry in the paper of Kawabata et al. [128]. Due to the Hermitian operator commute with TRS, PHS, and CS operators,

the Hermitian A, AIII, AI, AII, C, D, CI, CII, BDI, and DIII classes of the AZ tenfold way corresponds to the non-Hermitian η_+A , η_+AIII , η_+AI , η_+AII , η_++C , η_++D , η_++CI , η_++CII , η_++BDI , and η_++DIII classes of the GBL 54-fold way in Kawabata-Shiozaki-Ueda-Sato's notation, respectively. According to the correspondence relations between Kawabata-Shiozaki-Ueda-Sato notation and Ref. [130]'s notation in Table VIII of Ref. [130], the non-Hermitian η_+A , η_+AIII , η_+AI , η_+AII , η_++C , η_++D , η_++CI , η_++CII , η_++BDI , and η_++DIII classes of the GBL 54-fold way in Kawabata-Shiozaki-Ueda-Sato's notation correspond to the non-Hermitian Qa, PQ1, QC1a, QC3a, QC7a, QC5a, PQC9a, PQC5, PQC1, and PQC11a classes of the GBL 54-fold way in Ref. [130]'s notation, respectively.

For the above 10 classes, our classification for the FO angle-gapped case in Table I reproduces Roy and Harper's periodic table [104] of Floquet Hermitian topological insulator with FH real gaps (or FO angle gaps). While for the FO angle-gapless case, our classification in Table II reproduces Higashikawa, Nakagawa, and Ueda's periodic table [148] of unitary Floquet operator. The superficial doubling of the topological invariants $\mathbb{Z}^{\times 2n}$, $\mathbb{Z}^{\times 2n_p}$, $\mathbb{Z}_2^{\times 2n}$, or $\mathbb{Z}_2^{\times 2n_p}$ appeared in Table I and II comes from the existence of the Q ($\epsilon_q = 1$) symmetry, which enforces the $\tilde{H}(\mathbf{k}, t)$ in Eq. (30) and $\tilde{H}(\mathbf{k})$ in Eq. (37) to be diagonalized into two irreducible blocks. Each block either corresponds to the 1 or the -1 eigenvalue of \tilde{Q} (note that $\tilde{Q}^2 = 1$), respectively. Consider Hermitian as a type- Q symmetry, we have $\epsilon_q = 1$, $\eta_q = 1$, and $q = \mathbb{I}$, the -1 eigensubspace of \tilde{Q} is vanish. By kicking out the half topological numbers that correspond to -1 eigensubspace, we are left with only the half topological numbers that correspond to the 1 eigensubspace and fully recover previous results for Floquet Hermitian topological phases.

We stress that the classification of Floquet topological insulator is equivalent to the topological classification of FO angle gapped Hermitian system. And unitary Floquet operator's topological classification is equivalent to the topological classification of FO angle gapless Hermitian system. They are different names for the same thing.

For example, according to Table I, the topological classification of the non-Hermitian 1-dimensional GBL PQC1 class FO angle gapped system is \mathbb{Z}^{2n_p} . Consider Hermitian as a type- Q symmetry, and we have $q = \mathbb{I}$. Thus, the -1 eigensubspace of \tilde{Q} vanish, we should kick out the half topological number (they correspond to -1 the eigensubspace and must be trivial). And the topological classification is \mathbb{Z}^{n_p} . According to Ref. [104] the topological classification of Hermitian 1-dimensional AZ BDI class Floquet topological insulator is \mathbb{Z}^{n_p} . Thus, our result is consistent with Roy and Harper's result [104]. Similarly, it is not difficult to verify that our results are consistent with Roy and Harper's results [104] for any dimensional and symmetry class. According to Table II, the topological classification of the non-Hermitian 1-dimensional GBL Qa class FO angle gapless system is \mathbb{Z}^2 . Consider

Hermitian as a type-Q symmetry, and we have $q = \mathbb{I}$. Thus, the -1 eigensubspace of \tilde{Q} vanish, we should kick out the half topological number (they correspond to -1 the eigensubspace and must be trivial). And the topological classification is \mathbb{Z} . According to Ref. [148], the topological classification of Hermitian 1-dimensional A

class unitary Floquet operator is \mathbb{Z} . Thus, our result is consistent with Higashikawa, Nakagawa, and Ueda's result [148]. Similarly, it is not difficult to verify that our results are consistent with Higashikawa, Nakagawa, and Ueda's results [148] for any dimensional and symmetry class.

TABLE I. Periodic table of Floquet non-Hermitian topological phases for FO angle gapped case. d is the spatial dimension. Each row corresponds to a specific generalized Bernard-LeClair (GBL) symmetry class, labeled by its name in the first column. The second column lists the symmetry-generator relations, including the signs of time-flipping, operator involution, and commutation relations. For the classes with P and at least one of the Q and K symmetries, only the cases of $\epsilon_q = 1$ or $\epsilon_k = 1$ are listed in the table. This is because the classes of $\epsilon_q = -1$ or $\epsilon_k = -1$ are equivalent to the corresponding classes of $\epsilon_q = 1$ or $\epsilon_k = 1$ in the presence of P symmetry, as can be seen from Eqs. (10)-(13). The third column gives the classifying space of each symmetry class. In the table, $n \in \mathbb{Z}^+$ is the total number of relevant spectrum gaps. $n_p = n_q + n_r$. And $n_r \in \{1, 2\}$ counts the relevant FO angle gaps at 0 and π . $n_q \in \mathbb{Z}^+ \cup \{0\}$ is the number of pairs of FO angle gaps at $(\theta_m, -\theta_m)$ ($m = 1, 2, \dots, n_q, \theta_m \neq 0, \pi$). The topological numbers in the table are stable strong topological numbers.

GBL	Gen. Rel.	Cl	$d = 0$	1	2	3	4	5	6	7
Non		$C_0^{\times n}$	$\mathbb{Z}^{\times n}$	0	$\mathbb{Z}^{\times n}$	0	$\mathbb{Z}^{\times n}$	0	$\mathbb{Z}^{\times n}$	0
P		$C_1^{\times n_p}$	0	$\mathbb{Z}^{\times n_p}$	0	$\mathbb{Z}^{\times n_p}$	0	$\mathbb{Z}^{\times n_p}$	0	$\mathbb{Z}^{\times n_p}$
Qa	$\epsilon_q = 1$	$C_0^{\times 2n}$	$\mathbb{Z}^{\times 2n}$	0	$\mathbb{Z}^{\times 2n}$	0	$\mathbb{Z}^{\times 2n}$	0	$\mathbb{Z}^{\times 2n}$	0
Qb	$\epsilon_q = -1$	$C_1^{\times n_p}$	0	$\mathbb{Z}^{\times n_p}$	0	$\mathbb{Z}^{\times n_p}$	0	$\mathbb{Z}^{\times n_p}$	0	$\mathbb{Z}^{\times n_p}$
K1a	$\epsilon_k = 1, \eta_k = 1$	$R_0^{\times n}$	$\mathbb{Z}^{\times n}$	0	0	0	$2\mathbb{Z}^{\times n}$	0	$\mathbb{Z}_2^{\times n}$	$\mathbb{Z}_2^{\times n}$
K1b	$\epsilon_k = -1, \eta_k = 1$	$R_2^{\times n_p}$	$\mathbb{Z}_2^{\times n_p}$	$\mathbb{Z}_2^{\times n_p}$	$\mathbb{Z}^{\times n_p}$	0	0	0	$2\mathbb{Z}^{\times n_p}$	0
K2a	$\epsilon_k = 1, \eta_k = -1$	$R_4^{\times n}$	$2\mathbb{Z}^{\times n}$	0	$\mathbb{Z}_2^{\times n}$	$\mathbb{Z}_2^{\times n}$	$\mathbb{Z}^{\times n}$	0	0	0
K2b	$\epsilon_k = -1, \eta_k = -1$	$R_6^{\times n_p}$	0	0	$2\mathbb{Z}^{\times n_p}$	0	$\mathbb{Z}_2^{\times n_p}$	$\mathbb{Z}_2^{\times n_p}$	$\mathbb{Z}^{\times n_p}$	0
C1	$\epsilon_c = 1, \eta_c = 1$	$R_3^{\times n}$	$\mathbb{Z}^{\times n}$	0	0	0	$2\mathbb{Z}^{\times n}$	0	$\mathbb{Z}_2^{\times n}$	$\mathbb{Z}_2^{\times n}$
C2	$\epsilon_c = 1, \eta_c = -1$	$R_4^{\times n}$	$2\mathbb{Z}^{\times n}$	0	$\mathbb{Z}_2^{\times n}$	$\mathbb{Z}_2^{\times n}$	$\mathbb{Z}^{\times n}$	0	0	0
C3	$\epsilon_c = -1, \eta_c = 1$	$R_2^{\times n_p}$	$\mathbb{Z}_2^{\times n_p}$	$\mathbb{Z}_2^{\times n_p}$	$\mathbb{Z}^{\times n_p}$	0	0	0	$2\mathbb{Z}^{\times n_p}$	0
C4	$\epsilon_c = -1, \eta_c = -1$	$R_6^{\times n_p}$	0	0	$2\mathbb{Z}^{\times n_p}$	0	$\mathbb{Z}_2^{\times n_p}$	$\mathbb{Z}_2^{\times n_p}$	$\mathbb{Z}^{\times n_p}$	0
PQ1	$\epsilon_q = 1, \epsilon_{pq} = 1$	$C_1^{\times 2n_p}$	0	$\mathbb{Z}^{\times 2n_p}$	0	$\mathbb{Z}^{\times 2n_p}$	0	$\mathbb{Z}^{\times 2n_p}$	0	$\mathbb{Z}^{\times 2n_p}$
PQ2	$\epsilon_q = 1, \epsilon_{pq} = -1$	$C_0^{\times n_p}$	$\mathbb{Z}^{\times n_p}$	0	$\mathbb{Z}^{\times n_p}$	0	$\mathbb{Z}^{\times n_p}$	0	$\mathbb{Z}^{\times n_p}$	0
PK1	$\epsilon_k = 1, \eta_k = 1, \epsilon_{pk} = 1$	$R_1^{\times n_p}$	$\mathbb{Z}_2^{\times n_p}$	$\mathbb{Z}^{\times n_p}$	0	0	0	$2\mathbb{Z}^{\times n_p}$	0	$\mathbb{Z}_2^{\times n_p}$
PK2	$\epsilon_k = 1, \eta_k = -1, \epsilon_{pk} = 1$	$R_5^{\times n_p}$	0	$2\mathbb{Z}^{\times n_p}$	0	$\mathbb{Z}_2^{\times n_p}$	$\mathbb{Z}_2^{\times n_p}$	$\mathbb{Z}^{\times n_p}$	0	0
PK3a	$\epsilon_k = 1, \eta_k = 1, \epsilon_{pk} = -1$	$R_7^{\times n_p}$	0	0	0	$2\mathbb{Z}^{\times n_p}$	0	$\mathbb{Z}_2^{\times n_p}$	$\mathbb{Z}_2^{\times n_p}$	$\mathbb{Z}^{\times n_p}$
PK3b	$\epsilon_k = 1, \eta_k = -1, \epsilon_{pk} = -1$	$R_3^{\times n_p}$	0	$\mathbb{Z}_2^{\times n_p}$	$\mathbb{Z}_2^{\times n_p}$	$\mathbb{Z}^{\times n_p}$	0	0	0	$2\mathbb{Z}^{\times n_p}$
PC1	$\frac{\epsilon_c = 1, \eta_c = 1, \epsilon_{pc} = 1}{\epsilon_c = -1, \eta_c = 1, \epsilon_{pc} = 1}$	$R_1^{\times n_p}$	$\mathbb{Z}_2^{\times n_p}$	$\mathbb{Z}^{\times n_p}$	0	0	0	$2\mathbb{Z}^{\times n_p}$	0	$\mathbb{Z}_2^{\times n_p}$
PC2	$\frac{\epsilon_c = 1, \eta_c = 1, \epsilon_{pc} = -1}{\epsilon_c = -1, \eta_c = -1, \epsilon_{pc} = -1}$	$R_7^{\times n_p}$	0	0	0	$2\mathbb{Z}^{\times n_p}$	0	$\mathbb{Z}_2^{\times n_p}$	$\mathbb{Z}_2^{\times n_p}$	$\mathbb{Z}^{\times n_p}$
PC3	$\frac{\epsilon_c = 1, \eta_c = -1, \epsilon_{pc} = 1}{\epsilon_c = -1, \eta_c = -1, \epsilon_{pc} = 1}$	$R_5^{\times n_p}$	0	$2\mathbb{Z}^{\times n_p}$	0	$\mathbb{Z}_2^{\times n_p}$	$\mathbb{Z}_2^{\times n_p}$	$\mathbb{Z}^{\times n_p}$	0	0
PC4	$\frac{\epsilon_c = 1, \eta_c = -1, \epsilon_{pc} = -1}{\epsilon_c = -1, \eta_c = 1, \epsilon_{pc} = -1}$	$R_3^{\times n_p}$	0	$\mathbb{Z}_2^{\times n_p}$	$\mathbb{Z}_2^{\times n_p}$	$\mathbb{Z}^{\times n_p}$	0	0	0	$2\mathbb{Z}^{\times n_p}$
QC1a	$\epsilon_q = 1, \epsilon_c = 1, \eta_c = 1, \epsilon_{qc} = 1$	$R_0^{\times 2n}$	$\mathbb{Z}^{\times 2n}$	0	0	0	$2\mathbb{Z}^{\times 2n}$	0	$\mathbb{Z}_2^{\times 2n}$	$\mathbb{Z}_2^{\times 2n}$
QC1b	$\epsilon_q = -1, \epsilon_c = 1, \eta_c = 1, \epsilon_{qc} = 1$	$R_1^{\times n_p}$	$\mathbb{Z}_2^{\times n_p}$	$\mathbb{Z}^{\times n_p}$	0	0	0	$2\mathbb{Z}^{\times n_p}$	0	$\mathbb{Z}_2^{\times n_p}$
QC2a	$\epsilon_q = 1, \epsilon_c = 1, \eta_c = 1, \epsilon_{qc} = -1$	$C_0^{\times n}$	$\mathbb{Z}^{\times n}$	0	$\mathbb{Z}^{\times n}$	0	$\mathbb{Z}^{\times n}$	0	$\mathbb{Z}^{\times n}$	0
QC2b	$\epsilon_q = -1, \epsilon_c = 1, \eta_c = 1, \epsilon_{qc} = -1$	$R_7^{\times n_p}$	0	0	0	$2\mathbb{Z}^{\times n_p}$	0	$\mathbb{Z}_2^{\times n_p}$	$\mathbb{Z}_2^{\times n_p}$	$\mathbb{Z}^{\times n_p}$
QC3a	$\epsilon_q = 1, \epsilon_c = 1, \eta_c = -1, \epsilon_{qc} = 1$	$R_3^{\times 2n}$	$2\mathbb{Z}^{\times 2n}$	0	$\mathbb{Z}_2^{\times 2n}$	$\mathbb{Z}_2^{\times 2n}$	$\mathbb{Z}^{\times 2n}$	0	0	0
QC3b	$\epsilon_q = -1, \epsilon_c = 1, \eta_c = -1, \epsilon_{qc} = 1$	$R_5^{\times n_p}$	0	$2\mathbb{Z}^{\times n_p}$	0	$\mathbb{Z}_2^{\times n_p}$	$\mathbb{Z}_2^{\times n_p}$	$\mathbb{Z}^{\times n_p}$	0	0
QC4a	$\epsilon_q = 1, \epsilon_c = 1, \eta_c = -1, \epsilon_{qc} = -1$	$C_0^{\times n}$	$\mathbb{Z}^{\times n}$	0	$\mathbb{Z}^{\times n}$	0	$\mathbb{Z}^{\times n}$	0	$\mathbb{Z}^{\times n}$	0
QC4b	$\epsilon_q = -1, \epsilon_c = 1, \eta_c = -1, \epsilon_{qc} = -1$	$R_3^{\times n_p}$	0	$\mathbb{Z}_2^{\times n_p}$	$\mathbb{Z}_2^{\times n_p}$	$\mathbb{Z}^{\times n_p}$	0	0	0	$2\mathbb{Z}^{\times n_p}$
QC5a	$\epsilon_q = 1, \epsilon_c = -1, \eta_c = 1, \epsilon_{qc} = 1$	$R_2^{\times 2n_p}$	$\mathbb{Z}_2^{\times 2n_p}$	$\mathbb{Z}_2^{\times 2n_p}$	$\mathbb{Z}^{\times 2n_p}$	0	0	0	$2\mathbb{Z}^{\times 2n_p}$	0
QC5b	$\epsilon_q = -1, \epsilon_c = -1, \eta_c = 1, \epsilon_{qc} = 1$	$R_1^{\times n_p}$	$\mathbb{Z}_2^{\times n_p}$	$\mathbb{Z}^{\times n_p}$	0	0	0	$2\mathbb{Z}^{\times n_p}$	0	$\mathbb{Z}_2^{\times n_p}$
QC6a	$\epsilon_q = 1, \epsilon_c = -1, \eta_c = 1, \epsilon_{qc} = -1$	$C_0^{\times n_p}$	$\mathbb{Z}^{\times n_p}$	0	$\mathbb{Z}^{\times n_p}$	0	$\mathbb{Z}^{\times n_p}$	0	$\mathbb{Z}^{\times n_p}$	0
QC6b	$\epsilon_q = -1, \epsilon_c = -1, \eta_c = 1, \epsilon_{qc} = -1$	$R_3^{\times n_p}$	0	$\mathbb{Z}_2^{\times n_p}$	$\mathbb{Z}_2^{\times n_p}$	$\mathbb{Z}^{\times n_p}$	0	0	0	$2\mathbb{Z}^{\times n_p}$
QC7a	$\epsilon_q = 1, \epsilon_c = -1, \eta_c = -1, \epsilon_{qc} = 1$	$R_6^{\times 2n_p}$	0	0	$2\mathbb{Z}^{\times 2n_p}$	0	$\mathbb{Z}_2^{\times 2n_p}$	$\mathbb{Z}_2^{\times 2n_p}$	$\mathbb{Z}^{\times 2n_p}$	0
QC7b	$\epsilon_q = -1, \epsilon_c = -1, \eta_c = -1, \epsilon_{qc} = 1$	$R_5^{\times n_p}$	0	$2\mathbb{Z}^{\times n_p}$	0	$\mathbb{Z}_2^{\times n_p}$	$\mathbb{Z}_2^{\times n_p}$	$\mathbb{Z}^{\times n_p}$	0	0
QC8a	$\epsilon_q = 1, \epsilon_c = -1, \eta_c = -1, \epsilon_{qc} = -1$	$C_0^{\times n_p}$	$\mathbb{Z}^{\times n_p}$	0	$\mathbb{Z}^{\times n_p}$	0	$\mathbb{Z}^{\times n_p}$	0	$\mathbb{Z}^{\times n_p}$	0
QC8b	$\epsilon_q = -1, \epsilon_c = -1, \eta_c = -1, \epsilon_{qc} = -1$	$R_7^{\times n_p}$	0	0	0	$2\mathbb{Z}^{\times n_p}$	0	$\mathbb{Z}_2^{\times n_p}$	$\mathbb{Z}_2^{\times n_p}$	$\mathbb{Z}^{\times n_p}$
PQC1	$\frac{\epsilon_c = 1, \eta_c = 1, \epsilon_{pq} = 1, \epsilon_{pc} = 1, \epsilon_{qc} = 1}{\epsilon_c = -1, \eta_c = 1, \epsilon_{pq} = 1, \epsilon_{pc} = 1, \epsilon_{qc} = 1}$	$R_1^{\times 2n_p}$	$\mathbb{Z}_2^{\times 2n_p}$	$\mathbb{Z}^{\times 2n_p}$	0	0	0	$2\mathbb{Z}^{\times 2n_p}$	0	$\mathbb{Z}_2^{\times 2n_p}$
PQC2	$\frac{\epsilon_c = 1, \eta_c = 1, \epsilon_{pq} = 1, \epsilon_{pc} = 1, \epsilon_{qc} = -1}{\epsilon_c = -1, \eta_c = 1, \epsilon_{pq} = 1, \epsilon_{pc} = 1, \epsilon_{qc} = -1}$	$C_1^{\times n_p}$	0	$\mathbb{Z}^{\times n_p}$	0	$\mathbb{Z}^{\times n_p}$	0	$\mathbb{Z}^{\times n_p}$	0	$\mathbb{Z}^{\times n_p}$
PQC3	$\frac{\epsilon_c = 1, \eta_c = 1, \epsilon_{pq} = -1, \epsilon_{pc} = -1, \epsilon_{qc} = 1}{\epsilon_c = -1, \eta_c = -1, \epsilon_{pq} = -1, \epsilon_{pc} = -1, \epsilon_{qc} = -1}$	$R_0^{\times n_p}$	$\mathbb{Z}^{\times n_p}$	0	0	0	$2\mathbb{Z}^{\times n_p}$	0	$\mathbb{Z}_2^{\times n_p}$	$\mathbb{Z}_2^{\times n_p}$
PQC4	$\frac{\epsilon_c = 1, \eta_c = 1, \epsilon_{pq} = -1, \epsilon_{pc} = -1, \epsilon_{qc} = -1}{\epsilon_c = -1, \eta_c = -1, \epsilon_{pq} = -1, \epsilon_{pc} = -1, \epsilon_{qc} = -1}$	$R_6^{\times n_p}$	0	0	$2\mathbb{Z}^{\times n_p}$	0	$\mathbb{Z}_2^{\times n_p}$	$\mathbb{Z}_2^{\times n_p}$	$\mathbb{Z}^{\times n_p}$	0

continued on next page

TABLE I — continued

PQC5	$\frac{\epsilon_c = 1, \eta_c = -1, \epsilon_{pq} = 1, \epsilon_{pc} = 1, \epsilon_{qc} = 1}{\epsilon_c = -1, \eta_c = -1, \epsilon_{pq} = 1, \epsilon_{pc} = 1, \epsilon_{qc} = 1}$	$R_5^{\times 2n_p}$	0	$2\mathbb{Z}^{\times 2n_p}$	0	$\mathbb{Z}_2^{\times 2n_p}$	$\mathbb{Z}_2^{\times 2n_p}$	$\mathbb{Z}^{\times 2n_p}$	0	0
PQC6	$\frac{\epsilon_c = 1, \eta_c = -1, \epsilon_{pq} = 1, \epsilon_{pc} = 1, \epsilon_{qc} = -1}{\epsilon_c = -1, \eta_c = -1, \epsilon_{pq} = 1, \epsilon_{pc} = 1, \epsilon_{qc} = -1}$	$C_1^{\times n_p}$	0	$\mathbb{Z}^{\times n_p}$	0	$\mathbb{Z}^{\times n_p}$	0	$\mathbb{Z}^{\times n_p}$	0	$\mathbb{Z}^{\times n_p}$
PQC7	$\frac{\epsilon_c = 1, \eta_c = -1, \epsilon_{pq} = -1, \epsilon_{pc} = -1, \epsilon_{qc} = 1}{\epsilon_c = -1, \eta_c = 1, \epsilon_{pq} = -1, \epsilon_{pc} = -1, \epsilon_{qc} = -1}$	$R_4^{\times n_p}$	$2\mathbb{Z}^{\times n_p}$	0	$\mathbb{Z}_2^{\times n_p}$	$\mathbb{Z}_2^{\times n_p}$	$\mathbb{Z}^{\times n_p}$	0	0	0
PQC8	$\frac{\epsilon_c = 1, \eta_c = -1, \epsilon_{pq} = -1, \epsilon_{pc} = -1, \epsilon_{qc} = -1}{\epsilon_c = -1, \eta_c = 1, \epsilon_{pq} = -1, \epsilon_{pc} = -1, \epsilon_{qc} = 1}$	$R_2^{\times n_p}$	$\mathbb{Z}_2^{\times n_p}$	$\mathbb{Z}_2^{\times n_p}$	$\mathbb{Z}^{\times n_p}$	0	0	0	$2\mathbb{Z}^{\times n_p}$	0
PQC9a	$\frac{\epsilon_c = 1, \eta_c = 1, \epsilon_{pq} = 1, \epsilon_{pc} = -1, \epsilon_{qc} = 1}{\epsilon_c = -1, \eta_c = 1, \epsilon_{pq} = 1, \epsilon_{pc} = -1, \epsilon_{qc} = 1}$	$R_7^{\times 2n_p}$	0	0	0	$2\mathbb{Z}^{\times 2n_p}$	0	$\mathbb{Z}_2^{\times 2n_p}$	$\mathbb{Z}_2^{\times 2n_p}$	$\mathbb{Z}^{\times 2n_p}$
PQC9b	$\frac{\epsilon_c = 1, \eta_c = 1, \epsilon_{pq} = 1, \epsilon_{pc} = -1, \epsilon_{qc} = -1}{\epsilon_c = -1, \eta_c = -1, \epsilon_{pq} = 1, \epsilon_{pc} = -1, \epsilon_{qc} = -1}$	$C_1^{\times n_p}$	0	$\mathbb{Z}^{\times n_p}$	0	$\mathbb{Z}^{\times n_p}$	0	$\mathbb{Z}^{\times n_p}$	0	$\mathbb{Z}^{\times n_p}$
PQC10a	$\frac{\epsilon_c = 1, \eta_c = 1, \epsilon_{pq} = -1, \epsilon_{pc} = 1, \epsilon_{qc} = 1}{\epsilon_c = -1, \eta_c = 1, \epsilon_{pq} = -1, \epsilon_{pc} = 1, \epsilon_{qc} = -1}$	$R_0^{\times n_p}$	$\mathbb{Z}^{\times n_p}$	0	0	0	$2\mathbb{Z}^{\times n_p}$	0	$\mathbb{Z}_2^{\times n_p}$	$\mathbb{Z}_2^{\times n_p}$
PQC10b	$\frac{\epsilon_c = 1, \eta_c = 1, \epsilon_{pq} = -1, \epsilon_{pc} = 1, \epsilon_{qc} = -1}{\epsilon_c = -1, \eta_c = -1, \epsilon_{pq} = -1, \epsilon_{pc} = 1, \epsilon_{qc} = 1}$	$R_2^{\times n_p}$	$\mathbb{Z}_2^{\times n_p}$	$\mathbb{Z}_2^{\times n_p}$	$\mathbb{Z}^{\times n_p}$	0	0	0	$2\mathbb{Z}^{\times n_p}$	0
PQC11a	$\frac{\epsilon_c = 1, \eta_c = -1, \epsilon_{pq} = 1, \epsilon_{pc} = -1, \epsilon_{qc} = 1}{\epsilon_c = -1, \eta_c = 1, \epsilon_{pq} = 1, \epsilon_{pc} = -1, \epsilon_{qc} = 1}$	$R_3^{\times 2n_p}$	0	$\mathbb{Z}_2^{\times 2n_p}$	$\mathbb{Z}_2^{\times 2n_p}$	$\mathbb{Z}^{\times 2n_p}$	0	0	0	$2\mathbb{Z}^{\times 2n_p}$
PQC11b	$\frac{\epsilon_c = 1, \eta_c = -1, \epsilon_{pq} = 1, \epsilon_{pc} = -1, \epsilon_{qc} = -1}{\epsilon_c = -1, \eta_c = 1, \epsilon_{pq} = 1, \epsilon_{pc} = -1, \epsilon_{qc} = -1}$	$C_1^{\times n_p}$	0	$\mathbb{Z}^{\times n_p}$	0	$\mathbb{Z}^{\times n_p}$	0	$\mathbb{Z}^{\times n_p}$	0	$\mathbb{Z}^{\times n_p}$
PQC12a	$\frac{\epsilon_c = 1, \eta_c = -1, \epsilon_{pq} = -1, \epsilon_{pc} = 1, \epsilon_{qc} = 1}{\epsilon_c = -1, \eta_c = -1, \epsilon_{pq} = -1, \epsilon_{pc} = 1, \epsilon_{qc} = -1}$	$R_4^{\times n_p}$	$2\mathbb{Z}^{\times n_p}$	0	$\mathbb{Z}_2^{\times n_p}$	$\mathbb{Z}_2^{\times n_p}$	$\mathbb{Z}^{\times n_p}$	0	0	0
PQC12b	$\frac{\epsilon_c = 1, \eta_c = -1, \epsilon_{pq} = -1, \epsilon_{pc} = 1, \epsilon_{qc} = -1}{\epsilon_c = -1, \eta_c = -1, \epsilon_{pq} = -1, \epsilon_{pc} = 1, \epsilon_{qc} = 1}$	$R_6^{\times n_p}$	0	0	$2\mathbb{Z}^{\times n_p}$	0	$\mathbb{Z}_2^{\times n_p}$	$\mathbb{Z}_2^{\times n_p}$	$\mathbb{Z}^{\times n_p}$	0

TABLE II. Periodic table of Floquet non-Hermitian topological phases for FO angle gapless case. d is the spatial dimension. The first two columns are the same as those of Table I. Each row corresponds to a specific generalized Bernard-LeClair (GBL) symmetry class, labeled by its name in the first column. The second column lists the symmetry generator relations, including the signs of time-flipping, operator involution, and commutation relations. The third column gives the classifying space of each symmetry class in the FO angle-gapless case, which is different from Table I. The topological numbers in the table are stable strong topological numbers.

GBL	Gen. Rel.	Cl	$d = 0$	1	2	3	4	5	6	7
Non		C_1	0	\mathbb{Z}	0	\mathbb{Z}	0	\mathbb{Z}	0	\mathbb{Z}
P		C_0	\mathbb{Z}	0	\mathbb{Z}	0	\mathbb{Z}	0	\mathbb{Z}	0
Qa	$\epsilon_q = 1$	C_1^2	0	$\mathbb{Z} \oplus \mathbb{Z}$	0	$\mathbb{Z} \oplus \mathbb{Z}$	0	$\mathbb{Z} \oplus \mathbb{Z}$	0	$\mathbb{Z} \oplus \mathbb{Z}$
Qb	$\epsilon_q = -1$	C_0	\mathbb{Z}	0	\mathbb{Z}	0	\mathbb{Z}	0	\mathbb{Z}	0
K1a	$\epsilon_k = 1, \eta_k = 1$	R_7	0	0	0	$2\mathbb{Z}$	0	\mathbb{Z}_2	\mathbb{Z}_2	\mathbb{Z}
K1b	$\epsilon_k = -1, \eta_k = 1$	R_1	\mathbb{Z}_2	\mathbb{Z}	0	0	0	$2\mathbb{Z}$	0	\mathbb{Z}_2
K2a	$\epsilon_k = 1, \eta_k = -1$	R_3	0	\mathbb{Z}_2	\mathbb{Z}_2	\mathbb{Z}	0	0	0	$2\mathbb{Z}$
K2b	$\epsilon_k = -1, \eta_k = -1$	R_5	0	$2\mathbb{Z}$	0	\mathbb{Z}_2	\mathbb{Z}_2	\mathbb{Z}	0	0
C1	$\epsilon_c = 1, \eta_c = 1$	R_7	0	0	0	$2\mathbb{Z}$	0	\mathbb{Z}_2	\mathbb{Z}_2	\mathbb{Z}
C2	$\epsilon_c = 1, \eta_c = -1$	R_3	0	\mathbb{Z}_2	\mathbb{Z}_2	\mathbb{Z}	0	0	0	$2\mathbb{Z}$
C3	$\epsilon_c = -1, \eta_c = 1$	R_1	\mathbb{Z}_2	\mathbb{Z}	0	0	0	$2\mathbb{Z}$	0	\mathbb{Z}_2
C4	$\epsilon_c = -1, \eta_c = -1$	R_5	0	$2\mathbb{Z}$	0	\mathbb{Z}_2	\mathbb{Z}_2	\mathbb{Z}	0	0
PQ1	$\epsilon_q = 1, \epsilon_{pq} = 1$	C_0^2	$\mathbb{Z} \oplus \mathbb{Z}$	0	$\mathbb{Z} \oplus \mathbb{Z}$	0	$\mathbb{Z} \oplus \mathbb{Z}$	0	$\mathbb{Z} \oplus \mathbb{Z}$	0
PQ2	$\epsilon_q = 1, \epsilon_{pq} = -1$	C_1	0	\mathbb{Z}	0	\mathbb{Z}	0	\mathbb{Z}	0	\mathbb{Z}
PK1	$\epsilon_k = 1, \eta_k = 1, \epsilon_{pk} = 1$	R_0	\mathbb{Z}	0	0	0	$2\mathbb{Z}$	0	\mathbb{Z}_2	\mathbb{Z}_2
PK2	$\epsilon_k = 1, \eta_k = -1, \epsilon_{pk} = 1$	R_4	$2\mathbb{Z}$	0	\mathbb{Z}_2	\mathbb{Z}_2	\mathbb{Z}	0	0	0
PK3a	$\epsilon_k = 1, \eta_k = 1, \epsilon_{pk} = -1$	R_6	0	0	$2\mathbb{Z}$	0	\mathbb{Z}_2	\mathbb{Z}_2	\mathbb{Z}	0
PK3b	$\epsilon_k = 1, \eta_k = -1, \epsilon_{pk} = -1$	R_2	\mathbb{Z}_2	\mathbb{Z}_2	\mathbb{Z}	0	0	0	$2\mathbb{Z}$	0
PC1	$\frac{\epsilon_c = 1, \eta_c = 1, \epsilon_{pc} = 1}{\epsilon_c = -1, \eta_c = 1, \epsilon_{pc} = 1}$	R_0	\mathbb{Z}	0	0	0	$2\mathbb{Z}$	0	\mathbb{Z}_2	\mathbb{Z}_2
PC2	$\frac{\epsilon_c = 1, \eta_c = 1, \epsilon_{pc} = -1}{\epsilon_c = -1, \eta_c = -1, \epsilon_{pc} = -1}$	R_6	0	0	$2\mathbb{Z}$	0	\mathbb{Z}_2	\mathbb{Z}_2	\mathbb{Z}	0
PC3	$\frac{\epsilon_c = 1, \eta_c = -1, \epsilon_{pc} = 1}{\epsilon_c = -1, \eta_c = -1, \epsilon_{pc} = 1}$	R_4	$2\mathbb{Z}$	0	\mathbb{Z}_2	\mathbb{Z}_2	\mathbb{Z}	0	0	0
PC4	$\frac{\epsilon_c = 1, \eta_c = -1, \epsilon_{pc} = -1}{\epsilon_c = -1, \eta_c = 1, \epsilon_{pc} = -1}$	R_2	\mathbb{Z}_2	\mathbb{Z}_2	\mathbb{Z}	0	0	0	$2\mathbb{Z}$	0
QC1a	$\epsilon_q = 1, \epsilon_c = 1, \eta_c = 1, \epsilon_{qc} = 1$	R_7^2	0	0	0	$2\mathbb{Z} \oplus 2\mathbb{Z}$	0	$\mathbb{Z}_2 \oplus \mathbb{Z}_2$	$\mathbb{Z}_2 \oplus \mathbb{Z}_2$	$\mathbb{Z} \oplus \mathbb{Z}$
QC1b	$\epsilon_q = -1, \epsilon_c = 1, \eta_c = 1, \epsilon_{qc} = 1$	R_0	\mathbb{Z}	0	0	0	$2\mathbb{Z}$	0	\mathbb{Z}_2	\mathbb{Z}_2
QC2a	$\epsilon_q = 1, \epsilon_c = 1, \eta_c = 1, \epsilon_{qc} = -1$	C_1	0	\mathbb{Z}	0	\mathbb{Z}	0	\mathbb{Z}	0	\mathbb{Z}
QC2b	$\epsilon_q = -1, \epsilon_c = 1, \eta_c = 1, \epsilon_{qc} = -1$	R_6	0	0	$2\mathbb{Z}$	0	\mathbb{Z}_2	\mathbb{Z}_2	\mathbb{Z}	0

continued on next page

IV. EXAMPLES OF FLOQUET NON-HERMITIAN TOPOLOGICAL PHASES

To get an intuitive understanding of our topological classification and the novel features of FNH topological phases, we demonstrate two explicit examples in this section. They correspond to the FO angle-gapped and FO angle-gapless cases, respectively. And we extract the physical meanings of the topological invariants.

A. FO angle-gapped topology

Let us consider a periodically driven two-dimensional honeycomb lattice, which contains two sublattices (denoted as A and B), as depicted in Fig. 2(a). The Floquet dynamics is implemented through a seven-step driving sequence, with each step described by a constant Hamiltonian H_j for time-lapse $n\tau + \frac{j-1}{7}\tau \leq t < n\tau + \frac{j}{7}\tau$ ($n \in \mathbb{Z}$, $j = 1, 2, \dots, 7$), τ is the driving period. The driving protocol is schematically shown in Fig. 2(b). The first three steps involve only nonreciprocal hoppings between the neighbouring A, B sites along three different edges, respectively. Their Hamiltonians are given by

$$\begin{aligned} H_1(\mathbf{k}) &= \begin{bmatrix} 0 & e^{g+i\mathbf{k}\cdot\mathbf{a}_1} \\ e^{-g-i\mathbf{k}\cdot\mathbf{a}_1} & 0 \end{bmatrix}; \\ H_2(\mathbf{k}) &= \begin{bmatrix} 0 & e^{-g+i\mathbf{k}\cdot\mathbf{a}_2} \\ e^{g-i\mathbf{k}\cdot\mathbf{a}_2} & 0 \end{bmatrix}; \\ H_3(\mathbf{k}) &= \begin{bmatrix} 0 & e^{-g+i\mathbf{k}\cdot\mathbf{a}_3} \\ e^{g-i\mathbf{k}\cdot\mathbf{a}_3} & 0 \end{bmatrix}, \end{aligned} \quad (44)$$

on the sublattice basis. Here $\mathbf{a}_1 = (-\frac{a}{2}, -\frac{a}{2\sqrt{3}})$, $\mathbf{a}_2 = (0, \frac{a}{\sqrt{3}})$, $\mathbf{a}_3 = (\frac{a}{2}, -\frac{a}{2\sqrt{3}})$, and $a = 1$ is the lattice constant. g is the nonreciprocal coefficient. When $g \neq 0$, the Hamiltonian is non-Hermitian. The next three steps repeat the first three steps, The final step is an onsite chemical potential term, i.e.,

$$H_4 = H_1, \quad H_5 = H_2, \quad H_6 = H_3, \quad H_7 = -V\sigma_z \quad (45)$$

Here σ_z is Pauli matrix. This model can be regarded as a non-Hermitian generalization of Kitagawa et al.'s model [101] and belongs to class Non in the GBL class.

We start from the ideal case with $V = 0$, $\tau = 3.5\pi$, and consider the motion of a single particle in the geometry depicted in Fig. 2(a). The Floquet dynamics are exactly solvable and depicted in Fig. 2(a). The bulk Floquet operator is $U(\mathbf{k}) = -\mathbb{I}$. An initial particle at the A site in bulk travels along the blue loci cyclically. And the particle returns to its initial position after one whole period. Similar, the particle at the bulk B site also returns to its initial position after one whole period. Thus, the bulk Floquet operator is trivial. The dynamics exhibit different behaviors on the edges. First, we consider the top edge. An initial particle located at B site moves along the edge towards the right (green arrow), and after one driving cycle, it passes through two unit cells. In comparison,

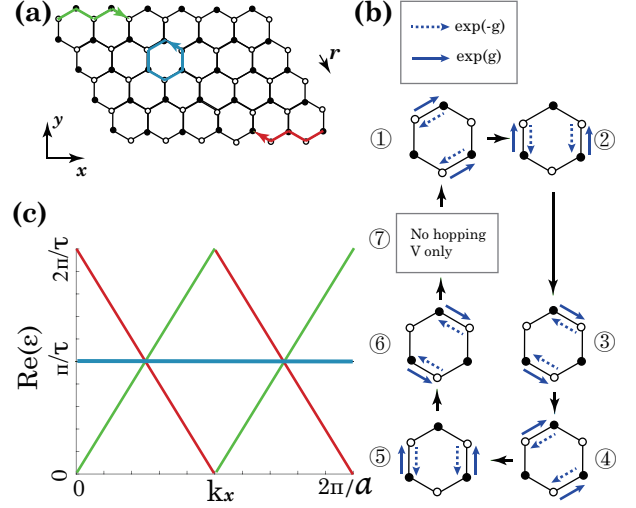


FIG. 2. Anomalous non-Hermitian edge modes on a two-dimensional Floquet driven honeycomb lattice. (a) Honeycomb lattice structure. Filled and open circles represent A and B sites, respectively. Red and green arrows depict the trajectories of a particle initially at the bottom edge A site and top edge B site in a driving period $t \in [0, \tau]$, respectively. A bulk particle follows the blue trajectory cyclically. (b) Driving protocol. In the first six steps, the spatially homogeneous hopping amplitudes are varied in a chiral way. In each step, only nonreciprocal hoppings along one specific bond are allowed. The dotted blue arrows and solid blue arrows denote hopping amplitudes e^{-g} and e^g , respectively. In the last step, the potential $-V$ and V are applied on the A and B lattice, respectively. (c) Quasienergy spectra (real part). The red and blue bands are for the chiral edge modes at the bottom and top zigzag edges, respectively; the flat bulk bands (blue) are pinned at $\epsilon = \pi/\tau$. The parameters are $V = 0$, $\tau = 3.5\pi$, and $g = \pi$.

an initial particle located at A site returns to itself. Second, we consider the bottom edge. An initial particle at A site moves along the bottom edge towards the left (red arrow) and passes through two unit cells after one driving cycle, while an initial particle at B site returns to itself. The topological edge modes at the top and bottom edge possess different imaginary quasienergies, which are also different from the imaginary quasienergies of the bulk modes. We can explicitly work out the edge dynamics of the ideal case. The effective Floquet Hamiltonians for the four edges are given by (up to $2\pi j/\tau$, $j \in \mathbb{Z}$)

$$\begin{aligned} \hat{H}_T &= \begin{bmatrix} \frac{-\pi}{\tau} & 0 \\ 0 & \frac{2k_x + 4gi}{\tau} \end{bmatrix}; \hat{H}_B = \begin{bmatrix} \frac{-2k_x + 4gi}{\tau} & 0 \\ 0 & \frac{-\pi}{\tau} \end{bmatrix}; \\ \hat{H}_L &= \begin{bmatrix} \frac{-2k_r}{\tau} & 0 \\ 0 & \frac{-\pi}{\tau} \end{bmatrix}; \hat{H}_R = \begin{bmatrix} \frac{-\pi}{\tau} & 0 \\ 0 & \frac{2k_r}{\tau} \end{bmatrix}. \end{aligned} \quad (46)$$

where T , B , L , and R refer to the top, bottom, left, and right edges, respectively. The k_x and k_r are the momenta along \mathbf{x} and \mathbf{r} directions labeled in Fig. 2(a).

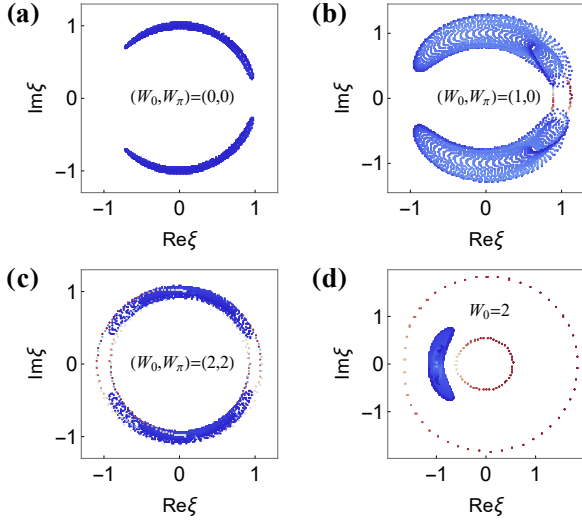


FIG. 3. Spectra of the Floquet operator for four topologically distinct FO angle-gapped phases. (a) $g = 0.01\pi$, $\tau = \pi$, and $V = 0.5\pi$. The $(W_0, W_\pi) = (0, 0)$ phase when both 0 and π FO angle gaps exist. (b) $g = 0.05\pi$, $\tau = \pi$, and $V = 0.05\pi$. The $(W_0, W_\pi) = (1, 0)$ phase with both 0 and π FO angle gaps. The colors represent the value of inverse partial ratio (IPR), which is defined as $\text{IPR} = (\sum_j |\psi_j|^4) / (\sum_j |\psi_j|^2)^2$, where j is the site index. The IPR clearly shows the appearance of edge states inside the 0 FO angle gap. (c) $g = 0.01\pi$, $\tau = 2.5\pi$, and $V = 0.5\pi$. The $(W_2, W_\pi) = (2, 2)$ phase with both 0 and π FO angle gaps. This is an anomalous Floquet phase with zero Chern number for each Floquet operator band. (d) $g = 0.05\pi$, $\tau = 3.2\pi$, and $V = 0.01\pi$. The $W_\pi = 2$ phase is unique to Floquet non-Hermitian system. There is only one FO angle gap at 0. The edge modes are fully detached from the bulk bands.

The quasienergy spectra of the above ideal case are illustrated in Fig. 2(c). Besides the flat bulk quasienergy bands located at π/τ , there exist two sets of chiral edge modes shown by the red and green lines. These edge modes describe the chiral motion on the top and bottom edges. The appearance of these edge modes in the π/τ real gap of the quasienergy spectra cannot be understood from the bulk Floquet Hamiltonian itself. These chiral edge states are intrinsically dynamical, and the system is in the Floquet anomalous topological phase. The dynamical topology can only be revealed from the time-evolution operator. According to Table I for the Non class, the topological invariant is $\mathbb{Z}^{\times n}$ with n the number of FO angle gaps. Formally, we can define the loop operator from $H_{F,\theta} = \frac{i}{\tau} \ln_{-\theta}[U(\mathbf{k})]$ as $U_{l,\theta} = U(\mathbf{k}, t) * e^{iH_{F,\theta}t}$, here $U(\mathbf{k}, t)$ is the time evolution operator of the system. The topological invariant defined for the loop operator is as follows:

$$W_\theta = \frac{1}{8\pi^2} \int_0^{2\pi} k_x \int_0^{2\pi} dk_y \int_0^\tau dt \times \text{Tr}(U_{l,\theta}^{-1} \partial_t U_{l,\theta} [U_{l,\theta}^{-1} \partial_{k_x} U_{l,\theta}, U_{l,\theta}^{-1} \partial_{k_y} U_{l,\theta}]). \quad (47)$$

W_θ is the so-called three-winding number in the

momentum-time space and directly gives the number of chiral edge modes located at the FO angle gap θ (equivalent to FH real gap θ/τ). For Fig. 2(c) case, $W_0 = 2$, which is consistent with the chiral motion across two unit cells in Fig. 2(a). There may exist multiple FO angle gaps when deviating from the ideal case. By tuning the parameters g , V , and T in this model, various FNH topological phases can appear. Let us consider four typical examples, with their spectra of the Floquet operator on the complex plane illustrated in Fig. 3. In Fig. 3(a), the spectra exhibit both 0 and π FO angle gaps. There is no topologically nontrivial edge state in these FO angle gaps, consistent with their topological invariants $(W_0, W_\pi) = (0, 0)$. By tuning parameters, the FO angle gap at 0 closes and further reopens, accompanied by the emergence of one chiral edge state (at the top edge) at the FO angle gap 0 as shown in Fig. 3(b). For this case, the topological invariants are $(W_0, W_\pi) = (1, 0)$. Fig. 3(c) depicts an anomalous case when the bulk Floquet Hamiltonian is topologically trivial. We can verify the Chern number for each Floquet operator band is zero. However, there exist both edge states inside the 0 and π FO angle gaps, dictated by topological invariants $(W_0, W_\pi) = (2, 2)$. In Fig. 3(d), we illustrate an unexpected case when there is no FO angle gap at π , and the Floquet operator possesses a FO angle gap at 0. The topological invariant for the FO angle gap 0 is $W_0 = 2$. Contrary to the general picture of boundary states connecting bulk bands in the two dimensional Hermitian topological phases, the two chiral edge states are fully detached from the bulk. They can be engineered independently without changing the bulk invariants. We emphasize that such a phase is intrinsic to Floquet non-Hermitian system and can be utilized, e.g., in boundary-state engineering in photonic waveguides [137].

B. FO angle-gapless topology

When the spectra of the Floquet operator enclose the origin without any FO angle gaps, the topology of the system is carried by its Floquet operator. We consider a one-dimensional two-band system with a two-step driving sequence generated by Hamiltonian \hat{H}_{o1} and \hat{H}_{o2} . The time-lapse of each step is $\tau/2$. The expressions of \hat{H}_{o1} and \hat{H}_{o2} are

$$\hat{H}_{o1} = -\frac{\pi}{\tau} \begin{bmatrix} 0 & e^{ik} \\ e^{-ik} & 0 \end{bmatrix}; \quad \hat{H}_{o2} = \frac{\pi}{\tau} \begin{bmatrix} 0 & e^g \\ e^{-g} & 0 \end{bmatrix}. \quad (48)$$

The Floquet operator $U(k) = e^{-iH_{o2}\tau/2} e^{-iH_{o1}\tau/2}$ is

$$U(k) = \begin{bmatrix} e^{-ik+g} & 0 \\ 0 & e^{ik-g} \end{bmatrix}. \quad (49)$$

This model can be regarded as a non-Hermitian generalization of Budich, Hu, and Zoller's model [151]. The system belongs to the Non class, and Floquet operator $U(k)$ is a reducible matrix. The quasienergy spectra of the Floquet Hamiltonian and the spectra of the

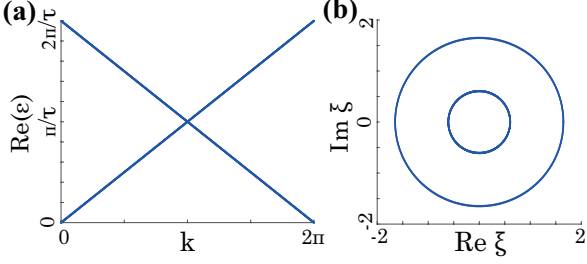


FIG. 4. Spectra of the FO angle-gapless system. (a) Quasienergy spectra (real part) with respect to momentum k . The two bands with opposite chirality wind around the quasienergy zone. (b) Spectra of the Floquet operator on the complex plane. The inner (outer) circle with winding number $W_{\pm} = \pm 1$ encloses the origin counter-clockwise (clockwise) by increasing k from 0 to 2π .

Floquet operator are depicted in Fig. 4(a) and (b), respectively. Due to the absence of the FO angle gap, the Floquet Hamiltonian bands (real part) wind around the quasienergy zone ($[0, 2\pi/\tau)$) and possess different imaginary parts (i.e., lifetimes). Such band structures only exist in Floquet driven systems and describe the chiral motions of opposite chirality. Each irreducible block ($U_+ := e^{-ik+g}$ and $U_- := e^{ik-g}$) is characterized by a winding number: $W_+ = \frac{i}{2\pi} \int_0^{2\pi} dk U_+^{-1} \partial_k U_+ = 1$ for U_+ and $W_- = \frac{i}{2\pi} \int_0^{2\pi} dk U_-^{-1} \partial_k U_- = -1$ for U_- . W_{\pm} corresponds to the number of right/left-moving chiral fermions in the Floquet Hamiltonian bands. Similarly, we can consider FO angle-gapless model in other dimensions. The above topological number in the FO angle gapless case gives rise to unidirectional topological charge pumping differs from the physical meaning of angle gapped topological number [138].

V. BOSONIC SYSTEMS

Our topological classification can be equally applied to the Floquet driving bosonic systems. Usually, the bosonic particle number is not conserved [152] in realistic experimental settings. Let us formally consider a generic tight-binding bosonic BdG-type Hamiltonian:

$$\hat{H}_b = \sum_{ij;\mu\nu} (h_{i\mu,j\nu} \hat{a}_{i\mu}^\dagger \hat{a}_{j\nu} + \frac{1}{2} \Delta_{i\mu,j\nu} \hat{a}_{i\mu}^\dagger \hat{a}_{j\nu}^\dagger + \frac{1}{2} \Delta_{i\mu,j\nu}^* \hat{a}_{i\mu} \hat{a}_{j\nu}). \quad (50)$$

Here $\hat{a}_{i\mu}^\dagger$ ($\hat{a}_{i\mu}$) is the creation (annihilation) operator of bosonic particles. i and μ label the unit cell and some internal degrees of freedom (e.g., spin, sublattice, or orbit), respectively. They satisfy the standard bosonic commutation relation $[\hat{a}_{i\mu}, \hat{a}_{j\nu}^\dagger] = \delta_{ij} \delta_{\mu\nu}$. $\Delta_{i\mu,j\nu} = \Delta_{j\nu,i\mu}$ is the pairing term. We define the two field operators: $\hat{\Psi} = (\hat{a}_{11}, \dots, \hat{a}_{1m}, \hat{a}_{21}, \dots, \hat{a}_{2m}, \dots, \hat{a}_{L1}, \dots, \hat{a}_{Lm})^T$,

and $\hat{\bar{\Psi}} = (\hat{a}_{11}^\dagger, \dots, \hat{a}_{1m}^\dagger, \hat{a}_{21}^\dagger, \dots, \hat{a}_{2m}^\dagger, \dots, \hat{a}_{L1}^\dagger, \dots, \hat{a}_{Lm}^\dagger)^T$. The Heisenberg equation of motion of the system is

$$\frac{d}{dt} \begin{pmatrix} \hat{\Psi} \\ \hat{\bar{\Psi}} \end{pmatrix} = -iM(t) \begin{pmatrix} \hat{\Psi} \\ \hat{\bar{\Psi}} \end{pmatrix}, \quad (51)$$

where

$$M(t) := \begin{pmatrix} h & \Delta \\ -\Delta^* & -h^T \end{pmatrix}. \quad (52)$$

The single-particle Hamiltonian h can be either Hermitian or non-Hermitian. The dynamics of the bosonic system are fully governed by the M matrices. M plays a similar role as the time-dependent Hamiltonian in the fermionic system. The topological classification of the bosonic system is for the $M(t)$ matrix, and our conclusions of FNH symmetry and topology can be directly applied. Specifically, for a Hermitian H_b with BdG pairing, the M matrix fulfills $\tau_x M(t) \tau_x = -M^*(t)$, $\tau_z M(t) \tau_z = M^\dagger(t)$ and $\tau_y M(t) \tau_y = -M^T(t)$. Thus, the $M(t)$ belongs to the GBL class QC8a. According to Table I, the topological invariant for the bosonic system in even (odd) dimensions is \mathbb{Z}^{n_p} (0) if the system is FO angle-gapped. Here $n_p = 1$ if there is only one FO angle gap at 0 or π , and $n_p = 2$ if there exist both 0 and π FO angle gaps. According to Table II, the topological invariant for the bosonic system in even (odd) dimensions is 0 (\mathbb{Z}) if the system is FO angle-gapless. In the following, we consider two representative examples to illustrate our classifications for the bosonic systems. One is a two-dimensional Floquet bosonic topological superconductor with FO angle gaps, which hosts anomalous Floquet bosonic edge modes without any static counterparts. The other one is a one-dimensional Floquet bosonic system without any FO angle gap, which can exhibit nontrivial spectral windings.

First example: FO angle-gapped bosonic system. We consider a similar driving protocol as in Fig. 2(a) on a bosonic honeycomb lattice, with bosons on neighbouring sites paired together. There are seven driven steps, each step determined by driven time $\tau/7$ and a static Hamiltonian. Written on the sublattice and BdG basis, the static Hamiltonian for each step is

$$\begin{aligned} \hat{H}_{bj} = \sum_{\mathbf{k}} \left[\begin{pmatrix} a_{\mathbf{k}A}^\dagger & a_{\mathbf{k}B}^\dagger \end{pmatrix} H_j(\mathbf{k}) \begin{pmatrix} a_{\mathbf{k}A} \\ a_{\mathbf{k}B} \end{pmatrix} \right. \\ \left. + \begin{pmatrix} a_{\mathbf{k}A}^\dagger & a_{\mathbf{k}B}^\dagger \end{pmatrix} \Delta(\mathbf{k}) \begin{pmatrix} a_{\mathbf{k}A}^\dagger \\ a_{\mathbf{k}B}^\dagger \end{pmatrix} \right. \\ \left. + \begin{pmatrix} a_{\mathbf{k}A} & a_{\mathbf{k}B} \end{pmatrix} \Delta^\dagger(\mathbf{k}) \begin{pmatrix} a_{\mathbf{k}A} \\ a_{\mathbf{k}B} \end{pmatrix} \right]. \end{aligned} \quad (53)$$

Here $H_j(\mathbf{k})$ is given by Eqs. (44) and (45), and $g = 0$ in these equations. $\Delta(\mathbf{k}) = \Delta_0 \sigma_0$, and Δ_0 is a complex number. The field operators are denoted by $\hat{\Psi} = (a_{\mathbf{k}A}, a_{\mathbf{k}B})^T$ and $\hat{\bar{\Psi}} = (a_{\mathbf{k}A}^\dagger, a_{\mathbf{k}B}^\dagger)^T$. When $\Delta_0 = 0$, the model reduces to the bosonic version of the model in Sec.

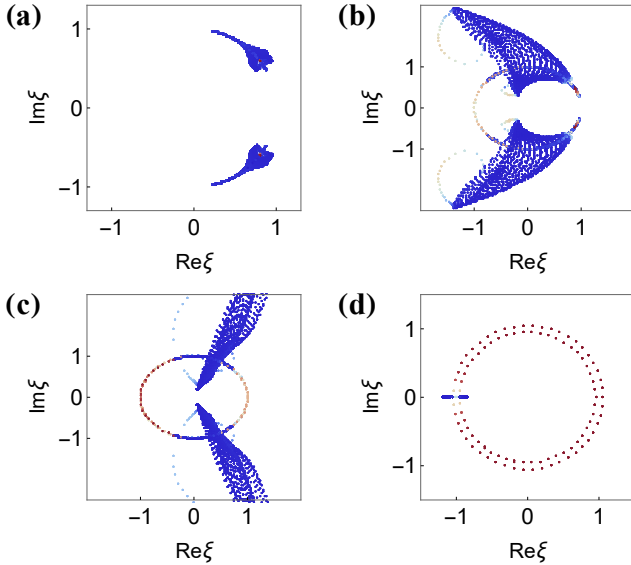


FIG. 5. Spectra of the M matrix's Floquet operator for four distinct FO angle-gapped bosonic topological phases. (a) $\Delta_1 = 0.1\pi$, $\tau = 0.5\pi$, and $V = \pi$. The $(W_0, W_\pi) = (0, 0)$ phase when both 0 and π FO angle gaps exist. (b) $\Delta_1 = 0.1\pi$, $\tau = 1.7\pi$, and $V = \pi$. The $(W_0, W_\pi) = (0, 2)$ phase with both 0 and π FO angle gaps. (c) $\Delta_1 = 0.1\pi$, $\tau = 3\pi$, and $V = \pi$. The $(W_2, W_\pi) = (4, 4)$ phase with both 0 and π FO angle gaps. It is an anomalous Floquet phase with zero Chern number for each Floquet operator band. (d) $\Delta_0 = 0.01\pi$, $\tau = 3.5\pi$, and $V = 0$. The $W_0 = 4$ phase is unique to Floquet non-Hermitian system. There is only one FO angle gap at 0. The edge modes are detached from the bulk bands. The colors represent the value of IPR, which clearly shows the appearance of edge states.

IV A. For the generic case with $\Delta_0 \neq 0$, the Floquet dynamics is described by the M matrix in Eq. (52).

Similar to the fermionic case, we can discuss the spectra and topological invariants of the M matrix. The system exhibits various topological phases by tuning the parameters Δ_0 , V , and τ . Figs. 5(a)-(d) depict the spectra of the M matrix's Floquet operator for four typical phases. Their topological invariants (W_0, W_π) are $(0, 0)$, $(0, 2)$, $(4, 4)$, and $(4, \text{undefined})$, respectively. The third case shown in Fig. 5(c) is dynamically anomalous, i.e., the bulk Chern number of each Floquet operator band is zero, yet with the appearance of edge states. For the fourth case shown in Fig. 5(d), there is only one FO angle gap at 0, and the topological invariant W_π is ill-defined due to the lack of a branch cut at the π FO angle gap. It is different from the fermionic Non class. Firstly, the M matrix's FO angle gaps, if any, must be pinned at either 0 or π or pairs at $(\theta_m, -\theta_m)$, compared to the fermionic Non class where the FO angle gap can be tuned anywhere. It is due to the additional symmetry constraints on the M matrix. Secondly, The topological invariants for the bosonic system are doubled due to the existence of BdG pairing.

Second example: FO angle-gapless bosonic system. We

consider a two equal-step driving sequence described by Hermitian Hamiltonian $H_{bo1} = -\frac{\pi}{\tau}\tau_0 \otimes [\cos(k)\sigma_x - \sin(k)\sigma_y]$, and

$$H_{bo2}(k) = \frac{\pi}{\tau}(\tau_0 \otimes \sigma_x + \Delta_1\tau_x \otimes \sigma_z) \quad (54)$$

Here τ_0 is a 2×2 identity matrix, $\tau_{x,y,z}$ are the Pauli matrices in the particle-hole space. Δ_1 is the real pairing amplitude. It is easy to check the M matrix of each step for this bosonic system is $M_{boj} = (\tau_z \otimes \sigma_0)H_{Boj}$ ($j = 1, 2$). The Floquet operator of M matrices is $U_{bo}(k, \tau) = e^{-iM_{bo2}\frac{\tau}{2}}e^{-iM_{bo1}\frac{\tau}{2}} = e^{-ik\tau_0 \otimes \sigma_z + \frac{\pi\Delta_1}{2}\tau_y \otimes \sigma_z}$. The M matrices' Floquet operator is reducible into four irreducible sub-blocks: $U_1 = e^{-ik - \pi\Delta_1/2}$, $U_2 = e^{-ik + \pi\Delta_1/2}$, $U_3 = e^{ik + \pi\Delta_1/2}$, and $U_4 = e^{ik - \pi\Delta_1/2}$. The corresponding M matrices' Floquet Hamiltonians for the four blocks are $\frac{1}{\tau}(\pm k \pm i\frac{\pi\Delta_1}{2})$. They describe the chiral bosonic modes, where the pairing term contributes to the lifetime of these modes. For each block, we can define an integer winding number as $W_m = \frac{i}{2\pi} \int_0^{2\pi} dk U_m^{-1} \partial_k U_m$ ($m = 1, 2, 3, 4$). It follows that $W_1 = W_2 = 1$ and $W_3 = W_4 = -1$. The number and chirality of each chiral bosonic mode are given by $|W_m|$ and the sign of W_m , respectively.

VI. CONCLUSIONS

In summary, we have developed a comprehensive classification of FNH topological phases using the K -theory based on the internal symmetries of the system and the FO angle gaps. We have demonstrated there exist 54 distinct GBL classes for time-dependent non-Hermitian Hamiltonians. We have obtained two periodic tables for the FO angle-gapped and FO angle-gapless FNH topological phases, respectively. Our scheme fully covers the previous topological classifications of Floquet Hermitian topological insulators and Floquet unitaries. Our classification can also be utilized to characterize the Floquet topological phases of bosonic systems. We have unveiled the physical meanings and consequences of the topological invariants through explicit examples, like the appearance of edge states in the FO angle gaps and charge transport.

Our topological classification of the FNH topological phase is based on the periodic boundary condition or Bloch Hamiltonian. According to the previous study of the topological classification of static non-Hermitian systems, the conclusions of topological classification don't change when the periodic boundary condition is transformed into the open boundary condition. The topological phase transition points may change due to the non-Hermitian skin effect. To recover the topological phase transition points, we can use non-Bloch band theory [75], biorthogonal bulk-boundary correspondence [76], or real space topological number [153]. Similarly, we think our results of topological classification don't change when the periodic boundary condition is transformed into the open boundary condition. We may need to use non-Bloch band

theory, biorthogonal bulk-boundary correspondence, or real space topological number to define the topological number in the open boundary condition when there is the non-Hermitian skin effect.

Our framework, together with the previous AZ tenfold way of static Hermitian topological phases [114–120], Roy and Harper’s periodic table of Floquet Hermitian topological insulators, [104] and Higashikawa, Nakagawa, and Ueda’s periodic table of Floquet unitaries [148] and the most recent classifications of static non-Hermitian Hamiltonians [14, 127–131], hence completes the whole classification map based on the internal symmetries. Our scheme may be extended to include other types of symmetries, e.g., crystalline symmetries [117, 118, 131, 156], and to higher-order Floquet topological phases [108–113]. Our scheme should be readily extended to include defects by changing $H(\mathbf{k}, t)$ to $H(\mathbf{k}, \mathbf{r}, t)$ [130], and include Floquet dislocation-induced non-Hermitian skin effect by discussing the wave function of H_F [154, 155]. Beyond its immediate significance for understanding the various topological phases unique to Floquet and non-Hermitian systems, our scheme should open a broad avenue to explore the novel dynamical phenomena and topological effects originating from the interplay of non-Hermiticity, topology, and Floquet engineering and further guide the experimental design and application in atomic and photonic systems.

ACKNOWLEDGMENTS

The work is supported by the NSFC under Grants No.12174436 and No.11974413 and the Strategic Priority Research Program of Chinese Academy of Sciences under Grant No. XDB33000000.

Appendix A: A full counting of the GBL classes

In this section, we give the details of the full count of the GBL classes. We need to count all possible group structures generated by Eqs. (6)-(9). From that the Hamiltonian is irreducible, we can get that $p^2 = \mathbb{I}, q^2 = \mathbb{I}, cc^* = \pm\mathbb{I}$, and $kk^* = \pm\mathbb{I}$. From the P, Q, C, and K commute with each other, we can get Eq. (14). And we can prove the following three propositions,

Proposition 1: If there are P and Q symmetry, we can define another Q-type symmetry labeled as Q' with $\epsilon_q =$

$-\epsilon_{q'}$.

Proposition 2: If there are P and C symmetry, we can define another C-type symmetry labeled as C' with $\epsilon_c = -\epsilon_{c'}$.

Proposition 3: If there are P and K symmetry, we can define another K-type symmetry labeled as K' with $\epsilon_k = -\epsilon_{k'}$.

The proof of Proposition 1: The system has Q and P symmetries, then it satisfies Eqs. (7) and (9). Then we can get that,

$$\begin{aligned} H(\mathbf{k}, t) &= \epsilon_q q H^\dagger(\mathbf{k}, \epsilon_q t) q^{-1} \\ &= \epsilon_q q [-p H(\mathbf{k}, -\epsilon_q t) p^{-1}]^\dagger q^{-1} \\ &= -\epsilon_q q p H^\dagger(\mathbf{k}, -\epsilon_q t) (q p)^{-1} \end{aligned} \quad (\text{A1})$$

According to Eq. (A1), we can define another type-Q symmetry, and we label it as Q' and $\epsilon_{q'} = -\epsilon_q, q' = \sqrt{\epsilon_{pq}} q p$. Thus, we get the proof of Propositions 1. Similarly, we can prove Propositions 2 and 3.

According to Propositions 1, 2, and 3, if the system has type-P symmetry, we can fix $\epsilon_q = \epsilon_c = \epsilon_k = 1$. To count all possible group structures, we should consider all possible situations:

- (1) When there is no symmetry, the number of group structures is 1.
- (2) When there is only type-P symmetry, the number of group structures is 1.
- (3) When there are only type-P and type-Q symmetries, we can fix $\epsilon_q = 1, \epsilon_{pq} = \pm 1$, the number of group structures is $2^1 = 2$.
- (4) When there are only type-P, type-Q, and type-C symmetries, we can fix $\epsilon_q = \epsilon_c = 1, \eta_c, \epsilon_{pq}, \epsilon_{pc}, \epsilon_{qc} = \pm 1$, the number of group structure is $2^4 = 16$.

Similarly, when there is only type-Q symmetry, the number of group structures is 2. When there is only type-C symmetry, the number of group structures is 4. When there is only type-K symmetry, the number of group structures is 4. When there are only type-P and type-C symmetries, the number of group structures is 4. When there are only type-P and type-K symmetries, the number of group structures is 4. When there are only type-C and type-Q symmetries, the number of group structures is 16. We summarize these conclusions in Table III. Adding all numbers of group structures of different situations, $1 + 1 + 2 + 4 + 4 + 2 + 4 + 4 + 16 + 16 = 54$. Thus, the total number of group structures is 54.

TABLE III. Counting all possible group structures generated by Eqs. (6)-(9).

System's symmetries	The variable can be ± 1	Number of group structure
Non		1
P		1
Q	ϵ_q	$2^1 = 2$
C	ϵ_c, η_c	$2^2 = 4$
K	ϵ_k, η_k	$2^2 = 4$
P,Q	ϵ_{pq}	$2^1 = 2$
P,C	η_c, ϵ_{pc}	$2^2 = 4$
P,K	η_k, ϵ_{pk}	$2^2 = 4$
Q,C	$\epsilon_q, \epsilon_c, \eta_c, \epsilon_{qc}$	$2^4 = 16$
P,Q,C	$\eta_c, \epsilon_{pc}, \epsilon_{pk}, \epsilon_{qc}$	$2^4 = 16$

Appendix B: Derivation of Eqs. (15)-(18) from Eqs. (10)-(13)

In the following, we derive the symmetry transformations on the time-evolution operator $U(\mathbf{k}, t)$ [Eqs. (15)-(18)] from the symmetry transformations on the time-dependent Hamiltonian $H(\mathbf{k}, t)$ [Eqs. (10)-(13)].

1.a. From $H(\mathbf{k}, t) = kH^*(-\mathbf{k}, -t)k^{-1}$ to $U^*(-\mathbf{k}, -t) = k^{-1}U(\mathbf{k}, t)k$.

$$\begin{aligned}
k^{-1}U(\mathbf{k}, t)k &= [1 - i\Delta tk^{-1}H(\mathbf{k}, t)k][1 - i\Delta tk^{-1}H(\mathbf{k}, t - \Delta t)k] \dots [1 - i\Delta tk^{-1}H(\mathbf{k}, \Delta t)k] \\
&= [1 - i\Delta tH^*(-\mathbf{k}, -t)][1 - i\Delta tH^*(-\mathbf{k}, -t + \Delta t)] \dots [1 - i\Delta tH^*(-\mathbf{k}, -\Delta t)] \\
&= \{[1 - i\Delta tH(-\mathbf{k}, -\Delta t)] \dots [1 - i\Delta tH(-\mathbf{k}, -t + \Delta t)][1 - i\Delta tH(-\mathbf{k}, -t)]\}^{-1*} \\
&= [U^*(-\mathbf{k}, 0, -t)]^{-1} \\
&= U^*(-\mathbf{k}, -t).
\end{aligned} \tag{B1}$$

1.b. From $H(\mathbf{k}, t) = -kH^*(-\mathbf{k}, t)k^{-1}$ to $U^*(-\mathbf{k}, t) = k^{-1}U(\mathbf{k}, t)k$.

$$\begin{aligned}
k^{-1}U(\mathbf{k}, t)k &= [1 - i\Delta tk^{-1}H(\mathbf{k}, t)k][1 - i\Delta tk^{-1}H(\mathbf{k}, t - \Delta t)k] \dots [1 - i\Delta tk^{-1}H(\mathbf{k}, \Delta t)k] \\
&= [1 + i\Delta tH^*(-\mathbf{k}, t)][1 + i\Delta tH^*(-\mathbf{k}, t - \Delta t)] \dots [1 + i\Delta tH^*(-\mathbf{k}, \Delta t)] \\
&= \{[1 - i\Delta tH(-\mathbf{k}, t)][1 - i\Delta tH(-\mathbf{k}, t - \Delta t)] \dots [1 - i\Delta tH(-\mathbf{k}, \Delta t)]\}^* \\
&= U^*(-\mathbf{k}, t).
\end{aligned} \tag{B2}$$

2.a. From $H(\mathbf{k}, t) = qH^\dagger(\mathbf{k}, t)q^{-1}$ to $[U^\dagger(\mathbf{k}, t)]^{-1} = q^{-1}U(\mathbf{k}, t)q$.

$$\begin{aligned}
q^{-1}U(\mathbf{k}, t)q &= [1 - i\Delta tq^{-1}H(\mathbf{k}, t)q][1 - i\Delta tq^{-1}H(\mathbf{k}, t - \Delta t)q] \dots [1 - i\Delta tq^{-1}H(\mathbf{k}, \Delta t)q] \\
&= [1 - i\Delta tH^\dagger(\mathbf{k}, t)][1 - i\Delta tH^\dagger(\mathbf{k}, t - \Delta t)] \dots [1 - i\Delta tH^\dagger(\mathbf{k}, \Delta t)] \\
&= \{[1 - i\Delta tH(\mathbf{k}, t)][1 - i\Delta tH(\mathbf{k}, t - \Delta t)] \dots [1 - i\Delta tH(\mathbf{k}, \Delta t)]\}^{\dagger-1} \\
&= [U^\dagger(\mathbf{k}, t)]^{-1}.
\end{aligned} \tag{B3}$$

2.b. From $H(\mathbf{k}, t) = -qH^\dagger(\mathbf{k}, -t)q^{-1}$ to $[U^\dagger(\mathbf{k}, -t)]^{-1} = q^{-1}U(\mathbf{k}, t)q$.

$$\begin{aligned}
q^{-1}U(\mathbf{k}, t)q &= [1 - i\Delta tq^{-1}H(\mathbf{k}, t)q][1 - i\Delta tq^{-1}H(\mathbf{k}, t - \Delta t)q] \dots [1 - i\Delta tq^{-1}H(\mathbf{k}, \Delta t)q] \\
&= [1 + i\Delta tH^\dagger(\mathbf{k}, -t)][1 + i\Delta tH^\dagger(\mathbf{k}, -t + \Delta t)] \dots [1 + i\Delta tH^\dagger(\mathbf{k}, -\Delta t)] \\
&= \{[1 - i\Delta tH(\mathbf{k}, -\Delta t)] \dots [1 - i\Delta tH(\mathbf{k}, -t + \Delta t)][1 - i\Delta tH(\mathbf{k}, -t)]\}^\dagger \\
&= [U(\mathbf{k}, 0, -t)]^\dagger \\
&= [U^\dagger(\mathbf{k}, -t)]^{-1}.
\end{aligned} \tag{B4}$$

3.a. From $H(\mathbf{k}, t) = -cH^\mathbf{T}(-\mathbf{k}, t)c^{-1}$ to $[U^\mathbf{T}(-\mathbf{k}, t)]^{-1} = c^{-1}U(\mathbf{k}, t)c$.

$$\begin{aligned}
c^{-1}U(\mathbf{k}, t)c &= [1 - i\Delta tc^{-1}H(\mathbf{k}, t)c][1 - i\Delta tc^{-1}H(\mathbf{k}, t - \Delta t)c] \dots [1 - i\Delta tc^{-1}H(\mathbf{k}, \Delta t)c] \\
&= [1 + i\Delta tH^\mathbf{T}(-\mathbf{k}, t)][1 + i\Delta tH^\mathbf{T}(-\mathbf{k}, t - \Delta t)] \dots [1 + i\Delta tH^\mathbf{T}(-\mathbf{k}, \Delta t)] \\
&= \{[1 - i\Delta tH(-\mathbf{k}, t)][1 - i\Delta tH(-\mathbf{k}, t - \Delta t)] \dots [1 - i\Delta tH(-\mathbf{k}, \Delta t)]\}^{-1\mathbf{T}} \\
&= [U^\mathbf{T}(-\mathbf{k}, t)]^{-1}.
\end{aligned} \tag{B5}$$

3.b. From $H(\mathbf{k}, t) = cH^{\mathbf{T}}(-\mathbf{k}, -t)c^{-1}$ to $[U^{\mathbf{T}}(-\mathbf{k}, -t)]^{-1} = c^{-1}U(\mathbf{k}, t)c$.

$$\begin{aligned}
c^{-1}U(\mathbf{k}, t)c &= [1 - i\Delta tc^{-1}H(\mathbf{k}, t)c][1 - i\Delta tc^{-1}H(\mathbf{k}, t - \Delta t)c] \dots [1 - i\Delta tc^{-1}H(\mathbf{k}, \Delta t)c] \\
&= [1 - i\Delta tH^{\mathbf{T}}(-\mathbf{k}, -t)][1 - i\Delta tH^{\mathbf{T}}(-\mathbf{k}, -t + \Delta t)] \dots [1 - i\Delta tH^{\mathbf{T}}(-\mathbf{k}, -\Delta t)] \\
&= \{[1 - i\Delta tH(-\mathbf{k}, -\Delta t)] \dots [1 - i\Delta tH(-\mathbf{k}, -t + \Delta t)][1 - i\Delta tH(-\mathbf{k}, -t)]\}^{\mathbf{T}} \\
&= [U^{\mathbf{T}}(-\mathbf{k}, 0, -t)] \\
&= [U^{\mathbf{T}}(-\mathbf{k}, -t)]^{-1}.
\end{aligned} \tag{B6}$$

4. From $H(\mathbf{k}, t) = -pH(\mathbf{k}, -t)p^{-1}$ to $U(\mathbf{k}, -t) = p^{-1}U(\mathbf{k}, t)p$.

$$\begin{aligned}
p^{-1}U(\mathbf{k}, t)p &= [1 - i\Delta tp^{-1}H(\mathbf{k}, t)p][1 - i\Delta tp^{-1}H(\mathbf{k}, t - \Delta t)p] \dots [1 - i\Delta tp^{-1}H(\mathbf{k}, \Delta t)p] \\
&= [1 + i\Delta tH(\mathbf{k}, -t)][1 + i\Delta tH(\mathbf{k}, -t + \Delta t)] \dots [1 + i\Delta tH(\mathbf{k}, -\Delta t)] \\
&= \{[1 - i\Delta tH(\mathbf{k}, -\Delta t)] \dots [1 - i\Delta tH(\mathbf{k}, -t + \Delta t)][1 - i\Delta tH(\mathbf{k}, -t)]\}^{-1} \\
&= [U(\mathbf{k}, 0, -t)]^{-1} \\
&= U(\mathbf{k}, -t).
\end{aligned} \tag{B7}$$

Appendix C: Derivation of Eqs. (20)-(23) from Eqs. (15)-(18)

First, we need to show:

Lemma 3. $U(\mathbf{k}, \epsilon\tau) = [U(\mathbf{k})]^{\epsilon}$, where $\epsilon = \pm 1$.

Proof: $\epsilon = 1$ is obvious. If $\epsilon = -1$. We have,

$$\begin{aligned}
U(\mathbf{k}, -\tau) &= U(\mathbf{k}, -\tau, 0) \\
&= U(\mathbf{k}, 0, \tau) \\
&= [U(\mathbf{k}, \tau, 0)]^{-1} \\
&= [U(\mathbf{k})]^{-1}.
\end{aligned} \tag{C1}$$

1. From $U^*(-\mathbf{k}, -t) = k^{-1}U(\mathbf{k}, \epsilon_k t)k$ to $[U^*(-\mathbf{k})]^{-\epsilon_k} = k^{-1}U(\mathbf{k})k$. First, we have $U^*(-\mathbf{k}, -\tau) = k^{-1}U(\mathbf{k}, \epsilon_k \tau)k$. Thus,

$$\begin{aligned}
&[U^*(-\mathbf{k})]^{-\epsilon_k} \\
&= [U^*(-\mathbf{k}, -\tau)]^{\epsilon_k} \\
&= [k^{-1}U(\mathbf{k}, \epsilon_k \tau)k]^{\epsilon_k} \\
&= \{k^{-1}[U(\mathbf{k})]^{\epsilon_k}k\}^{\epsilon_k} \\
&= k^{-1}U(\mathbf{k})k.
\end{aligned} \tag{C2}$$

2. From $[U^{\dagger}(\mathbf{k}, t)]^{-1} = q^{-1}U(\mathbf{k}, \epsilon_q t)q$ to $[U^{\dagger}(\mathbf{k})]^{-\epsilon_q} = q^{-1}U(\mathbf{k})q$. First, we have $[U^{\dagger}(\mathbf{k}, \tau)]^{-1} = q^{-1}U(\mathbf{k}, \epsilon_q \tau)q$. Thus,

$$\begin{aligned}
&[U^{\dagger}(\mathbf{k})]^{-\epsilon_q} \\
&= [U^{\dagger}(\mathbf{k}, \tau)]^{-\epsilon_q} \\
&= [q^{-1}U(\mathbf{k}, \epsilon_q \tau)q]^{\epsilon_q} \\
&= \{q^{-1}[U(\mathbf{k}, \tau)]^{\epsilon_q}q\}^{\epsilon_q} \\
&= q^{-1}U(\mathbf{k}, \tau)q.
\end{aligned} \tag{C3}$$

3. From $[U^{\mathbf{T}}(-\mathbf{k}, t)]^{-1} = c^{-1}U(\mathbf{k}, -\epsilon_c t)c$ to $[U^{\mathbf{T}}(-\mathbf{k})]^{\epsilon_c} = c^{-1}U(\mathbf{k})c$. First, we have $[U^{\mathbf{T}}(-\mathbf{k}, \tau)]^{-1} =$

$c^{-1}U(\mathbf{k}, -\epsilon_c \tau)c$. Thus,

$$\begin{aligned}
&[U^{\mathbf{T}}(-\mathbf{k})]^{\epsilon_c} \\
&= [U^{\mathbf{T}}(-\mathbf{k}, \tau)]^{\epsilon_c} \\
&= [c^{-1}U(\mathbf{k}, -\epsilon_c \tau)c]^{-\epsilon_c} \\
&= \{c^{-1}[U(\mathbf{k}, \tau)]^{-\epsilon_c}c\}^{-\epsilon_c} \\
&= c^{-1}U(\mathbf{k}, \tau)c.
\end{aligned} \tag{C4}$$

4. From $U(\mathbf{k}, -t) = p^{-1}U(\mathbf{k}, t)p$ to $[U(\mathbf{k})]^{-1} = p^{-1}U(\mathbf{k})p$. First, we have $U(\mathbf{k}, -\tau) = p^{-1}U(\mathbf{k}, \tau)p$. Thus,

$$\begin{aligned}
&[U(\mathbf{k})]^{-1} \\
&= U(\mathbf{k}, -\tau) \\
&= p^{-1}U(\mathbf{k}, \tau)p \\
&= p^{-1}U(\mathbf{k})p.
\end{aligned} \tag{C5}$$

Appendix D: Proof of Lemma 1

Lemma 1 states that the composition of two time-evolution generated by Hamiltonian $H_1(\mathbf{k}, t)$ and $H_2(\mathbf{k}, t)$ does not alter the underlying symmetry class. Here we consider all the four symmetries K, Q, C, P and denote the composition as $H(\mathbf{k}, t) = H_1 * H_2$.

1. K symmetry with $\epsilon_k = 1$. We have $H_1(\mathbf{k}, t) = kH_1^*(-\mathbf{k}, -t)k^{-1}$ and $H_2(\mathbf{k}, t) = kH_2^*(-\mathbf{k}, -t)k^{-1}$. We need to derive $H(\mathbf{k}, t) = kH^*(-\mathbf{k}, -t)k^{-1}$. The conditions are equivalent to $H_1(-\mathbf{k}, -t) = kH_1^*(\mathbf{k}, t)k^{-1}$ and $H_2(-\mathbf{k}, -t) = kH_2^*(\mathbf{k}, t)k^{-1}$.

1a. When $0 \leq t \leq \tau/4$,

$$\begin{aligned}
&kH^*(\mathbf{k}, t)k^{-1} \\
&= kH_2^*(\mathbf{k}, 2t)k^{-1} \\
&= H_2(-\mathbf{k}, -2t),
\end{aligned} \tag{D1}$$

$$\begin{aligned}
& H(-\mathbf{k}, -t) \\
& = H(-\mathbf{k}, \tau - t) \\
& = H_2(-\mathbf{k}, 2\tau - 2t - \tau) \\
& = H_2(-\mathbf{k}, -2t),
\end{aligned} \tag{D2}$$

Thus, $kH^*(\mathbf{k}, t)k^{-1} = H(-\mathbf{k}, -t)$.

1b. When $\tau/4 < t < 3\tau/4$,

$$\begin{aligned}
& kH^*(\mathbf{k}, t)k^{-1} \\
& = kH_1^*(\mathbf{k}, 2t - \tau/2)k^{-1} \\
& = H_1(-\mathbf{k}, \tau/2 - 2t),
\end{aligned} \tag{D3}$$

$$\begin{aligned}
& H(-\mathbf{k}, -t) \\
& = H(-\mathbf{k}, \tau - t) \\
& = H_1(-\mathbf{k}, 2\tau - 2t - \tau/2) \\
& = H_1(-\mathbf{k}, \tau/2 - 2t),
\end{aligned} \tag{D4}$$

Thus, $kH^*(\mathbf{k}, t)k^{-1} = H(-\mathbf{k}, -t)$.

1c. When $3\tau/4 \leq t \leq \tau$,

$$\begin{aligned}
& kH^*(\mathbf{k}, t)k^{-1} \\
& = kH_2^*(\mathbf{k}, 2t - \tau)k^{-1} \\
& = H_2(-\mathbf{k}, \tau - 2t),
\end{aligned} \tag{D5}$$

$$\begin{aligned}
& H(-\mathbf{k}, -t) \\
& = H(-\mathbf{k}, \tau - t) \\
& = H_2(-\mathbf{k}, 2\tau - 2t) \\
& = H_2(-\mathbf{k}, \tau - 2t),
\end{aligned} \tag{D6}$$

Thus, $kH^*(\mathbf{k}, t)k^{-1} = H(-\mathbf{k}, -t)$

2. K symmetry with $\epsilon_k = -1$. From $H_1(\mathbf{k}, t) = -kH_1^*(-\mathbf{k}, t)k^{-1}$ and $H_2(\mathbf{k}, t) = -kH_2^*(-\mathbf{k}, t)k^{-1}$ to $H(\mathbf{k}, t) = -kH^*(-\mathbf{k}, t)k^{-1}$.

2a. When $0 \leq t \leq \tau/4$,

$$\begin{aligned}
& -kH^*(-\mathbf{k}, t)k^{-1} \\
& = -kH_2^*(-\mathbf{k}, 2t)k^{-1} \\
& = H_2(\mathbf{k}, 2t) \\
& = H(\mathbf{k}, t),
\end{aligned} \tag{D7}$$

Thus, $-kH^*(-\mathbf{k}, t)k^{-1} = H(\mathbf{k}, t)$.

2b. When $\tau/4 < t < 3\tau/4$,

$$\begin{aligned}
& -kH^*(-\mathbf{k}, t)k^{-1} \\
& = -kH_1^*(-\mathbf{k}, 2t - \tau/2)k^{-1} \\
& = H_1(\mathbf{k}, 2t - \tau/2) \\
& = H(\mathbf{k}, t),
\end{aligned} \tag{D8}$$

Thus, $-kH^*(-\mathbf{k}, t)k^{-1} = H(\mathbf{k}, t)$.

2c. When $3\tau/4 \leq t \leq \tau$,

$$\begin{aligned}
& -kH^*(-\mathbf{k}, t)k^{-1} \\
& = -kH_2^*(-\mathbf{k}, 2t - \tau)k^{-1} \\
& = H_2(\mathbf{k}, 2t - \tau) \\
& = H(\mathbf{k}, t),
\end{aligned} \tag{D9}$$

Thus, $-kH^*(-\mathbf{k}, t)k^{-1} = H(\mathbf{k}, t)$.

3. Q symmetry with $\epsilon_q = -1$. From $H_1(\mathbf{k}, t) = -qH_1^\dagger(\mathbf{k}, -t)q^{-1}$ and $H_2(\mathbf{k}, t) = -qH_2^\dagger(\mathbf{k}, -t)q^{-1}$ to $H(\mathbf{k}, t) = -qH^\dagger(\mathbf{k}, -t)q^{-1}$. It is equivalent to "From $H_1(\mathbf{k}, -t) = -qH_1^\dagger(\mathbf{k}, t)q^{-1}$ and $H_2(\mathbf{k}, -t) = -qH_2^\dagger(\mathbf{k}, t)q^{-1}$ to $H(\mathbf{k}, -t) = -qH^\dagger(\mathbf{k}, t)q^{-1}$ ".

3a. When $0 \leq t \leq \tau/4$,

$$\begin{aligned}
& -qH^\dagger(\mathbf{k}, t)q^{-1} \\
& = -qH_2^\dagger(\mathbf{k}, 2t)q^{-1} \\
& = H_2(\mathbf{k}, -2t),
\end{aligned} \tag{D10}$$

$$\begin{aligned}
& H(\mathbf{k}, -t) \\
& = H(\mathbf{k}, \tau - t) \\
& = H_2(\mathbf{k}, 2\tau - 2t - \tau) \\
& = H_2(\mathbf{k}, -2t),
\end{aligned} \tag{D11}$$

Thus, $H(\mathbf{k}, -t) = -qH^\dagger(\mathbf{k}, t)q^{-1}$.

3b. When $\tau/4 < t < 3\tau/4$,

$$\begin{aligned}
& -qH^\dagger(\mathbf{k}, t)q^{-1} \\
& = -qH_1^\dagger(\mathbf{k}, 2t - \tau/2)q^{-1} \\
& = H_1(\mathbf{k}, \tau/2 - 2t),
\end{aligned} \tag{D12}$$

$$\begin{aligned}
& H(\mathbf{k}, -t) \\
& = H(\mathbf{k}, \tau - t) \\
& = H_1(\mathbf{k}, 2\tau - 2t - \tau/2) \\
& = H_1(\mathbf{k}, \tau/2 - 2t),
\end{aligned} \tag{D13}$$

Thus, $H(\mathbf{k}, -t) = -qH^\dagger(\mathbf{k}, t)q^{-1}$.

3c. When $3\tau/4 \leq t \leq \tau$,

$$\begin{aligned}
& -qH^\dagger(\mathbf{k}, t)q^{-1} \\
& = -qH_2^\dagger(\mathbf{k}, 2t - \tau)q^{-1} \\
& = H_2(\mathbf{k}, \tau - 2t),
\end{aligned} \tag{D14}$$

$$\begin{aligned}
& H(\mathbf{k}, -t) \\
& = H(\mathbf{k}, \tau - t) \\
& = H_2(\mathbf{k}, 2\tau - 2t - \tau) \\
& = H_2(\mathbf{k}, \tau - 2t),
\end{aligned} \tag{D15}$$

Thus, $H(\mathbf{k}, -t) = -qH^\dagger(\mathbf{k}, t)q^{-1}$.

4. Q symmetry with $\epsilon_q = 1$. From $H_1(\mathbf{k}, t) = qH_1^\dagger(\mathbf{k}, t)q^{-1}$ and $H_2(\mathbf{k}, t) = qH_2^\dagger(\mathbf{k}, t)q^{-1}$ to $H(\mathbf{k}, t) = qH^\dagger(\mathbf{k}, t)q^{-1}$.

4a. When $0 \leq t \leq \tau/4$,

$$\begin{aligned}
& qH^\dagger(\mathbf{k}, t)q^{-1} \\
& = qH_2^\dagger(\mathbf{k}, 2t)q^{-1} \\
& = H_2(\mathbf{k}, 2t) \\
& = H(\mathbf{k}, t),
\end{aligned} \tag{D16}$$

Thus, $H(\mathbf{k}, t) = qH^\dagger(\mathbf{k}, t)q^{-1}$.

4b. When $\tau/4 < t < 3\tau/4$,

$$\begin{aligned} & qH^\dagger(\mathbf{k}, t)q^{-1} \\ &= qH_1^\dagger(\mathbf{k}, 2t - \tau/2)q^{-1} \\ &= H_1(\mathbf{k}, 2t - \tau/2) \\ &= H(\mathbf{k}, t), \end{aligned} \quad (\text{D17})$$

Thus, $H(\mathbf{k}, t) = qH^\dagger(\mathbf{k}, t)q^{-1}$.

4c. When $3\tau/4 \leq t \leq \tau$,

$$\begin{aligned} & qH^\dagger(\mathbf{k}, t)q^{-1} \\ &= qH_2^\dagger(\mathbf{k}, 2t - \tau)q^{-1} \\ &= H_2(\mathbf{k}, 2t - \tau) \\ &= H(\mathbf{k}, t), \end{aligned} \quad (\text{D18})$$

Thus, $H(\mathbf{k}, t) = qH^\dagger(\mathbf{k}, t)q^{-1}$.

5. C symmetry with $\epsilon_c = 1$. From $H_1(\mathbf{k}, t) = cH_1^\mathbf{T}(-\mathbf{k}, -t)c^{-1}$ and $H_2(\mathbf{k}, t) = cH_2^\mathbf{T}(-\mathbf{k}, -t)c^{-1}$ to $H(\mathbf{k}, t) = cH^\mathbf{T}(-\mathbf{k}, -t)c^{-1}$. It is equivalent to “From $H_1(-\mathbf{k}, -t) = cH_1^\mathbf{T}(\mathbf{k}, t)c^{-1}$ and $H_2(-\mathbf{k}, -t) = cH_2^\mathbf{T}(\mathbf{k}, t)c^{-1}$ to $H(-\mathbf{k}, -t) = cH^\mathbf{T}(\mathbf{k}, t)c^{-1}$ ”.

5a. When $0 \leq t \leq \tau/4$,

$$\begin{aligned} & cH^\mathbf{T}(\mathbf{k}, t)c^{-1} \\ &= cH_2^\mathbf{T}(\mathbf{k}, 2t)c^{-1} \\ &= H_2(-\mathbf{k}, -2t), \end{aligned} \quad (\text{D19})$$

$$\begin{aligned} & H(-\mathbf{k}, -t) \\ &= H(-\mathbf{k}, \tau - t) \\ &= H_2(-\mathbf{k}, 2\tau - 2t - \tau) \\ &= H_2(-\mathbf{k}, -2t), \end{aligned} \quad (\text{D20})$$

Thus, $H(-\mathbf{k}, -t) = cH^\mathbf{T}(\mathbf{k}, t)c^{-1}$.

5b. When $\tau/4 < t < 3\tau/4$,

$$\begin{aligned} & cH^\mathbf{T}(\mathbf{k}, t)c^{-1} \\ &= cH_1^\mathbf{T}(\mathbf{k}, 2t - \tau/2)c^{-1} \\ &= H_1(-\mathbf{k}, \tau/2 - 2t), \end{aligned} \quad (\text{D21})$$

$$\begin{aligned} & H(-\mathbf{k}, -t) \\ &= H(-\mathbf{k}, \tau - t) \\ &= H_1(-\mathbf{k}, 2\tau - 2t - \tau/2) \\ &= H_1(-\mathbf{k}, \tau/2 - 2t), \end{aligned} \quad (\text{D22})$$

Thus, $H(-\mathbf{k}, -t) = cH^\mathbf{T}(\mathbf{k}, t)c^{-1}$.

5c. When $3\tau/4 \leq t \leq \tau$,

$$\begin{aligned} & cH^\mathbf{T}(\mathbf{k}, t)c^{-1} \\ &= cH_2^\mathbf{T}(\mathbf{k}, 2t - \tau)c^{-1} \\ &= H_2(-\mathbf{k}, \tau - 2t), \end{aligned} \quad (\text{D23})$$

$$\begin{aligned} & H(-\mathbf{k}, -t) \\ &= H(-\mathbf{k}, \tau - t) \\ &= H_2(-\mathbf{k}, 2\tau - 2t) \\ &= H_2(-\mathbf{k}, \tau - 2t), \end{aligned} \quad (\text{D24})$$

Thus, $H(-\mathbf{k}, -t) = cH^\mathbf{T}(\mathbf{k}, t)c^{-1}$.

6. C symmetry with $\epsilon_c = -1$. From $H_1(\mathbf{k}, t) = -cH_1^\mathbf{T}(-\mathbf{k}, t)c^{-1}$ and $H_2(\mathbf{k}, t) = -cH_2^\mathbf{T}(-\mathbf{k}, t)c^{-1}$ to $H(\mathbf{k}, t) = -cH^\mathbf{T}(-\mathbf{k}, t)c^{-1}$.

6a. When $0 \leq t \leq \tau/4$,

$$\begin{aligned} & -cH^\mathbf{T}(-\mathbf{k}, t)c^{-1} \\ &= -cH_2^\mathbf{T}(-\mathbf{k}, 2t)c^{-1} \\ &= H_2(\mathbf{k}, 2t) \\ &= H(\mathbf{k}, t), \end{aligned} \quad (\text{D25})$$

Thus, $H(\mathbf{k}, t) = -cH^\mathbf{T}(-\mathbf{k}, t)c^{-1}$.

6b. When $\tau/4 < t < 3\tau/4$,

$$\begin{aligned} & -cH^\mathbf{T}(-\mathbf{k}, t)c^{-1} \\ &= -cH_1^\mathbf{T}(-\mathbf{k}, 2t - \tau/2)c^{-1} \\ &= H_1(\mathbf{k}, 2t - \tau/2) \\ &= H(\mathbf{k}, t), \end{aligned} \quad (\text{D26})$$

Thus, $H(\mathbf{k}, t) = -cH^\mathbf{T}(-\mathbf{k}, t)c^{-1}$.

6c. When $3\tau/4 \leq t \leq \tau$,

$$\begin{aligned} & -cH^\mathbf{T}(-\mathbf{k}, t)c^{-1} \\ &= -cH_2^\mathbf{T}(-\mathbf{k}, 2t - \tau)c^{-1} \\ &= H_2(\mathbf{k}, 2t - \tau) \\ &= H(\mathbf{k}, t), \end{aligned} \quad (\text{D27})$$

Thus, $H(\mathbf{k}, t) = -cH^\mathbf{T}(-\mathbf{k}, t)c^{-1}$.

7. P symmetry. From $-H_1(\mathbf{k}, t) = pH_1(\mathbf{k}, -t)p^{-1}$ and $-H_2(\mathbf{k}, t) = pH_2(\mathbf{k}, -t)p^{-1}$ to $-H(\mathbf{k}, t) = pH(\mathbf{k}, -t)p^{-1}$. It is equivalent to “From $-H_1(\mathbf{k}, -t) = pH_1(\mathbf{k}, t)p^{-1}$ and $-H_2(\mathbf{k}, -t) = pH_2(\mathbf{k}, t)p^{-1}$ to $-H(\mathbf{k}, -t) = pH(\mathbf{k}, t)p^{-1}$ ”.

7a. When $0 \leq t \leq \tau/4$,

$$\begin{aligned} & pH(\mathbf{k}, t)p^{-1} \\ &= pH_2(\mathbf{k}, 2t)p^{-1} \\ &= -H_2(\mathbf{k}, -2t), \end{aligned} \quad (\text{D28})$$

$$\begin{aligned} & -H(\mathbf{k}, -t) \\ &= -H(\mathbf{k}, \tau - t) \\ &= -H_2(\mathbf{k}, 2\tau - 2t - \tau) \\ &= -H_2(\mathbf{k}, -2t), \end{aligned} \quad (\text{D29})$$

Thus, $-H(\mathbf{k}, -t) = pH(\mathbf{k}, t)p^{-1}$.

7b. When $\tau/4 < t < 3\tau/4$,

$$\begin{aligned} & pH(\mathbf{k}, t)p^{-1} \\ &= pH_1(\mathbf{k}, 2t - \tau/2)p^{-1} \\ &= -H_1(\mathbf{k}, \tau/2 - 2t), \end{aligned} \quad (\text{D30})$$

$$\begin{aligned}
& -H(\mathbf{k}, -t) \\
&= -H(\mathbf{k}, \tau - t) \\
&= -H_1(\mathbf{k}, 2\tau - 2t - \tau/2) \\
&= -H_1(\mathbf{k}, \tau/2 - 2t),
\end{aligned} \tag{D31}$$

Thus, $-H(\mathbf{k}, -t) = pH(\mathbf{k}, t)p^{-1}$.

7c. When $3\tau/4 \leq t \leq \tau$,

$$\begin{aligned}
& pH(\mathbf{k}, t)p^{-1} \\
&= pH_2(\mathbf{k}, 2t - \tau)p^{-1} \\
&= -H_2(\mathbf{k}, \tau - 2t),
\end{aligned} \tag{D32}$$

$$\begin{aligned}
& -H(\mathbf{k}, -t) \\
&= -H(\mathbf{k}, \tau - t) \\
&= -H_2(\mathbf{k}, 2\tau - 2t) \\
&= -H_2(\mathbf{k}, \tau - 2t),
\end{aligned} \tag{D33}$$

Thus, $-H(\mathbf{k}, -t) = pH(\mathbf{k}, t)p^{-1}$.

Appendix E: Proof of Lemma 2

To prove Lemma 2, we first need to show Lemma 4-9 as listed below.

Lemma 7. $H_{F,\theta} + \frac{2\pi}{\tau} = H_{F,\theta+2\pi}$.

Proof:

$$\begin{aligned}
H_{F,\theta} + \frac{2\pi}{\tau} &= \frac{i}{\tau} \ln_{-\theta}[U(\mathbf{k})] + \frac{2\pi}{\tau} \\
&= \sum_n \frac{i}{\tau} \ln_{-\theta}(\lambda_n) |\psi_{n,R}\rangle \langle \psi_{n,L}| + \frac{2\pi}{\tau} \\
&= \sum_n \frac{i}{\tau} (\ln_{-\theta}(\lambda_n) - 2\pi i) |\psi_{n,R}\rangle \langle \psi_{n,L}| \\
&= \sum_n \frac{i}{\tau} (\ln_{-\theta-2\pi}(\lambda_n)) |\psi_{n,R}\rangle \langle \psi_{n,L}| = H_{F,\theta+2\pi}.
\end{aligned} \tag{E1}$$

Lemma 8. For any unitary matrix p_1 and any evolution operator $U(\mathbf{k})$, $\ln_{\theta}[p_1^{-1}U(\mathbf{k})p_1] = p_1^{-1} \ln_{\theta}[U(\mathbf{k})]p_1$.

Proof:

$$\begin{aligned}
& \ln_{\theta}[p_1^{-1}U(\mathbf{k})p_1] \\
&= \sum_n \frac{i}{\tau} \ln_{\theta}(\lambda_n) p_1^{-1} |\psi_{n,R}\rangle \langle \psi_{n,L}| p_1 \\
&= p_1^{-1} \left[\sum_n \frac{i}{\tau} \ln_{\theta}(\lambda_n) |\psi_{n,R}\rangle \langle \psi_{n,L}| \right] p_1 \\
&= p_1^{-1} \ln_{\theta}[U(\mathbf{k})] p_1
\end{aligned}$$

Lemma 4. For a complex number λ and $\ln_{\theta}(\lambda)$ is well defined, $\ln_{\theta}(\lambda) + \ln_{-\theta}(\lambda^{-1}) = 2\pi i$.

Proof: There always exist $\phi_1 \in (\theta, \theta + 2\pi)$ and ϕ_2 , satisfying $e^{i\phi_1 + \phi_2} = \lambda$. $\ln_{\theta}(\lambda) = i\phi_1 + \phi_2$ and $-\phi_1 \in (-\theta - 2\pi, -\theta)$. Thus, $-\phi_1 + 2\pi \in (-\theta, -\theta + 2\pi)$. $\ln_{-\theta}(\lambda^{-1}) = \ln_{-\theta}(e^{-i\phi_1 - \phi_2}) = -i\phi_1 + 2\pi i - \phi_2$. Hence $\ln_{\theta}(\lambda) + \ln_{-\theta}(\lambda^{-1}) = 2\pi i$.

Lemma 5. For a complex number λ and $\ln_{-\theta}(\lambda)$ is well defined, $\ln_{-\theta}(\lambda^*) - [\ln_{\theta}(\lambda)]^* = 2\pi i$.

Proof: There always exist $\phi_1 \in (\theta, \theta + 2\pi)$ and ϕ_2 , satisfying $e^{i\phi_1 + \phi_2} = \lambda$. $\ln_{\theta}(\lambda) = i\phi_1 + \phi_2$ and $-\phi_1 \in (-\theta - 2\pi, -\theta)$. Thus, $-\phi_1 + 2\pi \in (-\theta, -\theta + 2\pi)$. $\ln_{-\theta}(\lambda^*) = \ln_{-\theta}(e^{-i\phi_1 + \phi_2}) = -i\phi_1 + 2\pi i + \phi_2$. Hence $\ln_{-\theta}(\lambda^*) - [\ln_{\theta}(\lambda)]^* = 2\pi i$.

Lemma 6. For a complex number λ and $\ln_{\theta}(\lambda)$ is well defined, $\ln_{\theta}(\lambda) + 2\pi i = \ln_{\theta+2\pi}(\lambda)$.

Proof: There always exist $\phi_1 \in (\theta, \theta + 2\pi)$ and ϕ_2 , satisfying $e^{i\phi_1 + \phi_2} = \lambda$. $\ln_{\theta}(\lambda) = i\phi_1 + \phi_2$. And $\phi_1 + 2\pi \in (\theta + 2\pi, \theta + 4\pi)$. Thus, $\ln_{\theta+2\pi}(\lambda) = \ln_{\theta+2\pi}(e^{i\phi_1 + \phi_2}) = i\phi_1 + 2\pi i + \phi_2$. Hence $\ln_{\theta}(\lambda) + 2\pi i = \ln_{\theta+2\pi}(\lambda)$.

Lemma 9. *If $H(\mathbf{k}, t)$ satisfies Eqs. (10)-(13), then $H_{F,\theta}$ respectively satisfies Eqs. (E2)-(E5) below:*

$$H_{F,\theta}(\mathbf{k}) = -\frac{(1-\epsilon_k)\pi}{\tau} + \epsilon_k k H_{F,\epsilon_k\theta}^*(-\mathbf{k}) k^{-1}, \quad k k^* = \eta_k \mathbb{I}, \quad K \text{ sym.} \quad (\text{E2})$$

$$H_{F,\theta}(\mathbf{k}) = -\frac{(1-\epsilon_q)\pi}{\tau} + \epsilon_q q H_{F,\epsilon_q\theta}^\dagger(\mathbf{k}) q^{-1}, \quad q^2 = \mathbb{I}, \quad Q \text{ sym.} \quad (\text{E3})$$

$$H_{F,\theta}(\mathbf{k}) = -\frac{(1-\epsilon_c)\pi}{\tau} + \epsilon_c c H_{F,\epsilon_c\theta}^\mathbf{T}(-\mathbf{k}) c^{-1}, \quad c c^* = \eta_c \mathbb{I}, \quad C \text{ sym.} \quad (\text{E4})$$

$$H_{F,\theta}(\mathbf{k}) = -\frac{2\pi}{\tau} - p H_{F,-\theta}(\mathbf{k}) p^{-1}, \quad p^2 = \mathbb{I}. \quad P \text{ sym.} \quad (\text{E5})$$

Proof: We go through the four symmetries one by one.

1. From $U^*(-\mathbf{k}) = k^{-1} U(\mathbf{k}) k$ to $H_{F,\theta}(\mathbf{k}) = -\frac{2\pi}{\tau} - k H_{F,-\theta}^*(-\mathbf{k}) k^{-1}$. It is equivalent to “From $\frac{i}{\tau} \ln_{-\theta}[U^*(-\mathbf{k})] = \frac{i}{\tau} \ln_{-\theta}[k^{-1} U(\mathbf{k}) k]$ to $k^{-1} H_{F,\theta}(\mathbf{k}) k = -\frac{2\pi}{\tau} - H_{F,-\theta}^*(-\mathbf{k})$ ”.

$$\begin{aligned} & \frac{i}{\tau} \ln_{-\theta}[U^*(-\mathbf{k})] \\ &= \sum_n \frac{i}{\tau} \ln_{-\theta}[\lambda_n^*(-\mathbf{k})] |\psi_{n,R}^*(-\mathbf{k})\rangle \langle \psi_{n,L}^*(-\mathbf{k})| \\ &= \sum_n \frac{i}{\tau} [[\ln_{\theta}[\lambda_n(-\mathbf{k})]]^* + 2\pi i] |\psi_{n,R}^*(-\mathbf{k})\rangle \langle \psi_{n,L}^*(-\mathbf{k})| \\ &= -\frac{2\pi}{\tau} + \sum_n \frac{i}{\tau} [\ln_{\theta}[\lambda_n(-\mathbf{k})]]^* |\psi_{n,R}^*(-\mathbf{k})\rangle \langle \psi_{n,L}^*(-\mathbf{k})| \\ &= -\frac{2\pi}{\tau} - \left[\sum_n \frac{i}{\tau} \ln_{\theta}[\lambda_n(-\mathbf{k})] |\psi_{n,R}(-\mathbf{k})\rangle \langle \psi_{n,L}(-\mathbf{k})| \right]^* \\ &= -\frac{2\pi}{\tau} - H_{F,-\theta}^*(-\mathbf{k}). \end{aligned} \quad (\text{E6})$$

And we have

$$\frac{i}{\tau} \ln_{-\theta}[k^{-1} U(\mathbf{k}) k] = k^{-1} \frac{i}{\tau} \ln_{-\theta}[U(\mathbf{k})] k = k^{-1} H_{F,\theta}(\mathbf{k}) k. \quad (\text{E7})$$

Thus, $k^{-1} H_{F,\theta}(\mathbf{k}) k = -\frac{2\pi}{\tau} - H_{F,-\theta}^*(-\mathbf{k})$.

2. From $U^{*-1}(-\mathbf{k}) = k^{-1} U(\mathbf{k}) k$ to $H_{F,\theta}(\mathbf{k}) = k H_{F,\theta}^*(-\mathbf{k}) k^{-1}$. It is equivalent to “From $\frac{i}{\tau} \ln_{-\theta}[U^{*-1}(-\mathbf{k})] = \frac{i}{\tau} \ln_{-\theta}[k^{-1} U(\mathbf{k}) k]$ to $k^{-1} H_{F,\theta}(\mathbf{k}) k = H_{F,\theta}^*(-\mathbf{k})$ ”.

$$\begin{aligned} & \frac{i}{\tau} \ln_{-\theta}[U^{*-1}(-\mathbf{k})] \\ &= \sum_n \frac{i}{\tau} \ln_{-\theta}[\lambda_n^{*-1}(-\mathbf{k})] |\psi_{n,R}^*(-\mathbf{k})\rangle \langle \psi_{n,L}^*(-\mathbf{k})| \\ &= \sum_n \frac{i}{\tau} [[\ln_{\theta}[\lambda_n^{-1}(-\mathbf{k})]]^* + 2\pi i] |\psi_{n,R}^*(-\mathbf{k})\rangle \langle \psi_{n,L}^*(-\mathbf{k})| \\ &= \sum_n \frac{i}{\tau} [[-\ln_{-\theta}[\lambda_n(-\mathbf{k})] + 2\pi i]^* + 2\pi i] |\psi_{n,R}^*(-\mathbf{k})\rangle \langle \psi_{n,L}^*(-\mathbf{k})| \\ &= \sum_n \frac{i}{\tau} [-\ln_{-\theta}[\lambda_n(-\mathbf{k})]]^* |\psi_{n,R}^*(-\mathbf{k})\rangle \langle \psi_{n,L}^*(-\mathbf{k})| \\ &= \left[\sum_n \frac{i}{\tau} \ln_{-\theta}[\lambda_n(-\mathbf{k})] |\psi_{n,R}(-\mathbf{k})\rangle \langle \psi_{n,L}(-\mathbf{k})| \right]^* \\ &= H_{F,\theta}^*(-\mathbf{k}) \end{aligned} \quad (\text{E8})$$

And we have

$$\frac{i}{\tau} \ln_{-\theta}[k^{-1} U(\mathbf{k}) k] = k^{-1} \frac{i}{\tau} \ln_{-\theta}[U(\mathbf{k})] k = k^{-1} H_{F,\theta}(\mathbf{k}) k. \quad (\text{E9})$$

Thus, $k^{-1}H_{F,\theta}(\mathbf{k})k = H_{F,\theta}^*(-\mathbf{k})$.

3. From $[U^\dagger(\mathbf{k})] = q^{-1}U(\mathbf{k})q$ to $H_{F,\theta}(\mathbf{k}) = -\frac{2\pi}{\tau} - qH_{F,-\theta}^\dagger(\mathbf{k})q^{-1}$. It is equivalent to “From $\frac{i}{\tau}\ln_{-\theta}[U^\dagger(\mathbf{k})] = \frac{i}{\tau}\ln_{-\theta}[q^{-1}U(\mathbf{k})q]$ to $q^{-1}H_{F,\theta}(\mathbf{k})q = -\frac{2\pi}{\tau} - H_{F,-\theta}^\dagger(\mathbf{k})$ ”.

$$\begin{aligned}
& \frac{i}{\tau}\ln_{-\theta}[U^\dagger(\mathbf{k})] \\
&= \sum_n \frac{i}{\tau}\ln_{-\theta}[\lambda_n^*(\mathbf{k})]|\psi_{n,L}(\mathbf{k})\rangle\langle\psi_{n,R}(\mathbf{k})| \\
&= \sum_n \frac{i}{\tau}[[\ln_{\theta}[\lambda_n(\mathbf{k})]]^* + 2\pi i]|\psi_{n,L}(\mathbf{k})\rangle\langle\psi_{n,R}(\mathbf{k})| \\
&= -\frac{2\pi}{\tau} + \sum_n \frac{i}{\tau}[\ln_{\theta}[\lambda_n(\mathbf{k})]]^*|\psi_{n,L}(\mathbf{k})\rangle\langle\psi_{n,R}(\mathbf{k})| \\
&= -\frac{2\pi}{\tau} - [\sum_n \frac{i}{\tau}\ln_{\theta}[\lambda_n(\mathbf{k})]|\psi_{n,R}(\mathbf{k})\rangle\langle\psi_{n,L}(\mathbf{k})|]^\dagger \\
&= -\frac{2\pi}{\tau} - H_{F,-\theta}^\dagger(\mathbf{k}).
\end{aligned} \tag{E10}$$

And we have

$$\frac{i}{\tau}\ln_{-\theta}[q^{-1}U(\mathbf{k})q] = q^{-1}\frac{i}{\tau}\ln_{-\theta}[U(\mathbf{k})]q = q^{-1}H_{F,\theta}(\mathbf{k})q. \tag{E11}$$

Thus, $q^{-1}H_{F,\theta}(\mathbf{k})q = -\frac{2\pi}{\tau} - H_{F,-\theta}^\dagger(\mathbf{k})$.

4. From $[U^\dagger(\mathbf{k})]^{-1} = q^{-1}U(\mathbf{k})q$ to $H_{F,\theta}(\mathbf{k}) = qH_{F,\theta}^\dagger(\mathbf{k})q^{-1}$. It is equivalent to “From $\frac{i}{\tau}\ln_{-\theta}[U^\dagger(\mathbf{k})]^{-1} = \frac{i}{\tau}\ln_{-\theta}[q^{-1}U(\mathbf{k})q]$ to $q^{-1}H_{F,\theta}(\mathbf{k})q = H_{F,\theta}^\dagger(\mathbf{k})$ ”.

$$\begin{aligned}
& \frac{i}{\tau}\ln_{-\theta}[U^\dagger(\mathbf{k})]^{-1} \\
&= \sum_n \frac{i}{\tau}\ln_{-\theta}[\lambda_n^{*-1}(\mathbf{k})]|\psi_{n,L}(\mathbf{k})\rangle\langle\psi_{n,R}(\mathbf{k})| \\
&= \sum_n \frac{i}{\tau}[[\ln_{\theta}[\lambda_n^{-1}(\mathbf{k})]]^* + 2\pi i]|\psi_{n,L}(\mathbf{k})\rangle\langle\psi_{n,R}(\mathbf{k})| \\
&= \sum_n \frac{i}{\tau}[-\ln_{-\theta}[\lambda_n(\mathbf{k})] + 2\pi i]^* + 2\pi i]|\psi_{n,L}(\mathbf{k})\rangle\langle\psi_{n,R}(\mathbf{k})| \\
&= \sum_n \frac{i}{\tau}[-\ln_{-\theta}[\lambda_n(\mathbf{k})]]^*|\psi_{n,L}(\mathbf{k})\rangle\langle\psi_{n,R}(\mathbf{k})| \\
&= [\sum_n \frac{i}{\tau}\ln_{-\theta}[\lambda_n(\mathbf{k})]|\psi_{n,R}(\mathbf{k})\rangle\langle\psi_{n,L}(\mathbf{k})|]^\dagger \\
&= H_{F,\theta}^\dagger(\mathbf{k}).
\end{aligned} \tag{E12}$$

And we have

$$\frac{i}{\tau}\ln_{-\theta}[q^{-1}U(\mathbf{k})q] = q^{-1}\frac{i}{\tau}\ln_{-\theta}[U(\mathbf{k})]q = q^{-1}H_{F,\theta}(\mathbf{k})q. \tag{E13}$$

Thus, $q^{-1}H_{F,\theta}(\mathbf{k})q = H_{F,\theta}^\dagger(\mathbf{k})$.

5. From $[U^\mathbf{T}(-\mathbf{k})] = c^{-1}U(\mathbf{k})c$ to $H_{F,\theta}(\mathbf{k}) = cH_{F,\theta}^\mathbf{T}(-\mathbf{k})c^{-1}$. It is equivalent to “From $\frac{i}{\tau}\ln_{-\theta}[U^\mathbf{T}(-\mathbf{k})] =$

$\frac{i}{\tau} \ln_{-\theta}[c^{-1}U(\mathbf{k})c]$ to $c^{-1}H_{F,\theta}(\mathbf{k})c = H_{F,\theta}^{\mathbf{T}}(-\mathbf{k})$ ”.

$$\begin{aligned}
& \frac{i}{\tau} \ln_{-\theta}[U^{\mathbf{T}}(-\mathbf{k})] \\
&= \sum_n \frac{i}{\tau} \ln_{-\theta}[\lambda_n(-\mathbf{k})] |\psi_{n,L}^*(-\mathbf{k})\rangle \langle \psi_{n,R}^*(-\mathbf{k})| \\
&= \left[\sum_n \frac{i}{\tau} \ln_{-\theta}[\lambda_n(-\mathbf{k})] |\psi_{n,R}(-\mathbf{k})\rangle \langle \psi_{n,L}(-\mathbf{k})| \right]^{\mathbf{T}} \\
&= H_{F,\theta}^{\mathbf{T}}(-\mathbf{k}).
\end{aligned} \tag{E14}$$

And we have

$$\frac{i}{\tau} \ln_{-\theta}[c^{-1}U(\mathbf{k})c] = c^{-1} \frac{i}{\tau} \ln_{-\theta}[U(\mathbf{k})]c = c^{-1}H_{F,\theta}(\mathbf{k})c. \tag{E15}$$

Thus, $c^{-1}H_{F,\theta}(\mathbf{k})c = H_{F,\theta}^{\mathbf{T}}(-\mathbf{k})$.

6. From $[U^{\mathbf{T}}(-\mathbf{k})]^{-1} = c^{-1}U(\mathbf{k})c$ to $H_{F,\theta}(\mathbf{k}) = -\frac{2\pi}{\tau} - cH_{F,-\theta}^{\mathbf{T}}(-\mathbf{k})c^{-1}$. It is equivalent to “From $\frac{i}{\tau} \ln_{-\theta}[U^{\mathbf{T}}(-\mathbf{k})]^{-1} = \frac{i}{\tau} \ln_{-\theta}[c^{-1}U(\mathbf{k})c]$ to $c^{-1}H_{F,\theta}(\mathbf{k})c = -\frac{2\pi}{\tau} - H_{F,-\theta}^{\mathbf{T}}(-\mathbf{k})$ ”.

$$\begin{aligned}
& \frac{i}{\tau} \ln_{-\theta}[U^{\mathbf{T}}(-\mathbf{k})]^{-1} \\
&= \sum_n \frac{i}{\tau} \ln_{-\theta}[\lambda_n^{-1}(-\mathbf{k})] |\psi_{n,L}^*(-\mathbf{k})\rangle \langle \psi_{n,R}^*(-\mathbf{k})| \\
&= \sum_n \frac{i}{\tau} [-\ln_{\theta}[\lambda_n(-\mathbf{k})] + 2\pi i] |\psi_{n,L}^*(-\mathbf{k})\rangle \langle \psi_{n,R}^*(-\mathbf{k})| \\
&= -\frac{2\pi}{\tau} + \sum_n \frac{i}{\tau} [-\ln_{\theta}[\lambda_n(-\mathbf{k})]] |\psi_{n,L}^*(-\mathbf{k})\rangle \langle \psi_{n,R}^*(-\mathbf{k})| \\
&= -\frac{2\pi}{\tau} - \left[\sum_n \frac{i}{\tau} \ln_{\theta}[\lambda_n(-\mathbf{k})] |\psi_{n,R}(-\mathbf{k})\rangle \langle \psi_{n,L}(-\mathbf{k})| \right]^{\mathbf{T}} \\
&= -\frac{2\pi}{\tau} - H_{F,-\theta}^{\mathbf{T}}(-\mathbf{k}).
\end{aligned} \tag{E16}$$

And we have

$$\frac{i}{\tau} \ln_{-\theta}[c^{-1}U(\mathbf{k})c] = c^{-1} \frac{i}{\tau} \ln_{-\theta}[U(\mathbf{k})]c = c^{-1}H_{F,\theta}(\mathbf{k})c. \tag{E17}$$

Thus, $c^{-1}H_{F,\theta}(\mathbf{k})c = -\frac{2\pi}{\tau} - H_{F,-\theta}^{\mathbf{T}}(-\mathbf{k})$.

7. From $[U(\mathbf{k})]^{-1} = p^{-1}U(\mathbf{k})p$ to $H_{F,\theta}(\mathbf{k}) = -\frac{2\pi}{\tau} - pH_{F,-\theta}(\mathbf{k})p^{-1}$. It is equivalent to “From $\frac{i}{\tau} \ln_{-\theta}[U(\mathbf{k})]^{-1} = \frac{i}{\tau} \ln_{-\theta}[p^{-1}U(\mathbf{k})p]$ to $p^{-1}H_{F,\theta}(\mathbf{k})p = -\frac{2\pi}{\tau} - H_{F,-\theta}(\mathbf{k})$ ”.

$$\begin{aligned}
& \frac{i}{\tau} \ln_{-\theta}[U(\mathbf{k})]^{-1} \\
&= \sum_n \frac{i}{\tau} \ln_{-\theta}[\lambda_n^{-1}(\mathbf{k})] |\psi_{n,R}(\mathbf{k})\rangle \langle \psi_{n,L}(\mathbf{k})| \\
&= \sum_n \frac{i}{\tau} [-\ln_{\theta}[\lambda_n(\mathbf{k})] + 2\pi i] |\psi_{n,R}(\mathbf{k})\rangle \langle \psi_{n,L}(\mathbf{k})| \\
&= -\frac{2\pi}{\tau} - \sum_n \frac{i}{\tau} \ln_{\theta}[\lambda_n(\mathbf{k})] |\psi_{n,R}(\mathbf{k})\rangle \langle \psi_{n,L}(\mathbf{k})| \\
&= -\frac{2\pi}{\tau} - H_{F,-\theta}(\mathbf{k}).
\end{aligned} \tag{E18}$$

And we have

$$\frac{i}{\tau} \ln_{-\theta}[p^{-1}U(\mathbf{k})p] = p^{-1} \frac{i}{\tau} \ln_{-\theta}[U(\mathbf{k})]p = p^{-1}H_{F,\theta}(\mathbf{k})p. \tag{E19}$$

Thus, $p^{-1}H_{F,\theta}(\mathbf{k})p = -\frac{2\pi}{\tau} - H_{F,-\theta}(\mathbf{k})$. Combining 1-7, we get the proof of Lemma 9. Now we are ready to prove Lemma 2 in the main text. According to Lemma 9, if $H(\mathbf{k}, t)$ satisfies Eqs. (10)-(13), then $H_{F,\pi}$ satisfies Eqs. (E20)-(E23) below:

$$H_{F,\pi}(\mathbf{k}) = -\frac{(1-\epsilon_k)\pi}{\tau} + \epsilon_k k H_{F,\epsilon_k\pi}^*(-\mathbf{k})k^{-1}, \quad kk^* = \eta_k \mathbb{I}, \quad K \text{ sym.} \quad (\text{E20})$$

$$H_{F,\pi}(\mathbf{k}) = -\frac{(1-\epsilon_q)\pi}{\tau} + \epsilon_q q H_{F,\epsilon_q\pi}^\dagger(\mathbf{k})q^{-1}, \quad q^2 = \mathbb{I}, \quad Q \text{ sym.} \quad (\text{E21})$$

$$H_{F,\pi}(\mathbf{k}) = -\frac{(1-\epsilon_c)\pi}{\tau} + \epsilon_c c H_{F,\epsilon_c\pi}^{\mathbf{T}}(-\mathbf{k})c^{-1}, \quad cc^* = \eta_c \mathbb{I}, \quad C \text{ sym.} \quad (\text{E22})$$

$$H_{F,\pi}(\mathbf{k}) = -\frac{2\pi}{\tau} - p H_{F,-\pi}(\mathbf{k})p^{-1}, \quad p^2 = \mathbb{I}. \quad P \text{ sym.} \quad (\text{E23})$$

According to Lemma 7, we have:

$$-\frac{(1-\epsilon_k)\pi}{\tau} + \epsilon_k k H_{F,\epsilon_k\pi}^*(-\mathbf{k})k^{-1} = \epsilon_k k H_{F,\epsilon_k\pi+(1-\epsilon_k)\pi}^*(-\mathbf{k})k^{-1} = \epsilon_k k H_{F,\pi}^*(-\mathbf{k})k^{-1}, \quad (\text{E24})$$

$$-\frac{(1-\epsilon_q)\pi}{\tau} + \epsilon_q q H_{F,\epsilon_q\pi}^\dagger(\mathbf{k})q^{-1} = \epsilon_q q H_{F,\epsilon_q\pi+(1-\epsilon_q)\pi}^\dagger(\mathbf{k})q^{-1} = \epsilon_q q H_{F,\pi}^\dagger(\mathbf{k})q^{-1}, \quad (\text{E25})$$

$$-\frac{(1-\epsilon_c)\pi}{\tau} + \epsilon_c c H_{F,\epsilon_c\pi}^{\mathbf{T}}(-\mathbf{k})c^{-1} = \epsilon_c c H_{F,\epsilon_c\pi+(1-\epsilon_c)\pi}^{\mathbf{T}}(-\mathbf{k})c^{-1} = \epsilon_c c H_{F,\pi}^{\mathbf{T}}(-\mathbf{k})c^{-1}, \quad (\text{E26})$$

$$-\frac{2\pi}{\tau} - p H_{F,-\pi}(\mathbf{k})p^{-1} = -p H_{F,-\pi+2\pi}(\mathbf{k})p^{-1} = -p H_{F,\pi}(\mathbf{k})p^{-1}. \quad (\text{E27})$$

Combining Eqs. (E20)-(E27), we can conclude that if $H(\mathbf{k}, t)$ satisfies Eqs. (10)-(13), then $H_{F,\pi}$ satisfies:

$$H_{F,\pi}(\mathbf{k}) = \epsilon_k k H_{F,\pi}^*(-\mathbf{k})k^{-1}, \quad kk^* = \eta_k \mathbb{I}, \quad K \text{ sym.} \quad (\text{E28})$$

$$H_{F,\pi}(\mathbf{k}) = \epsilon_q q H_{F,\pi}^\dagger(\mathbf{k})q^{-1}, \quad q^2 = \mathbb{I}, \quad Q \text{ sym.} \quad (\text{E29})$$

$$H_{F,\pi}(\mathbf{k}) = \epsilon_c c H_{F,\pi}^{\mathbf{T}}(-\mathbf{k})c^{-1}, \quad cc^* = \eta_c \mathbb{I}, \quad C \text{ sym.} \quad (\text{E30})$$

$$H_{F,\pi}(\mathbf{k}) = -p H_{F,\pi}(\mathbf{k})p^{-1}, \quad p^2 = \mathbb{I}. \quad P \text{ sym.} \quad (\text{E31})$$

Thus, $H_{F,\pi}(\mathbf{k})$ and $H(\mathbf{k}, t)$ belong to same GBL class. The loop operator is $U_{l,\pi}(\mathbf{k}, t) = U(\mathbf{k}, t) * e^{iH_{F,\pi}(\mathbf{k})t}$. According to Lemma 1 in the main text, $H_{F,\pi}(\mathbf{k})$, $U_{l,\pi}$, and $H(\mathbf{k}, t)$ belong to same GBL class. We remark that $H_{F,\pi}(\mathbf{k})$ has (continuous) time-translation symmetry but $H(\mathbf{k})$ only has discrete time-translation symmetry. In general $H_{F,\pi}(\mathbf{k})$ has more symmetries than $H(\mathbf{k})$.

Appendix F: Proof of Theorem 1

The proof can be done in a similar vein with that of the Hermitian case (see Appendix C of Ref. [104]). Here we decompose the proof into Lemma 10 and Lemma 11.

Lemma 10. *The time evolution operator $U(\mathbf{k}, t)$ with FH real gap at π/τ can continuously transform to $U_f(\mathbf{k}, t) = L * C$, with L a loop operator and C a constant (time-independent) Hamiltonian evolution. One of the L is $L = U_{l,\pi}(\mathbf{k}, t)$. And the corresponding C is the constant evolution with Hamiltonian $H_{F,\pi}$. The continuous transformation preserves the GBL symmetries.*

To see this, we define the constant evolution $C_\pm(s) := e^{\mp i s H_{F,\pi} t}$. According to Lemma 9, $C_\pm(s)$ and $U(\mathbf{k}, t)$ belong to same GBL class. We further define $U_0(s) := U(\mathbf{k}, t) * C_-(s)$ and $h(s) := U_0(s) * C_+(s)$. According to Lemma 1, $C_\pm(s)$, $U(\mathbf{k}, t)$, $U_0(s)$, and $h(s)$ belong to same

GBL class. $h(s)$ is a continuous function and satisfies:

$$\begin{aligned} h(0) &= U(\mathbf{k}, t); \\ h(1) &= U_0(1) * C_+(1) = U_{l,\pi} * e^{-iH_{F,\pi}t}. \end{aligned} \quad (\text{F1})$$

Lemma 11. *In Lemma 10, if we have two $U_f(\mathbf{k}, t)$ labeled as U_{f1} and U_{f2} . And $U_{f1} = L_1 * C_1$ and $U_{f2} = L_2 * C_2$. We then have that $L_1 \approx L_2$ and $C_1 \approx C_2$. Here \approx is the homotopy equivalence.*

As $U(\mathbf{k}, t) \approx U_{f1}$ and $U(\mathbf{k}, t) \approx U_{f2}$, we have $U_{f1} \approx U_{f2}$. Thus, there exists continuous function $g_s(\mathbf{k}, t)$ such that $g_0 = U_{f1} = L_1 * C_1$, $g_1 = U_{f2} = L_2 * C_2$, and time evolution operator $g_s(\mathbf{k}, t)$ has FH real gap at π/τ for any s . And $U(\mathbf{k}, t)$ and g_s belong to same GBL class. We can define the continuous function:

$$h_s^F(\mathbf{k}) := \frac{i}{\tau} \ln_{-\pi} [g_s(\mathbf{k}, \tau)], \quad (\text{F2})$$

$$g_s^\pm(\mathbf{k}, t) := e^{\mp i h_s^F t}, \quad (\text{F3})$$

$$g_s^1(\mathbf{k}, t) := g_s * g_s^-. \quad (\text{F4})$$

According to Lemma 9, $U(\mathbf{k}, t)$, and $g_s^\pm(\mathbf{k}, t)$ belong to same GBL class. According to Lemma 1, $U(\mathbf{k}, t)$, $g_s^\pm(\mathbf{k}, t)$, and $g_s^1(\mathbf{k}, t)$ belong to same GBL class, and

$$g_0^+(\mathbf{k}, t) = e^{-ih_0^F t} = C_1; \quad (\text{F5})$$

$$g_1^+(\mathbf{k}, t) = e^{-ih_1^F t} = C_2; \quad (\text{F6})$$

$$g_0^1(\mathbf{k}, t) := g_0 * g_0^- \approx L_1; \quad (\text{F7})$$

$$g_1^1(\mathbf{k}, t) := g_1 * g_1^- \approx L_2. \quad (\text{F8})$$

Appendix G: Derivation of Eqs. (31)-(34) from Eqs. (15)-(18)

1. From $U_{l,\pi}^*(-\mathbf{k}, -t) = k^{-1}U_{l,\pi}(\mathbf{k}, \epsilon_k t)k$ to $\tilde{H}(-\mathbf{k}, -\epsilon_k t) = \tilde{K}\tilde{H}(\mathbf{k}, t)\tilde{K}^{-1}$.

$$\begin{aligned} & \tilde{K}\tilde{H}(\mathbf{k}, t)\tilde{K}^{-1} \\ &= \begin{bmatrix} k & 0 \\ 0 & k \end{bmatrix} \begin{bmatrix} 0 & U_{l,\pi}^*(\mathbf{k}, t) \\ U_{l,\pi}^{\mathbf{T}}(\mathbf{k}, t) & 0 \end{bmatrix} \begin{bmatrix} k^{-1} & 0 \\ 0 & k^{-1} \end{bmatrix} \\ &= \begin{bmatrix} 0 & kU_{l,\pi}^*(\mathbf{k}, t)k^{-1} \\ kU_{l,\pi}^{\mathbf{T}}(\mathbf{k}, t)k^{-1} & 0 \end{bmatrix} \quad (\text{G1}) \\ &= \begin{bmatrix} 0 & U_{l,\pi}(-\mathbf{k}, -\epsilon_k t) \\ U_{l,\pi}^\dagger(-\mathbf{k}, -\epsilon_k t) & 0 \end{bmatrix} \\ &= \tilde{H}(-\mathbf{k}, -\epsilon_k t). \end{aligned}$$

2. From $[U_{l,\pi}^\dagger(\mathbf{k}, t)]^{-1} = q^{-1}U_{l,\pi}(\mathbf{k}, \epsilon_q t)q$ to $\tilde{H}(\mathbf{k}, \epsilon_q t) = \tilde{Q}\tilde{H}(\mathbf{k}, t)\tilde{Q}^{-1}$.

$$\begin{aligned} & \tilde{Q}\tilde{H}(\mathbf{k}, t)\tilde{Q}^{-1} \\ &= \begin{bmatrix} q & 0 \\ 0 & q \end{bmatrix} \begin{bmatrix} 0 & U_{l,\pi}(\mathbf{k}, t) \\ U_{l,\pi}^\dagger(\mathbf{k}, t) & 0 \end{bmatrix} \begin{bmatrix} q^{-1} & 0 \\ 0 & q^{-1} \end{bmatrix} \\ &= \begin{bmatrix} 0 & qU_{l,\pi}(\mathbf{k}, t)q^{-1} \\ qU_{l,\pi}^\dagger(\mathbf{k}, t)q^{-1} & 0 \end{bmatrix} \\ &= \begin{bmatrix} 0 & (U_{l,\pi}^\dagger(\mathbf{k}, \epsilon_q t))^{-1} \\ (U_{l,\pi}(\mathbf{k}, \epsilon_q t))^{-1} & 0 \end{bmatrix} \quad (\text{G2}) \\ &= \begin{bmatrix} 0 & U_{l,\pi}(\mathbf{k}, \epsilon_q t) \\ U_{l,\pi}^\dagger(\mathbf{k}, \epsilon_q t) & 0 \end{bmatrix}^{-1} \\ &= [\tilde{H}(\mathbf{k}, \epsilon_q t)]^{-1} \\ &= \tilde{H}(\mathbf{k}, \epsilon_q t). \end{aligned}$$

3. From $[U_{l,\pi}^{\mathbf{T}}(-\mathbf{k}, t)]^{-1} = c^{-1}U_{l,\pi}(\mathbf{k}, -\epsilon_c t)c$ to

$$\tilde{H}(-\mathbf{k}, -\epsilon_c t) = \tilde{C}\tilde{H}(\mathbf{k}, t)\tilde{C}^{-1}.$$

$$\begin{aligned} & \tilde{C}\tilde{H}(\mathbf{k}, t)\tilde{C}^{-1} \\ &= \begin{bmatrix} c & 0 \\ 0 & c \end{bmatrix} \begin{bmatrix} 0 & U_{l,\pi}^*(\mathbf{k}, t) \\ U_{l,\pi}^{\mathbf{T}}(\mathbf{k}, t) & 0 \end{bmatrix} \begin{bmatrix} c^{-1} & 0 \\ 0 & c^{-1} \end{bmatrix} \\ &= \begin{bmatrix} 0 & cU_{l,\pi}^*(\mathbf{k}, t)c^{-1} \\ cU_{l,\pi}^{\mathbf{T}}(\mathbf{k}, t)c^{-1} & 0 \end{bmatrix} \\ &= \begin{bmatrix} 0 & (U_{l,\pi}^\dagger(-\mathbf{k}, -\epsilon_c t))^{-1} \\ (U_{l,\pi}(-\mathbf{k}, -\epsilon_c t))^{-1} & 0 \end{bmatrix} \quad (\text{G3}) \\ &= \begin{bmatrix} 0 & U_{l,\pi}(-\mathbf{k}, -\epsilon_c t) \\ U_{l,\pi}^\dagger(-\mathbf{k}, -\epsilon_c t) & 0 \end{bmatrix}^{-1} \\ &= [\tilde{H}(-\mathbf{k}, -\epsilon_c t)]^{-1} \\ &= \tilde{H}(-\mathbf{k}, -\epsilon_c t). \end{aligned}$$

4. From $U_{l,\pi}(\mathbf{k}, -t) = p^{-1}U_{l,\pi}(\mathbf{k}, t)p$ to $\tilde{H}(\mathbf{k}, -t) = \tilde{P}\tilde{H}(\mathbf{k}, t)\tilde{P}^{-1}$.

$$\begin{aligned} & \tilde{P}\tilde{H}(\mathbf{k}, t)\tilde{P}^{-1} \\ &= \begin{bmatrix} p & 0 \\ 0 & p \end{bmatrix} \begin{bmatrix} 0 & U_{l,\pi}(\mathbf{k}, t) \\ U_{l,\pi}^\dagger(\mathbf{k}, t) & 0 \end{bmatrix} \begin{bmatrix} p^{-1} & 0 \\ 0 & p^{-1} \end{bmatrix} \\ &= \begin{bmatrix} 0 & pU_{l,\pi}(\mathbf{k}, t)p^{-1} \\ pU_{l,\pi}^\dagger(\mathbf{k}, t)p^{-1} & 0 \end{bmatrix} \quad (\text{G4}) \\ &= \begin{bmatrix} 0 & U_{l,\pi}(\mathbf{k}, -t) \\ U_{l,\pi}^\dagger(\mathbf{k}, -t) & 0 \end{bmatrix} \\ &= \tilde{H}(\mathbf{k}, -t). \end{aligned}$$

Appendix H: Derivation of Eqs. (38)-(41) from Eqs. (20)-(23)

1. From $[U^*(-\mathbf{k})]^{-1} = k^{-1}U(\mathbf{k})k$ to $\tilde{H}(-\mathbf{k}) = \tilde{K}\tilde{H}(\mathbf{k})\tilde{K}^{-1}$ and $\tilde{K} = \sigma_x \otimes k\mathcal{K}$. First, we have that $kU^*(-\mathbf{k})k^{-1} = [U(\mathbf{k})]^{-1}$. Thus,

$$\begin{aligned} & \tilde{K}\tilde{H}(\mathbf{k})\tilde{K}^{-1} \\ &= \begin{bmatrix} 0 & k \\ k & 0 \end{bmatrix} \begin{bmatrix} 0 & U^*(\mathbf{k}) \\ U^{\mathbf{T}}(\mathbf{k}) & 0 \end{bmatrix} \begin{bmatrix} 0 & k^{-1} \\ k^{-1} & 0 \end{bmatrix} \\ &= \begin{bmatrix} 0 & kU^{\mathbf{T}}(\mathbf{k})k^{-1} \\ kU^*(\mathbf{k})k^{-1} & 0 \end{bmatrix} \quad (\text{H1}) \\ &= \begin{bmatrix} 0 & (U^\dagger(-\mathbf{k}))^{-1} \\ (U(-\mathbf{k}))^{-1} & 0 \end{bmatrix} \\ &= \begin{bmatrix} 0 & U(-\mathbf{k}) \\ U^\dagger(-\mathbf{k}) & 0 \end{bmatrix}^{-1} \\ &= [\tilde{H}(-\mathbf{k})]^{-1} = \tilde{H}(-\mathbf{k}). \end{aligned}$$

2. From $U^*(-\mathbf{k}) = k^{-1}U(\mathbf{k})k$ to $\tilde{H}(-\mathbf{k}) = \tilde{K}\tilde{H}(\mathbf{k})\tilde{K}^{-1}$ and $\tilde{K} = \sigma_0 \otimes k\mathcal{K}$. First, we have that

$kU^*(-\mathbf{k})k^{-1} = U(\mathbf{k})$. Thus,

$$\begin{aligned}
& \bar{K}\tilde{H}(\mathbf{k})\bar{K}^{-1} \\
&= \begin{bmatrix} k & 0 \\ 0 & k \end{bmatrix} \begin{bmatrix} 0 & U^*(\mathbf{k}) \\ U^{\mathbf{T}}(\mathbf{k}) & 0 \end{bmatrix} \begin{bmatrix} k^{-1} & 0 \\ 0 & k^{-1} \end{bmatrix} \\
&= \begin{bmatrix} 0 & kU^*(\mathbf{k})k^{-1} \\ kU^{\mathbf{T}}(\mathbf{k})k^{-1} & 0 \end{bmatrix} \\
&= \begin{bmatrix} 0 & U(-\mathbf{k}) \\ U^\dagger(-\mathbf{k}) & 0 \end{bmatrix} \\
&= \tilde{H}(-\mathbf{k}).
\end{aligned} \tag{H2}$$

3. From $[U^\dagger(\mathbf{k})]^{-1} = q^{-1}U(\mathbf{k})q$ to $\tilde{H}(\mathbf{k}) = \bar{Q}\tilde{H}(\mathbf{k})\bar{Q}^{-1}$ and $\bar{Q} = \sigma_0 \otimes q$.

$$\begin{aligned}
& \bar{Q}\tilde{H}(\mathbf{k})\bar{Q}^{-1} \\
&= \begin{bmatrix} q & 0 \\ 0 & q \end{bmatrix} \begin{bmatrix} 0 & U(\mathbf{k}) \\ U^\dagger(\mathbf{k}) & 0 \end{bmatrix} \begin{bmatrix} q^{-1} & 0 \\ 0 & q^{-1} \end{bmatrix} \\
&= \begin{bmatrix} 0 & qU(\mathbf{k})q^{-1} \\ qU^\dagger(\mathbf{k})q^{-1} & 0 \end{bmatrix} \\
&= \begin{bmatrix} 0 & (U^\dagger(\mathbf{k}))^{-1} \\ (U(\mathbf{k}))^{-1} & 0 \end{bmatrix} \\
&= \begin{bmatrix} 0 & U(\mathbf{k}) \\ U^\dagger(\mathbf{k}) & 0 \end{bmatrix}^{-1} \\
&= [\tilde{H}(\mathbf{k})]^{-1} = \tilde{H}(\mathbf{k}).
\end{aligned} \tag{H3}$$

4. From $U^\dagger(\mathbf{k}) = q^{-1}U(\mathbf{k})q$ to $\tilde{H}(\mathbf{k}) = \bar{Q}\tilde{H}(\mathbf{k})\bar{Q}^{-1}$ and $\bar{Q} = \sigma_x \otimes q$.

$$\begin{aligned}
& \bar{Q}\tilde{H}(\mathbf{k})\bar{Q}^{-1} \\
&= \begin{bmatrix} 0 & q \\ q & 0 \end{bmatrix} \begin{bmatrix} 0 & U(\mathbf{k}) \\ U^\dagger(\mathbf{k}) & 0 \end{bmatrix} \begin{bmatrix} 0 & q^{-1} \\ q^{-1} & 0 \end{bmatrix} \\
&= \begin{bmatrix} 0 & qU^\dagger(\mathbf{k})q^{-1} \\ qU(\mathbf{k})q^{-1} & 0 \end{bmatrix} \\
&= \begin{bmatrix} 0 & U(\mathbf{k}) \\ U^\dagger(\mathbf{k}) & 0 \end{bmatrix} \\
&= \tilde{H}(\mathbf{k}).
\end{aligned} \tag{H4}$$

5. From $U^{\mathbf{T}}(-\mathbf{k}) = c^{-1}U(\mathbf{k})c$ to $\tilde{H}(-\mathbf{k}) = \bar{C}\tilde{H}^*(\mathbf{k})\bar{C}^{-1}$ and $\bar{C} = \sigma_x \otimes c\mathcal{K}$.

$$\begin{aligned}
& \bar{C}\tilde{H}^*(\mathbf{k})\bar{C}^{-1} \\
&= \begin{bmatrix} 0 & c \\ c & 0 \end{bmatrix} \begin{bmatrix} 0 & U^*(\mathbf{k}) \\ U^{\mathbf{T}}(\mathbf{k}) & 0 \end{bmatrix} \begin{bmatrix} 0 & c^{-1} \\ c^{-1} & 0 \end{bmatrix} \\
&= \begin{bmatrix} 0 & cU^{\mathbf{T}}(\mathbf{k})c^{-1} \\ cU^*(\mathbf{k})c^{-1} & 0 \end{bmatrix} \\
&= \begin{bmatrix} 0 & U(-\mathbf{k}) \\ U^\dagger(-\mathbf{k}) & 0 \end{bmatrix} \\
&= \tilde{H}(-\mathbf{k}).
\end{aligned} \tag{H5}$$

6. From $[U^{\mathbf{T}}(-\mathbf{k})]^{-1} = c^{-1}U(\mathbf{k})c$ to $\tilde{H}(-\mathbf{k}) =$

$\bar{C}\tilde{H}^*(\mathbf{k})\bar{C}^{-1}$ and $\bar{C} = \sigma_0 \otimes c\mathcal{K}$.

$$\begin{aligned}
& \bar{C}\tilde{H}^*(\mathbf{k})\bar{C}^{-1} \\
&= \begin{bmatrix} c & 0 \\ 0 & c \end{bmatrix} \begin{bmatrix} 0 & U^*(\mathbf{k}) \\ U^{\mathbf{T}}(\mathbf{k}) & 0 \end{bmatrix} \begin{bmatrix} c^{-1} & 0 \\ 0 & c^{-1} \end{bmatrix} \\
&= \begin{bmatrix} 0 & cU^*(\mathbf{k})c^{-1} \\ cU^{\mathbf{T}}(\mathbf{k})c^{-1} & 0 \end{bmatrix} \\
&= \begin{bmatrix} 0 & (U^\dagger(-\mathbf{k}))^{-1} \\ (U(-\mathbf{k}))^{-1} & 0 \end{bmatrix} \\
&= \begin{bmatrix} 0 & U(-\mathbf{k}) \\ U^\dagger(-\mathbf{k}) & 0 \end{bmatrix}^{-1} \\
&= [\tilde{H}(-\mathbf{k})]^{-1} = \tilde{H}(-\mathbf{k}).
\end{aligned} \tag{H6}$$

7. From $[U(\mathbf{k})]^{-1} = p^{-1}U(\mathbf{k})p$ to $\tilde{H}(\mathbf{k}) = \bar{P}\tilde{H}(\mathbf{k})\bar{P}^{-1}$ and $\bar{P} = \sigma_x \otimes p$.

$$\begin{aligned}
& \bar{P}\tilde{H}(\mathbf{k})\bar{P}^{-1} \\
&= \begin{bmatrix} 0 & p \\ p & 0 \end{bmatrix} \begin{bmatrix} 0 & U(\mathbf{k}) \\ U^\dagger(\mathbf{k}) & 0 \end{bmatrix} \begin{bmatrix} 0 & p^{-1} \\ p^{-1} & 0 \end{bmatrix} \\
&= \begin{bmatrix} 0 & pU^\dagger(\mathbf{k})p^{-1} \\ pU(\mathbf{k})p^{-1} & 0 \end{bmatrix} \\
&= \begin{bmatrix} 0 & (U^\dagger(\mathbf{k}))^{-1} \\ (U(\mathbf{k}))^{-1} & 0 \end{bmatrix} \\
&= \begin{bmatrix} 0 & U(\mathbf{k}) \\ U^\dagger(\mathbf{k}) & 0 \end{bmatrix}^{-1} \\
&= [\tilde{H}(\mathbf{k})]^{-1} = \tilde{H}(\mathbf{k}).
\end{aligned} \tag{H7}$$

Appendix I: Clifford algebra's extension for $\tilde{H}(\mathbf{k}, t)$ and $\tilde{H}(\mathbf{k})$

Table IV and Table V list the Clifford algebra's extensions for $\tilde{H}(\mathbf{k}, t)$ and $\tilde{H}(\mathbf{k})$, respectively.

Lemma 12. For any GBL class in Table IV and Table V, the classification space is C_n , C_n^2 , R_m , or R_m^2 ($n = 0, 1, m = 0, 1, \dots, 7$). The space of mass term of the corresponding GBL class in dimension d is C_{n-d} , C_{n-d}^2 , R_{m-d} , or R_{m-d}^2 , respectively.

Proof: First for classes with \tilde{K} and \tilde{C} . We note that the anti-unitary symmetry operators \tilde{K} and \tilde{C} always reverse the momentum ($\mathbf{k} \rightarrow -\mathbf{k}$) while the unitary symmetry operators \tilde{P} and \tilde{Q} don't. When adding $\gamma_1, \gamma_2, \dots, \gamma_d$ into the Clifford algebra's extension in Table IV and Table V, the difference between the coefficient of $\gamma_1, \gamma_2, \dots, \gamma_d$ and the coefficient of γ_0 can always be chosen as J or $-J$. For class without \tilde{K} and \tilde{C} , when adding $\gamma_1, \gamma_2, \dots, \gamma_d$ into the Clifford algebra's extension in Table IV and Table V, the coefficients of $\gamma_1, \gamma_2, \dots, \gamma_d$ and the coefficient of γ_0 are can be chosen as the same. Hence Lemma 12 is proved. Let us consider for example:

Class P in Table IV. The Clifford algebra's extension in d dimensions is $\{\tilde{\gamma}_t, \gamma_1, \gamma_2, \dots, \gamma_d, \Sigma, \tilde{\gamma}_t\tilde{P}\} \rightarrow$

TABLE IV. The construction of Clifford algebra's extension and its corresponding classifying space (Cl) for $\tilde{H}(\mathbf{k}, t)$ in all GBL classes. $J = i$ is the imaginary unit.

GBL	Clifford algebra's extension	Cl
Non	$\{\tilde{\gamma}_1, \dots, \tilde{\gamma}_d, \tilde{\gamma}_t, \Sigma\} \rightarrow \{\tilde{\gamma}_0, \tilde{\gamma}_1, \dots, \tilde{\gamma}_d, \tilde{\gamma}_t, \Sigma\} = Cl_{d+2} \rightarrow Cl_{d+3}$	C_0
P	$\{\tilde{\gamma}_t, \Sigma, \tilde{\gamma}_t \tilde{P}\} \rightarrow \{\tilde{\gamma}_0, \tilde{\gamma}_t, \Sigma, \tilde{\gamma}_t \tilde{P}\} = Cl_3 \rightarrow Cl_4$	C_1
Qa	$\{\tilde{\gamma}_t, \Sigma\} \otimes \{\tilde{Q}\} \rightarrow \{\tilde{\gamma}_0, \tilde{\gamma}_t, \Sigma\} \otimes \{\tilde{Q}\} = Cl_2 \otimes Cl_1 \rightarrow Cl_3 \otimes Cl_1$	$C_0^{\times 2}$
Qb	$\{\tilde{\gamma}_t, \Sigma, \tilde{\gamma}_t \tilde{Q}\} \rightarrow \{\tilde{\gamma}_0, \tilde{\gamma}_t, \Sigma, \tilde{\gamma}_t \tilde{Q}\} = Cl_3 \rightarrow Cl_4$	C_1
K1a	$\{\tilde{\gamma}_t, J\Sigma, \tilde{K}, J\tilde{K}\} \rightarrow \{J\tilde{\gamma}_0, \tilde{\gamma}_t, J\Sigma, \tilde{K}, J\tilde{K}\} = Cl_{1,3} \rightarrow Cl_{2,3}$	R_0
K1b	$\{J\tilde{\gamma}_t, J\Sigma, \tilde{K}, J\tilde{K}\} \rightarrow \{J\tilde{\gamma}_0, J\tilde{\gamma}_t, J\Sigma, \tilde{K}, J\tilde{K}\} = Cl_{2,2} \rightarrow Cl_{3,2}$	R_2
K2a	$\{\tilde{\gamma}_t, J\Sigma, \tilde{K}, J\tilde{K}\} \rightarrow \{J\tilde{\gamma}_0, \tilde{\gamma}_t, J\Sigma, \tilde{K}, J\tilde{K}\} = Cl_{3,1} \rightarrow Cl_{4,1}$	R_4
K2b	$\{J\tilde{\gamma}_t, J\Sigma, \tilde{K}, J\tilde{K}\} \rightarrow \{J\tilde{\gamma}_0, J\tilde{\gamma}_t, J\Sigma, \tilde{K}, J\tilde{K}\} = Cl_{4,0} \rightarrow Cl_{5,0}$	R_6
C1	$\{\tilde{\gamma}_t, J\Sigma, \tilde{C}, J\tilde{C}\} \rightarrow \{J\tilde{\gamma}_0, \tilde{\gamma}_t, J\Sigma, \tilde{C}, J\tilde{C}\} = Cl_{1,3} \rightarrow Cl_{2,3}$	R_0
C2	$\{\tilde{\gamma}_t, J\Sigma, \tilde{C}, J\tilde{C}\} \rightarrow \{J\tilde{\gamma}_0, \tilde{\gamma}_t, J\Sigma, \tilde{C}, J\tilde{C}\} = Cl_{3,1} \rightarrow Cl_{4,1}$	R_4
C3	$\{J\tilde{\gamma}_t, J\Sigma, \tilde{C}, J\tilde{C}\} \rightarrow \{J\tilde{\gamma}_0, J\tilde{\gamma}_t, J\Sigma, \tilde{C}, J\tilde{C}\} = Cl_{2,2} \rightarrow Cl_{3,2}$	R_2
C4	$\{J\tilde{\gamma}_t, J\Sigma, \tilde{C}, J\tilde{C}\} \rightarrow \{J\tilde{\gamma}_0, J\tilde{\gamma}_t, J\Sigma, \tilde{C}, J\tilde{C}\} = Cl_{4,0} \rightarrow Cl_{5,0}$	R_6
PQ1	$\{\tilde{\gamma}_t, \Sigma, \tilde{\gamma}_t \tilde{P}\} \otimes \{\tilde{Q}\} \rightarrow \{\tilde{\gamma}_0, \tilde{\gamma}_t, \Sigma, \tilde{\gamma}_t \tilde{P}\} \otimes \{\tilde{Q}\} = Cl_3 \otimes Cl_1 \rightarrow Cl_4 \otimes Cl_1$	$C_1^{\times 2}$
PQ2	$\{\tilde{\gamma}_t, \Sigma, \tilde{\gamma}_t \tilde{P}, \tilde{\gamma}_t \tilde{P} \tilde{Q}\} \rightarrow \{\tilde{\gamma}_0, \tilde{\gamma}_t, \Sigma, \tilde{\gamma}_t \tilde{P}, \tilde{\gamma}_t \tilde{P} \tilde{Q}\} = Cl_4 \rightarrow Cl_5$	C_0
PK1	$\{\tilde{\gamma}_t, J\Sigma, \tilde{\gamma}_t \tilde{P}, \tilde{K}, J\tilde{K}\} \rightarrow \{J\tilde{\gamma}_0, \tilde{\gamma}_t, J\Sigma, \tilde{\gamma}_t \tilde{P}, \tilde{K}, J\tilde{K}\} = Cl_{2,3} \rightarrow Cl_{3,3}$	R_1
PK2	$\{\tilde{\gamma}_t, J\Sigma, \tilde{\gamma}_t \tilde{P}, \tilde{K}, J\tilde{K}\} \rightarrow \{J\tilde{\gamma}_0, \tilde{\gamma}_t, J\Sigma, \tilde{\gamma}_t \tilde{P}, \tilde{K}, J\tilde{K}\} = Cl_{4,1} \rightarrow Cl_{5,1}$	R_5
PK3a	$\{\tilde{\gamma}_t, J\Sigma, J\tilde{\gamma}_t \tilde{P}, \tilde{K}, J\tilde{K}\} \rightarrow \{J\tilde{\gamma}_0, \tilde{\gamma}_t, J\Sigma, J\tilde{\gamma}_t \tilde{P}, \tilde{K}, J\tilde{K}\} = Cl_{1,4} \rightarrow Cl_{2,4}$	R_7
PK3b	$\{\tilde{\gamma}_t, J\Sigma, J\tilde{\gamma}_t \tilde{P}, \tilde{K}, J\tilde{K}\} \rightarrow \{J\tilde{\gamma}_0, \tilde{\gamma}_t, J\Sigma, J\tilde{\gamma}_t \tilde{P}, \tilde{K}, J\tilde{K}\} = Cl_{3,2} \rightarrow Cl_{4,2}$	R_3
PC1	$\{\tilde{\gamma}_t, J\Sigma, J\tilde{P}, \tilde{C}, J\tilde{C}\} \rightarrow \{J\tilde{\gamma}_0, \tilde{\gamma}_t, J\Sigma, J\tilde{P}, \tilde{C}, J\tilde{C}\} = Cl_{2,3} \rightarrow Cl_{3,3}$	R_1
PC2	$\{\tilde{\gamma}_t, J\Sigma, J\tilde{\gamma}_t \tilde{P}, \tilde{C}, J\tilde{C}\} \rightarrow \{J\tilde{\gamma}_0, \tilde{\gamma}_t, J\Sigma, J\tilde{\gamma}_t \tilde{P}, \tilde{C}, J\tilde{C}\} = Cl_{1,4} \rightarrow Cl_{2,4}$	R_7
PC3	$\{\tilde{\gamma}_t, J\Sigma, \tilde{\gamma}_t \tilde{P}, \tilde{C}, J\tilde{C}\} \rightarrow \{J\tilde{\gamma}_0, \tilde{\gamma}_t, J\Sigma, \tilde{\gamma}_t \tilde{P}, \tilde{C}, J\tilde{C}\} = Cl_{4,1} \rightarrow Cl_{5,1}$	R_5
PC4	$\{\tilde{\gamma}_t, J\Sigma, J\tilde{\gamma}_t \tilde{P}, \tilde{C}, J\tilde{C}\} \rightarrow \{J\tilde{\gamma}_0, \tilde{\gamma}_t, J\Sigma, J\tilde{\gamma}_t \tilde{P}, \tilde{C}, J\tilde{C}\} = Cl_{3,2} \rightarrow Cl_{4,2}$	R_3
QC1a	$\{\tilde{\gamma}_t, J\Sigma, \tilde{C}, J\tilde{C}\} \otimes \{\tilde{Q}\} \rightarrow \{J\tilde{\gamma}_0, \tilde{\gamma}_t, J\Sigma, \tilde{C}, J\tilde{C}\} \otimes \{\tilde{Q}\} = Cl_{1,3} \otimes Cl_{0,1} \rightarrow Cl_{2,3} \otimes Cl_{0,1}$	$R_0^{\times 2}$
QC1b	$\{\tilde{\gamma}_t, J\Sigma, \tilde{C}, J\tilde{C}, \tilde{\gamma}_t \tilde{Q}\} \rightarrow \{J\tilde{\gamma}_0, \tilde{\gamma}_t, J\Sigma, \tilde{C}, J\tilde{C}, \tilde{\gamma}_t \tilde{Q}\} = Cl_{2,3} \rightarrow Cl_{3,3}$	R_1
QC2a	$\{\tilde{\gamma}_t, J\Sigma, \tilde{C}, J\tilde{C}\} \otimes \{J\tilde{Q}\} \rightarrow \{J\tilde{\gamma}_0, \tilde{\gamma}_t, J\Sigma, \tilde{C}, J\tilde{C}\} \otimes \{J\tilde{Q}\} = Cl_{1,3} \otimes Cl_{1,0} \rightarrow Cl_{2,3} \otimes Cl_{1,0}$	C_0
QC2b	$\{\tilde{\gamma}_t, J\Sigma, \tilde{C}, J\tilde{C}, J\tilde{\gamma}_t \tilde{Q}\} \rightarrow \{J\tilde{\gamma}_0, \tilde{\gamma}_t, J\Sigma, \tilde{C}, J\tilde{C}, J\tilde{\gamma}_t \tilde{Q}\} = Cl_{1,4} \rightarrow Cl_{2,4}$	R_7
QC3a	$\{\tilde{\gamma}_t, J\Sigma, \tilde{C}, J\tilde{C}\} \otimes \{\tilde{Q}\} \rightarrow \{J\tilde{\gamma}_0, \tilde{\gamma}_t, J\Sigma, \tilde{C}, J\tilde{C}\} \otimes \{\tilde{Q}\} = Cl_{3,1} \otimes Cl_{0,1} \rightarrow Cl_{4,1} \otimes Cl_{0,1}$	$R_4^{\times 2}$
QC3b	$\{\tilde{\gamma}_t, J\Sigma, \tilde{C}, J\tilde{C}, \tilde{\gamma}_t \tilde{Q}\} \rightarrow \{J\tilde{\gamma}_0, \tilde{\gamma}_t, J\Sigma, \tilde{C}, J\tilde{C}, \tilde{\gamma}_t \tilde{Q}\} = Cl_{4,1} \rightarrow Cl_{5,1}$	R_5
QC4a	$\{\tilde{\gamma}_t, J\Sigma, \tilde{C}, J\tilde{C}\} \otimes \{J\tilde{Q}\} \rightarrow \{J\tilde{\gamma}_0, \tilde{\gamma}_t, J\Sigma, \tilde{C}, J\tilde{C}\} \otimes \{J\tilde{Q}\} = Cl_{3,1} \otimes Cl_{1,0} \rightarrow Cl_{4,1} \otimes Cl_{1,0}$	C_0
QC4b	$\{\tilde{\gamma}_t, J\Sigma, \tilde{C}, J\tilde{C}, J\tilde{\gamma}_t \tilde{Q}\} \rightarrow \{J\tilde{\gamma}_0, \tilde{\gamma}_t, J\Sigma, \tilde{C}, J\tilde{C}, J\tilde{\gamma}_t \tilde{Q}\} = Cl_{3,2} \rightarrow Cl_{4,2}$	R_3

continued on next page

$\{\tilde{\gamma}_0, \gamma_1, \gamma_2, \dots, \gamma_d, \tilde{\gamma}_t, \Sigma, \tilde{\gamma}_t \tilde{P}\} = Cl_{3+d} \rightarrow Cl_{4+d}$. The space of mass term is $C_{3+d} \simeq C_{1-d}$.

Class Qa in Table IV. The Clifford algebra's extension in d dimensions is $\{\tilde{\gamma}_t, \gamma_1, \gamma_2, \dots, \gamma_d, \Sigma\} \otimes \{\tilde{Q}\} \rightarrow \{\tilde{\gamma}_0, \gamma_1, \gamma_2, \dots, \gamma_d, \tilde{\gamma}_t, \Sigma\} \otimes \{\tilde{Q}\} = Cl_{2+d} \otimes Cl_1 \rightarrow Cl_{3+d} \otimes Cl_1$. The space of mass term is $C_{2+d}^2 \simeq C_{-d}^2$.

Class K1a in Table IV. The Clifford algebra's extension in d dimensions is $\{\tilde{\gamma}_t, \gamma_1, \gamma_2, \dots, \gamma_d, J\Sigma, \tilde{K}, J\tilde{K}\} \rightarrow$

$\{J\tilde{\gamma}_0, \gamma_1, \gamma_2, \dots, \gamma_d, \tilde{\gamma}_t, J\Sigma, \tilde{K}, J\tilde{K}\} = Cl_{1,3+d} \rightarrow Cl_{2,3+d}$. The space of mass term is R_{-d} .

Class QC1a in Table IV. The Clifford algebra's extension in d dimensions is $\{\tilde{\gamma}_t, \gamma_1, \gamma_2, \dots, \gamma_d, J\Sigma, \tilde{C}, J\tilde{C}\} \otimes \{\tilde{Q}\} \rightarrow \{J\tilde{\gamma}_0, \gamma_1, \gamma_2, \dots, \gamma_d, \tilde{\gamma}_t, J\Sigma, \tilde{C}, J\tilde{C}\} \otimes \{\tilde{Q}\} = Cl_{1,3+d} \otimes Cl_{0,1} \rightarrow Cl_{2,3+d} \otimes Cl_{0,1}$. The space of mass term is R_{-d}^2 .

TABLE V. The construction of Clifford algebra's extension and its corresponding classifying space (Cl) for $\tilde{H}(\mathbf{k})$ in all GBL classes. $J = i$ is imaginary unit. For convenience, we use P, Q, C, K to represent $\tilde{P}, \tilde{Q}, \tilde{C}, \tilde{K}$ when we construct the Clifford algebra's extension (in the second column of the table).

GBL	Clifford algebra's extension	Cl
Non	$\{\gamma_1, \dots, \gamma_d, \Sigma\} \rightarrow \{\gamma_0, \gamma_1, \dots, \gamma_d, \Sigma\} = Cl_{d+1} \rightarrow Cl_{d+2}$	C_1
P	$\{\Sigma, P\Sigma\} \rightarrow \{\gamma_0, \Sigma, P\Sigma\} = Cl_2 \rightarrow Cl_3$	C_0
Qa	$\{\Sigma\} \otimes \{Q\} \rightarrow \{\gamma_0, \Sigma\} \otimes \{Q\} = Cl_1 \otimes Cl_1 \rightarrow Cl_2 \otimes Cl_1$	C_1^2
Qb	$\{\Sigma, Q\Sigma\} \rightarrow \{\gamma_0, \Sigma, Q\Sigma\} = Cl_2 \rightarrow Cl_3$	C_0
K1a	$\{\Sigma, \Sigma K, J\Sigma K\} \rightarrow \{\gamma_0, \Sigma, \Sigma K, J\Sigma K\} = Cl_{2,1} \rightarrow Cl_{2,2}$	R_7
K1b	$\{J\Sigma, K, JK\} \rightarrow \{J\gamma_0, J\Sigma, K, JK\} = Cl_{1,2} \rightarrow Cl_{2,2}$	R_1
K2a	$\{\Sigma, \Sigma K, J\Sigma K\} \rightarrow \{\gamma_0, \Sigma, \Sigma K, J\Sigma K\} = Cl_{0,3} \rightarrow Cl_{0,4}$	R_3
K2b	$\{J\Sigma, K, JK\} \rightarrow \{J\gamma_0, J\Sigma, K, JK\} = Cl_{3,0} \rightarrow Cl_{4,0}$	R_5
C1	$\{\Sigma, C, JC\} \rightarrow \{J\gamma_0, \Sigma, C, JC\} = Cl_{0,3} \rightarrow Cl_{1,3}$	R_7
C2	$\{\Sigma, C, JC\} \rightarrow \{J\gamma_0, \Sigma, C, JC\} = Cl_{2,1} \rightarrow Cl_{3,1}$	R_3
C3	$\{J\Sigma, C, JC\} \rightarrow \{J\gamma_0, J\Sigma, C, JC\} = Cl_{1,2} \rightarrow Cl_{2,2}$	R_1
C4	$\{J\Sigma, C, JC\} \rightarrow \{J\gamma_0, J\Sigma, C, JC\} = Cl_{3,0} \rightarrow Cl_{4,0}$	R_5
PQ1	$\{\Sigma, \Sigma P\} \otimes \{Q\} \rightarrow \{\gamma_0, \Sigma, \Sigma P\} \otimes \{Q\} = Cl_2 \otimes Cl_1 \rightarrow Cl_3 \otimes Cl_1$	C_0^2
PQ2	$\{\Sigma, \Sigma P, \Sigma P Q\} \rightarrow \{\gamma_0, \Sigma, \Sigma P, \Sigma P Q\} = Cl_3 \rightarrow Cl_4$	C_1
PK1	$\{\Sigma, \Sigma P, K, JK\} \rightarrow \{J\gamma_0, \Sigma, \Sigma P, K, JK\} = Cl_{1,3} \rightarrow Cl_{2,3}$	R_0
PK2	$\{\Sigma, \Sigma P, K, JK\} \rightarrow \{J\gamma_0, \Sigma, \Sigma P, K, JK\} = Cl_{3,1} \rightarrow Cl_{4,1}$	R_4
PK3a	$\{\Sigma, J\Sigma P, K, JK\} \rightarrow \{J\gamma_0, \Sigma, J\Sigma P, K, JK\} = Cl_{0,4} \rightarrow Cl_{1,4}$	R_6
PK3b	$\{\Sigma, J\Sigma P, K, JK\} \rightarrow \{J\gamma_0, \Sigma, J\Sigma P, K, JK\} = Cl_{2,2} \rightarrow Cl_{3,2}$	R_2
PC1	$\{\Sigma, \Sigma P, C, JC\} \rightarrow \{J\gamma_0, \Sigma, \Sigma P, C, JC\} = Cl_{1,3} \rightarrow Cl_{2,3}$	R_0
PC2	$\{\Sigma, J\Sigma P, C, JC\} \rightarrow \{J\gamma_0, \Sigma, J\Sigma P, C, JC\} = Cl_{0,4} \rightarrow Cl_{1,4}$	R_6
PC3	$\{\Sigma, \Sigma P, C, JC\} \rightarrow \{J\gamma_0, \Sigma, \Sigma P, C, JC\} = Cl_{3,1} \rightarrow Cl_{4,1}$	R_4
PC4	$\{\Sigma, J\Sigma P, C, JC\} \rightarrow \{J\gamma_0, \Sigma, J\Sigma P, C, JC\} = Cl_{2,2} \rightarrow Cl_{3,2}$	R_2
QC1a	$\{\Sigma, C, JC\} \otimes \{Q\} \rightarrow \{J\gamma_0, \Sigma, C, JC\} \otimes \{Q\} = Cl_{0,3} \otimes Cl_{0,1} \rightarrow Cl_{1,3} \otimes Cl_{0,1}$	R_7^2
QC1b	$\{\Sigma, C, JC, \Sigma Q\} \rightarrow \{J\gamma_0, \Sigma, C, JC, \Sigma Q\} = Cl_{1,3} \rightarrow Cl_{2,3}$	R_0
QC2a	$\{\Sigma, C, JC\} \otimes \{JQ\} \rightarrow \{J\gamma_0, \Sigma, C, JC\} \otimes \{JQ\} = Cl_{0,3} \otimes Cl_{1,0} \rightarrow Cl_{1,3} \otimes Cl_{1,0}$	C_1
QC2b	$\{\Sigma, C, JC, J\Sigma Q\} \rightarrow \{J\gamma_0, \Sigma, C, JC, J\Sigma Q\} = Cl_{0,4} \rightarrow Cl_{1,4}$	R_6
QC3a	$\{\Sigma, C, JC\} \otimes \{Q\} \rightarrow \{J\gamma_0, \Sigma, C, JC\} \otimes \{Q\} = Cl_{2,1} \otimes Cl_{0,1} \rightarrow Cl_{3,1} \otimes Cl_{0,1}$	R_3^2
QC3b	$\{\Sigma, C, JC, \Sigma Q\} \rightarrow \{J\gamma_0, \Sigma, C, JC, \Sigma Q\} = Cl_{3,1} \rightarrow Cl_{4,1}$	R_4
QC4a	$\{\Sigma, C, JC\} \otimes \{JQ\} \rightarrow \{J\gamma_0, \Sigma, C, JC\} \otimes \{JQ\} = Cl_{2,1} \otimes Cl_{1,0} \rightarrow Cl_{3,1} \otimes Cl_{1,0}$	C_1
QC4b	$\{\Sigma, C, JC, J\Sigma Q\} \rightarrow \{J\gamma_0, \Sigma, C, JC, J\Sigma Q\} = Cl_{2,2} \rightarrow Cl_{3,2}$	R_2
QC5a	$\{J\Sigma, C, JC\} \otimes \{Q\} \rightarrow \{J\gamma_0, J\Sigma, C, JC\} \otimes \{Q\} = Cl_{1,2} \otimes Cl_{0,1} \rightarrow Cl_{2,2} \otimes Cl_{0,1}$	R_1^2
QC5b	$\{J\Sigma, C, JC, J\Sigma Q\} \rightarrow \{J\gamma_0, J\Sigma, C, JC, J\Sigma Q\} = Cl_{1,3} \rightarrow Cl_{2,3}$	R_0
QC6a	$\{J\Sigma, C, JC\} \otimes \{JQ\} \rightarrow \{J\gamma_0, J\Sigma, C, JC\} \otimes \{JQ\} = Cl_{1,2} \otimes Cl_{1,0} \rightarrow Cl_{2,2} \otimes Cl_{1,0}$	C_1
QC6b	$\{J\Sigma, C, JC, \Sigma Q\} \rightarrow \{J\gamma_0, J\Sigma, C, JC, \Sigma Q\} = Cl_{2,2} \rightarrow Cl_{3,2}$	R_2
QC7a	$\{J\Sigma, C, JC\} \otimes \{Q\} \rightarrow \{J\gamma_0, J\Sigma, C, JC\} \otimes \{Q\} = Cl_{3,0} \otimes Cl_{0,1} \rightarrow Cl_{4,0} \otimes Cl_{0,1}$	R_5^2
QC7b	$\{J\Sigma, C, JC, J\Sigma Q\} \rightarrow \{J\gamma_0, J\Sigma, C, JC, J\Sigma Q\} = Cl_{3,1} \rightarrow Cl_{4,1}$	R_4
QC8a	$\{J\Sigma, C, JC\} \otimes \{JQ\} \rightarrow \{J\gamma_0, J\Sigma, C, JC\} \otimes \{JQ\} = Cl_{3,0} \otimes Cl_{1,0} \rightarrow Cl_{4,0} \otimes Cl_{1,0}$	C_1
QC8b	$\{J\Sigma, C, JC, \Sigma Q\} \rightarrow \{J\gamma_0, J\Sigma, C, JC, \Sigma Q\} = Cl_{4,0} \rightarrow Cl_{5,0}$	R_6
PQC1	$\{\Sigma, \Sigma P, C, JC\} \otimes \{Q\} \rightarrow \{J\gamma_0, \Sigma, \Sigma P, C, JC\} \otimes \{Q\} = Cl_{1,3} \otimes Cl_{0,1} \rightarrow Cl_{2,3} \otimes Cl_{0,1}$	R_0^2
PQC2	$\{\Sigma, \Sigma P, C, JC\} \otimes \{JQ\} \rightarrow \{J\gamma_0, \Sigma, \Sigma P, C, JC\} \otimes \{JQ\} = Cl_{1,3} \otimes Cl_{1,0} \rightarrow Cl_{2,3} \otimes Cl_{1,0}$	C_0
PQC3	$\{\Sigma, J\Sigma P, C, JC, J\Sigma P Q\} \rightarrow \{J\gamma_0, \Sigma, J\Sigma P, C, JC, J\Sigma P Q\} = Cl_{1,4} \rightarrow Cl_{2,4}$	R_7
PQC4	$\{\Sigma, J\Sigma P, C, JC, \Sigma P Q\} \rightarrow \{J\gamma_0, \Sigma, J\Sigma P, C, JC, \Sigma P Q\} = Cl_{0,5} \rightarrow Cl_{1,5}$	R_5
PQC5	$\{\Sigma, \Sigma P, C, JC\} \otimes \{Q\} \rightarrow \{J\gamma_0, \Sigma, \Sigma P, C, JC\} \otimes \{Q\} = Cl_{3,1} \otimes Cl_{0,1} \rightarrow Cl_{4,1} \otimes Cl_{0,1}$	R_4^2
PQC6	$\{\Sigma, \Sigma P, C, JC\} \otimes \{JQ\} \rightarrow \{J\gamma_0, \Sigma, \Sigma P, C, JC\} \otimes \{JQ\} = Cl_{3,1} \otimes Cl_{1,0} \rightarrow Cl_{4,1} \otimes Cl_{1,0}$	C_0
PQC7	$\{\Sigma, J\Sigma P, C, JC, J\Sigma P Q\} \rightarrow \{J\gamma_0, \Sigma, J\Sigma P, C, JC, J\Sigma P Q\} = Cl_{3,2} \rightarrow Cl_{4,2}$	R_3
PQC8	$\{\Sigma, J\Sigma P, C, JC, \Sigma P Q\} \rightarrow \{J\gamma_0, \Sigma, J\Sigma P, C, JC, \Sigma P Q\} = Cl_{2,3} \rightarrow Cl_{3,3}$	R_1
PQC9a	$\{\Sigma, J\Sigma P, C, JC\} \otimes \{Q\} \rightarrow \{J\gamma_0, \Sigma, J\Sigma P, C, JC\} \otimes \{Q\} = Cl_{0,4} \otimes Cl_{0,1} \rightarrow Cl_{1,4} \otimes Cl_{0,1}$	R_6^2
PQC9b	$\{\Sigma, J\Sigma P, C, JC\} \otimes \{JQ\} \rightarrow \{J\gamma_0, \Sigma, J\Sigma P, C, JC\} \otimes \{JQ\} = Cl_{0,4} \otimes Cl_{1,0} \rightarrow Cl_{1,4} \otimes Cl_{1,0}$	C_0
PQC10a	$\{\Sigma, \Sigma P, C, JC, \Sigma P Q\} \rightarrow \{J\gamma_0, \Sigma, \Sigma P, C, JC, \Sigma P Q\} = Cl_{1,4} \rightarrow Cl_{2,4}$	R_7
PQC10b	$\{\Sigma, \Sigma P, C, JC, J\Sigma P Q\} \rightarrow \{J\gamma_0, \Sigma, \Sigma P, C, JC, J\Sigma P Q\} = Cl_{2,3} \rightarrow Cl_{3,3}$	R_1
PQC11a	$\{\Sigma, J\Sigma P, C, JC\} \otimes \{Q\} \rightarrow \{J\gamma_0, \Sigma, J\Sigma P, C, JC\} \otimes \{Q\} = Cl_{2,2} \otimes Cl_{0,1} \rightarrow Cl_{3,2} \otimes Cl_{0,1}$	R_2^2
PQC11b	$\{\Sigma, J\Sigma P, C, JC\} \otimes \{JQ\} \rightarrow \{J\gamma_0, \Sigma, J\Sigma P, C, JC\} \otimes \{JQ\} = Cl_{2,2} \otimes Cl_{1,0} \rightarrow Cl_{3,2} \otimes Cl_{1,0}$	C_0
PQC12a	$\{\Sigma, \Sigma P, C, JC, \Sigma P Q\} \rightarrow \{J\gamma_0, \Sigma, \Sigma P, C, JC, \Sigma P Q\} = Cl_{3,2} \rightarrow Cl_{4,2}$	R_3
PQC12b	$\{\Sigma, \Sigma P, C, JC, J\Sigma P Q\} \rightarrow \{J\gamma_0, \Sigma, \Sigma P, C, JC, J\Sigma P Q\} = Cl_{4,1} \rightarrow Cl_{5,1}$	R_5

-
- [1] M. Z. Hasan and C. L. Kane, *Colloquium: Topological insulators*, *Rev. Mod. Phys.* **82**, 3045 (2010).
- [2] X.-L. Qi and S.-C. Zhang, *Topological insulators and superconductors*, *Rev. Mod. Phys.* **83**, 1057 (2011).
- [3] B. A. Bernevig and T. L. Hughes, *Topological Insulators and Topological Superconductors* (Princeton University Press, Princeton, NJ, 2013).
- [4] J. K. Asboth, L. Oroszlany, and A. Palyi, *A Short Course on Topological Insulators* (Springer, 2016).
- [5] S.-Q. Shen, *Topological Insulators: Dirac Equation in Condensed Matter* (Springer, 2018).
- [6] C. M. Bender, Making sense of non-Hermitian Hamiltonians, *Rep. Prog. Phys.* **70**, 947 (2007).
- [7] I. Rotter, A non-Hermitian Hamilton operator and the physics of open quantum systems, *J. Phys. A: Math. Theor.* **42**, 153001 (2009).
- [8] V. M. Martinez Alvarez, J. E. Barrios Vargas, M. Berdakin, and L. E. F. Foa Torres, Topological states of non-Hermitian systems, *Eur. Phys. J. Spec. Top.* **227**, 1295 (2018).
- [9] R. El-Ganainy, K. G. Makris, M. Khajavikhan, Z. H. Musslimani, S. Rotter, and D. N. Christodoulides, Non-Hermitian physics and symmetry, *Nat. Phys.* **14**, 11 (2018).
- [10] E. J. Bergholtz, J. C. Budich, and F. K. Kunst, Exceptional Topology of Non-Hermitian Systems, *Rev. Mod. Phys.* **93**, 15005 (2021).
- [11] N. Moiseyev, *Non-Hermitian Quantum Mechanics* (Cambridge University Press, New York, 2011).
- [12] A. Ghatak and T. Das, New topological invariants in non-Hermitian systems, *J. Phys.: Condens. Matter* **31**, 263001 (2019).
- [13] L. E. F. Foa Torres, Perspective on Topological States of Non-Hermitian Systems, *J. Phys. Mater.* **3**, 014002 (2019).
- [14] Y. Ashida, Z. Gong, and Masahito Ueda, Non-Hermitian Physics, *Advances in Physics* **69**, 3 (2020).
- [15] M. Aspelmeyer, T. J. Kippenberg, and F. Marquardt, Cavity optomechanics, *Rev. Mod. Phys.* **86**, 1391 (2014).
- [16] H. Cao and J. Wiersig, Dielectric microcavities: Model systems for wave chaos and non-Hermitian physics, *Rev. Mod. Phys.* **87**, 61 (2015).
- [17] T. Gao, E. Estrecho, K. Y. Bliokh, T. C. H. Liew, M. D. Fraser, S. Brodbeck, M. Kamp, C. Schneider, S. Höfling, Y. Yamamoto, F. Nori, Y. S. Kivshar, A. G. Truscott, R. G. Dall, and E. A. Ostrovskaya, Observation of non-Hermitian degeneracies in a chaotic exciton-polariton billiard, *Nature* **526**, 554 (2015).
- [18] J. Doppler, A. A. Mailybaev, J. Böhm, U. Kuhl, A. Girschik, F. Libisch, T. J. Milburn, P. Rabl, N. Moiseyev, and S. Rotter, Dynamically encircling an exceptional point for asymmetric mode switching, *Nature* **537**, 76 (2016).
- [19] P. Peng, W. Cao, C. Shen, W. Qu, J. Wen, L. Jiang, and Y. Xiao, Anti-parity-time symmetry with flying atoms, *Nature Physics* **12**, 1139 (2016).
- [20] H. Xu, D. Mason, L. Jiang, and J. G. E. Harris, Topological energy transfer in an optomechanical system with exceptional points, *Nature* **537**, 80 (2016).
- [21] B. Zhen, C. W. Hsu, Y. Igarashi, L. Lu, I. Kaminer, A. Pick, S.-L. Chua, J. D. Joannopoulos, and M. Soljačić, Spawning rings of exceptional points out of Dirac cones, *Nature (London)* **525**, 354 (2015).
- [22] V. Kozii and L. Fu, Non-Hermitian Topological Theory of Finite-Lifetime Quasiparticles: Prediction of Bulk Fermi Arc due to Exceptional Point, [arXiv:1708.05841](https://arxiv.org/abs/1708.05841).
- [23] H. Shen and L. Fu, Quantum Oscillation from In-Gap States and Non-Hermitian Landau Level Problem, *Phys. Rev. Lett.* **121**, 026403 (2018).
- [24] T. Yoshida, R. Peters, and N. Kawakami, Non-Hermitian perspective of the band structure in heavy-fermion systems, *Phys. Rev. B* **98**, 035141 (2018).
- [25] Y. Xu, S.-T. Wang, and L.-M. Duan, Weyl Exceptional Rings in a Three-Dimensional Dissipative Cold Atomic Gas, *Phys. Rev. Lett.* **118**, 045701 (2017).
- [26] M. Papaž, H. Isobe, and L. Fu, Nodal arc of disordered Dirac fermions and non-Hermitian band theory, *Phys. Rev. B* **99**, 201107(R) (2019).
- [27] J. Li, A. K. Harter, J. Liu, L. de Melo, Y. N. Joglekar, and L. Luo, Observation of parity-time symmetry breaking transitions in a dissipative Floquet system of ultracold atoms, *Nat. Commun.* **10**, 855 (2019).
- [28] Y. Ashida, S. Furukawa, and M. Ueda, Parity-time-symmetric quantum critical phenomena, *Nat. Commun.* **8**, 15791 (2017).
- [29] S. Diehl, E. Rico, M. A. Baranov, and P. Zoller, Topology by dissipation in atomic quantum wires, *Nat. Phys.* **7**, 971 (2011).
- [30] D. S. Borgnia, A. J. Kruchkov, and R.-J. Slager, Non-Hermitian Boundary Modes and Topology, *Phys. Rev. Lett.* **124**, 056802 (2020).
- [31] A. McDonald, T. Pereg-Barnea, and A. A. Clerk, Phase-Dependent Chiral Transport and Effective Non-Hermitian Dynamics in a Bosonic Kitaev-Majorana Chain, *Phys. Rev. X* **8**, 041031(2018).
- [32] S. Lieu, Topological symmetry classes for non-Hermitian models and connections to the bosonic Bogoliubov–de Gennes equation, *Phys. Rev. B* **98**, 115135(2018).
- [33] Z. Yang, Non-perturbative Breakdown of Bloch’s Theorem and Hermitian Skin Effects, [arXiv:2012.03333](https://arxiv.org/abs/2012.03333).
- [34] K. Yokomizo and S. Murakami, Non-Bloch band theory in bosonic Bogoliubov–de Gennes systems, *Phys. Rev. B* **103**, 165123(2021).
- [35] Q.-R. Xu, V. P. Flynn, A. Alase, E. Cobanera, L. Viola, and G. Ortiz, Squaring the fermion: The three-fold way and the fate of zero modes, *Phys. Rev. B* **102**, 125127(2020).
- [36] I. Zapata and F. Sols, Andreev Reflection in Bosonic Condensates, *Phys. Rev. Lett.* **102**, 180405(2009).
- [37] B. Wu and Q. Niu, Landau and dynamical instabilities of the superflow of Bose-Einstein condensates in optical lattices, *Phys. Rev. A* **64**, 061603(R)(2001).
- [38] R. Barnett, Edge-state instabilities of bosons in a topological band, *Phys. Rev. A* **88**, 063631(2013).
- [39] B. Galilo, D. K. K. Lee, and R. Barnett, Selective Population of Edge States in a 2D Topological Band System, *Phys. Rev. Lett.* **115**, 245302(2015).
- [40] B. Wu and Q. Niu, Superfluidity of Bose–Einstein condensate in an optical lattice: Landau–Zener tunnelling and dynamical instability, *New J. Phys.* **5**, 104 (2003).

- [41] J. Dereziński, Bosonic quadratic Hamiltonians, *J. Math. Phys.* **58**, 121101 (2017).
- [42] I. Gohberg, P. Lancaster, and L. Rodman, *Indefinite Linear Algebra and Applications* (Birkhauser, Basel, 2005).
- [43] Y. Kawaguchi and M. Ueda, Spinor Bose–Einstein condensates, *Phys. Rep.* **520**, 253 (2012).
- [44] G. E. Blonder, M. Tinkham, and T. M. Klapwijk, Transition from metallic to tunneling regimes in superconducting microconstrictions: Excess current, charge imbalance, and supercurrent conversion, *Phys. Rev. B* **25**, 4515 (1982).
- [45] K. Katsura, N. Nagaosa, and P. A. Lee, Theory of the Thermal Hall Effect in Quantum Magnets, *Phys. Rev. Lett.* **104**, 066403 (2010).
- [46] H. Kondo, Y. Akagi, and H. Katsura, \mathbb{Z}_2 topological invariant for magnon spin Hall systems, *Phys. Rev. B* **99**, 041110(R) (2019).
- [47] G. Lindblad, On the generators of quantum dynamical semigroups, *Commun. Math. Phys.* **48**, 119 (1976).
- [48] F. Song, S. Yao, and Z. Wang, Non-Hermitian Skin Effect and Chiral Damping in Open Quantum Systems, *Phys. Rev. Lett.* **123**, 170401 (2019).
- [49] C.-H. Liu, K. Zhang, Z. Yang, and S. Chen, Helical damping and dynamical critical skin effect in open quantum systems, *Phys. Rev. Research*, **2**, 043167 (2020).
- [50] C.-H. Liu and S. Chen, Information constraint in open quantum systems, *Phys. Rev. B* **104**, 174305 (2021).
- [51] K. G. Makris, R. El-Ganainy, D. N. Christodoulides, and Z. H. Musslimani, Beam Dynamics in \mathcal{PT} Symmetric Optical Lattices, *Phys. Rev. Lett.* **100**, 103904 (2008).
- [52] A. Regensburger, C. Bersch, M.-A. Miri, G. Onishchukov, D. N. Christodoulides, and U. Peschel, Parity-time synthetic photonic lattices, *Nature (London)* **488**, 167 (2012).
- [53] B. Peng, Ş. K. Özdemir, S. Rotter, H. Yilmaz, M. Liertzer, F. Monifi, C. M. Bender, F. Nori, and L. Yang, Loss-induced suppression and revival of lasing, *Science* **346**, 328 (2014).
- [54] H. Jing, S. K. Özdemir, X.-Y. Lü, J. Zhang, L. Yang, and F. Nori, \mathcal{PT} -Symmetric Phonon Laser, *Phys. Rev. Lett.* **113**, 053604 (2014).
- [55] S. Malzard, C. Poli, and H. Schomerus, Topologically Protected Defect States in Open Photonic Systems with Non-Hermitian Charge-Conjugation and Parity-Time Symmetry, *Phys. Rev. Lett.* **115**, 200402 (2015).
- [56] J. M. Zeuner, M. C. Rechtsman, Y. Plotnik, Y. Lumer, S. Nolte, M. S. Rudner, M. Segev, and A. Szameit, Observation of a Topological Transition in the Bulk of a non-Hermitian System, *Phys. Rev. Lett.* **115**, 040402 (2015).
- [57] Lei Xiao, Kunkun Wang, Xiang Zhan, Zhihao Bian, Kohei Kawabata, Masahito Ueda, Wei Yi, and Peng Xue, Observation of Critical Phenomena in Parity-Time-Symmetric Quantum Dynamics, *Phys. Rev. Lett.* **123**, 230401 (2019).
- [58] Lei Xiao, Tianshu Deng, Kunkun Wang, Zhong Wang, Wei Yi, and Peng Xue, Observation of Non-Bloch Parity-Time Symmetry and Exceptional Points, *Phys. Rev. Lett.* **126**, 230402 (2021).
- [59] C. Poli, M. Bellec, U. Kuhl, F. Mortessagne, and H. Schomerus, Selective enhancement of topologically induced interface states in a dielectric resonator chain, *Nat. Commun.* **6**, 6710 (2015).
- [60] S. Weimann, M. Kremer, Y. Plotnik, Y. Lumer, S. Nolte, K. G. Makris, M. Segev, M. C. Rechtsman, and A. Szameit, Topologically protected bound states in photonic parity–time-symmetric crystals, *Nat. Mater.* **16**, 433 (2017).
- [61] P. St-Jean, V. Goblot, E. Galopin, A. Lemaître, T. Ozawa, L. Le Gratiet, I. Sagnes, J. Bloch, and A. Amo, Lasing in topological edge states of a one-dimensional lattice, *Nat. Photon.* **11**, 651 (2017).
- [62] L. Xiao et al., Observation of topological edge states in parity-time-symmetric quantum walks, *Nat. Phys.* **13**, 1117 (2017).
- [63] X. Zhan, L. Xiao, Z. Bian, K. Wang, X. Qiu, B. C. Sanders, W. Yi, and P. Xue, Detecting Topological Invariants in Nonunitary Discrete-Time Quantum Walks, *Phys. Rev. Lett.* **119**, 130501 (2017).
- [64] C. E. Ruter, K. G. Makris, R. El-Ganainy, D. N. Christodoulides, M. Segev, and D. Kip, Observation of parity–time symmetry in optics, *Nat. Phys.* **6**, 192 (2010).
- [65] J. Bartlett, H. Hu, and E. Zhao, Illuminating the bulk-boundary correspondence of a non-Hermitian stub lattice with Majorana stars, *Phys. Rev. B* **104**, 195131 (2021).
- [66] H. Hu, E. Zhao, and W. V. Liu, Dynamical signatures of point-gap Weyl semimetal, [arXiv:2107.02135](https://arxiv.org/abs/2107.02135).
- [67] M. V. Berry, Physics of Nonhermitian Degeneracies, *Czech. J. Phys.* **54**, 1039 (2004).
- [68] W D Heiss, The physics of exceptional points, *J. Phys. A: Math. Theor.* **45**, 444016 (2012).
- [69] M.-A. Miri and A. Alù, Exceptional points in optics and photonics, *Science* **363**, eaar7709 (2019).
- [70] K. Kawabata, T. Bessho, and M. Sato, Classification of Exceptional Points and Non-Hermitian Topological Semimetals, *Phys. Rev. Lett.* **123**, 066405 (2019).
- [71] T. Yoshida, R. Peters, N. Kawakami, and Y. Hatsugai, Symmetry-protected exceptional rings in two-dimensional correlated systems with chiral symmetry, *Phys. Rev. B* **99**, 121101(R) (2019).
- [72] T. Yoshida and Y. Hatsugai, Exceptional rings protected by emergent symmetry for mechanical systems, *Phys. Rev. B* **100**, 054109 (2019).
- [73] S. Lin, L. Jin, and Z. Song, Symmetry protected topological phases characterized by isolated exceptional points, *Phys. Rev. B* **99**, 165148 (2019).
- [74] H. Hu, S. Sun, and S. Chen, Knot Topology of Exceptional Point and Non-Hermitian No-Go Theorem, [arXiv: 2111.11346](https://arxiv.org/abs/2111.11346).
- [75] S. Yao and Z. Wang, Edge States and Topological Invariants of Non-Hermitian Systems, *Phys. Rev. Lett.* **121**, 086803 (2018).
- [76] F. K. Kunst, E. Edvardsson, J. C. Budich, and E. J. Bergholtz, Biorthogonal Bulk-Boundary Correspondence in non-Hermitian Systems, *Phys. Rev. Lett.* **121**, 026808 (2018).
- [77] S. Yao, F. Song, and Z. Wang, Non-Hermitian Chern Bands, *Phys. Rev. Lett.* **121**, 136802 (2018).
- [78] Y. Xiong, Why does bulk boundary correspondence fail in some non-Hermitian topological models, *J. Phys. Commun.* **2**, 035043 (2018).
- [79] T. E. Lee, Anomalous Edge State in a Non-Hermitian Lattice, *Phys. Rev. Lett.* **116**, 133903 (2016).

- [80] K. Yokomizo and S. Murakami, Non-Bloch Band Theory of Non-Hermitian Systems, *Phys. Rev. Lett.* **123**, 066404 (2019).
- [81] V. M. Martinez Alvarez, J. E. Barrios Vargas, and L. E. F. Foa Torres, Non-Hermitian robust edge states in one-dimension: Anomalous localization and eigenspace condensation at exceptional points, *Phys. Rev. B* **97**, 121401(R) (2018).
- [82] C. H. Lee and R. Thomale, Anatomy of skin modes and topology in non-Hermitian systems, *Phys. Rev. B* **99**, 201103(R) (2019).
- [83] L. Li, C. H. Lee, S. Mu, J. Gong, Critical non-Hermitian Skin Effect, *Nat Commun* **11**, 5491 (2020).
- [84] Z. Yang, K. Zhang, C. Fang, and J. Hu, Non-Hermitian Bulk-Boundary Correspondence and Auxiliary Generalized Brillouin Zone Theory, *Phys. Rev. Lett.* **125**, 226402 (2020).
- [85] C. H. Lee, L. Li, R. Thomale, and J. Gong, Unraveling non-Hermitian pumping: emergent spectral singularities and anomalous responses, *Phys. Rev. B* **102**, 085151(2020).
- [86] A. Ghatak, M. Brandenbourger, J. van Wezel, and C. Coulais, Observation of non-Hermitian topology and its bulk-edge correspondence in an active mechanical metamaterial, *Proc. Natl. Ac. Sc. U.S.A.* **117**, 29561 (2020).
- [87] T. Helbig, T. Hofmann, S. Imhof, M. Abdelghany, T. Kiessling, L. W. Molenkamp, C. H. Lee, A. Szameit, M. Greiter, and R. Thomale, Generalized bulk-boundary correspondence in non-Hermitian topoelectrical circuits, *Nat. Phys.* **16**, 747 (2020).
- [88] L. Xiao, T. Deng, K. Wang, G. Zhu, Z. Wang, W. Yi, and P. Xue, Observation of non-hermitian bulk-boundary correspondence in quantum dynamics, *Nat. Phys.* **16**, 761 (2020).
- [89] T. Hofmann et al., Reciprocal skin effect and its realization in a topoelectrical circuit, *Phys. Rev. Research* **2**, 023265 (2020).
- [90] J. Cayssol, B. Dóra, F. Simon, and R. Moessner, Floquet topological insulators, *Phys. Status Solidi RRL* **7**, 101 (2013).
- [91] M. Bukov, L. D'Alessio, and A. Polkovnikov, Universal high-frequency behavior of periodically driven systems: from dynamical stabilization to Floquet engineering, *Adv. Phys.* **64**, 139 (2015).
- [92] T. Kitagawa, M. A. Broome, A. Fedrizzi, and M. S. Rudner, Observation of topologically protected bound states in photonic quantum walks, *Nat. Commun.* **3**, 882 (2012).
- [93] M. C. Rechtsman, J. M. Zeuner, Y. Plotnik, Y. Lumer, D. Podolsky, F. Dreisow, S. Nolte, M. Segev, and A. Szameit, Photonic Floquet topological insulators, *Nature (London)* **496**, 196 (2013).
- [94] L. J. Maczewsky, J. M. Zeuner, S. Nolte, and A. Szameit, Observation of photonic anomalous Floquet topological insulators, *Nat. Commun.* **8**, 13756 (2017).
- [95] F. Cardano, A. D'Errico, A. Dauphin, M. Maffei, B. Piccirillo, C. de Lisis, G. De Filippis, V. Cataudella, E. Santamato, L. Marrucci, M. Lewenstein, and P. Massignan, Detection of Zak phases and topological invariants in a chiral quantum walk of twisted photons, *Nat. Commun.* **8**, 15516 (2017).
- [96] G. Jotzu, M. Messer, R. Desbuquois, and M. Lebrat, Experimental realization of the topological Haldane model with ultracold fermions, *Nature (London)* **515**, 237 (2014).
- [97] K. Jiménez-García, L. J. LeBlanc, R. A. Williams, M. C. Beeler, C. Qu, M. Gong, C. Zhang, and I. B. Spielman, Tunable Spin-Orbit Coupling via Strong Driving in Ultracold-Atom Systems, *Phys. Rev. Lett.* **114**, 125301 (2015).
- [98] G. Floquet, Sur les équations différentielles linéaires à coefficients périodiques, *Ann. Sci. Éc. Norm. Super.* **12**, 4788 (1883).
- [99] L. Jiang, T. Kitagawa, J. Alicea, A. R. Akhmerov, D. Pekker, G. Refael, J. I. Cirac, E. Demler, M. D. Lukin, and P. Zoller, Majorana Fermions in Equilibrium and in Driven Cold-Atom Quantum Wires, *Phys. Rev. Lett.* **106**, 220402 (2011).
- [100] N. H. Lindner, G. Refael, V. Galitski, Floquet Topological Insulator in Semiconductor Quantum Wells, *Nat. Phys.* **7**, 490 (2011).
- [101] T. Kitagawa, E. Berg, M. Rudner, E. Demler, Topological characterization of periodically driven quantum systems, *Phys. Rev. B* **82**, 235114 (2010).
- [102] D. J. Thouless, Quantization of particle transport, *Phys. Rev. B* **27**, 6083(1983).
- [103] M. Fruchart, Complex classes of periodically driven topological lattice systems, *Phys. Rev. B* **93**, 115429 (2016).
- [104] R. Roy and F. Harper, Periodic table for Floquet topological insulators, *Phys. Rev. B* **96**, 155118(2017).
- [105] S. Yao, Z. Yan, and Z. Wang, Topological invariants of Floquet systems: General formulation, special properties, and Floquet topological defects, *Phys. Rev. B* **96**, 195303 (2017).
- [106] M. S. Rudner, N. H. Lindner, E. Berg, and M. Levin, Anomalous Edge States and the Bulk-Edge Correspondence for Periodically Driven Two-Dimensional Systems, *Phys. Rev. X* **3**, 031005 (2013).
- [107] K. Wintersperger, C. Braun, F. N. Ünal, André Eckardt, M. D. Liberto, N. Goldman, I. Bloch, and M. Aidelsburger, Realization of an anomalous Floquet topological system with ultracold atoms, *Nat. Phys.* **16**, 1058 (2020).
- [108] H. Hu, B. Huang, E. Zhao, and W. V. Liu, Dynamical Singularities of Floquet Higher-Order Topological Insulators, *Phys. Rev. Lett.* **124**, 057001 (2020).
- [109] B. Huang and W. V. Liu, Floquet Higher-Order Topological Insulators with Anomalous Dynamical Polarization, *Phys. Rev. Lett.* **124**, 216601 (2020).
- [110] M. Rodriguez-Vega, A. Kumar, B. Seradjeh, Higher-order Floquet topological phases with corner and bulk bound states, *Phys. Rev. B* **100**, 085138 (2019).
- [111] R. W. Bomantara, L. Zhou, J. Pan, and J. Gong, Coupled-wire construction of static and Floquet second-order topological insulators, *Phys. Rev. B* **99**, 045441 (2019).
- [112] Y. Peng and G. Refael, Floquet Second-Order Topological Insulators from Nonsymmorphic Space-Time Symmetries, *Phys. Rev. Lett.* **123**, 016806 (2019).
- [113] R. Seshadri, A. Dutta, and D. Sen, Generating a second-order topological insulator with multiple corner states by periodic driving, *Phys. Rev. B* **100**, 115403 (2019).
- [114] A. Altland and M. R. Zirnbauer, Nonstandard symmetry classes in mesoscopic normal-superconducting hybrid structures, *Phys. Rev. B* **55**, 1142 (1997).
- [115] C.-K. Chiu, J. C. Y. Teo, A. P. Schnyder, and S. Ryu,

- Classification of topological quantum matter with symmetries, *Rev. Mod. Phys.* **88**, 035005 (2016).
- [116] M. Stone, C.-K. Chiu, and A. Roy, Symmetries, dimensions and topological insulators: the mechanism behind the face of the Bott clock, *J. Phys. A* **44**, 045001 (2010). (2011).
- [117] C.-K. Chiu, H. Yao, and S. Ryu, Classification of topological insulators and superconductors in the presence of reflection symmetry, *Phys. Rev. B* **88**, 075142 (2013). (2013).
- [118] T. Morimoto and A. Furusaki, Topological classification with additional symmetries from Clifford algebras, *Phys. Rev. B* **88**, 125129 (2013).
- [119] A. Kitaev, Periodic table for topological insulators and superconductors, *AIP Conf. Proc.* **1134**, 22 (2009).
- [120] A. P. Schnyder, S. Ryu, A. Furusaki, and A. W. Ludwig, Classification of topological insulators and superconductors in three spatial dimensions, *Phys. Rev. B* **78**, 195125 (2008).
- [121] H. Shen, B. Zhen, and L. Fu, Topological Band Theory for Non-Hermitian Hamiltonians, *Phys. Rev. Lett.* **120**, 146402 (2018).
- [122] D. Bernard and A. LeClair, A classification of 2D random Dirac fermions, *J. Phys. A: Math. Gen.* **35**, 2555 (2002).
- [123] U. Magnea, Random matrices beyond the Cartan classification, *Journal of Physics A: Mathematical and Theoretical* **41**, 045203 (2008).
- [124] C. C. Wojcik, X.-Q. Sun, T. Bzdušek, and S. Fan, Homotopy characterization of non-Hermitian Hamiltonians, *Phys. Rev. B* **101**, 205417 (2020).
- [125] Z. Li and R. S. K. Mong, Homotopical classification of non-Hermitian band structures, *Phys. Rev. B* **103**, 155129 (2021).
- [126] H. Hu and E. Zhao, Knots and Non-Hermitian Bloch Bands, *Phys. Rev. Lett.* **126**, 010401 (2021).
- [127] Z. Gong, Y. Ashida, K. Kawabata, K. Takasan, S. Higashikawa, and M. Ueda, Topological Phases of Non-Hermitian Systems, *Phys. Rev. X* **8**, 031079 (2018).
- [128] K. Kawabata, K. Shiozaki, M. Ueda, and M. Sato, Symmetry and Topology in Non-Hermitian Physics, *Phys. Rev. X* **9**, 140015(2019).
- [129] H. Zhou and J. Y. Lee, Periodic table for topological bands with non-Hermitian symmetries, *Phys. Rev. B* **99**, 235112 (2019).
- [130] C.-H. Liu and S. Chen, Topological classification of defects in non-Hermitian systems, *Phys. Rev. B* **100**,144106(2019).
- [131] C.-H. Liu, H. Jiang, and S. Chen, Topological classification of non-Hermitian systems with reflection symmetry, *Phys. Rev. B* **99**, 125103 (2019).
- [132] C. Yuce, PT symmetric Floquet topological phase, *Eur. Phys. J. D* **69**, 184 (2015).
- [133] Z. Turkera, S. Tombuloglub, and C. Yuce, PT symmetric Floquet topological phase in SSH model, *Phys. Lett. A* **382**, 2013 (2018).
- [134] D. Kim, M. Ken, N. Kawakami, H. Obuse, Bulk-edge correspondence in nonunitary Floquet systems with chiral symmetry, *Phys. Rev. A* **102**. 062202(2020).
- [135] J. Gong and Q. Wang, Stabilizing non-Hermitian systems by periodic driving, *Phys. Rev. A* **91**, 042135 (2015).
- [136] X. Lü, H. Jing, J. Ma, and Y. Wu, \mathcal{PT} -Symmetry-Breaking Chaos in Optomechanics, *Phys. Rev. Lett.* **114**, 253601 (2015).
- [137] B. Höckendorf, A. Alvermann, and H. Fehske, Non-Hermitian Boundary State Engineering in Anomalous Floquet Topological Insulators, *Phys. Rev. Lett.* **123**, 190403 (2019).
- [138] B. Höckendorf, A. Alvermann, and H. Fehske, Topological origin of quantized transport in non-Hermitian Floquet chains, *Phys. Rev. Research* **2**, 023235 (2020).
- [139] L. Zhou and J. Gong, Non-Hermitian Floquet topological phases with arbitrarily many real-quasienergy edge states, *Phys. Rev. B* **98**, 205417 (2018).
- [140] L. Zhou, Y. Gu, and J. Gong, Dual topological characterization of non-Hermitian Floquet phases, *Phys. Rev. B* **103**, L041404 (2021).
- [141] H. Wu and J.-H. An, Floquet topological phases of non-Hermitian systems, *Phys. Rev. B* **102**, 041119(R) (2020).
- [142] S. Diehl, A. Micheli, A. Kantian, B. Kraus, H. P. Büchler, and P. Zoller, Quantum states and phases in driven open quantum systems with cold atoms, *Nat. Phys.* **4**, 878 (2008).
- [143] F. Schäfer, T. Fukuhara, S. Sugawa, Y. Takasu, and Y. Takahashi, Tools for quantum simulation with ultracold atoms in optical lattices, *Nat. Rev. Phys.* **2**, 411 (2020).
- [144] M. Lemesko and H. Weimer, Dissipative binding of atoms by non-conservative forces, *Nat. Commun.* **4**, 2230 (2013).
- [145] J. Otterbach and M. Lemesko, Dissipative Preparation of Spatial Order in Rydberg-Dressed Bose-Einstein Condensates, *Phys. Rev. Lett.* **113**, 070401 (2014).
- [146] R. Bouganne, M. B. Aguilera, A. Ghermaoui, J. Beugnon, and F. Gerbier, Anomalous decay of coherence in a dissipative many-body system, *Nat. Phys.* **16**, 21 (2020).
- [147] S. Attal, F. Petruccione, and I. Sinayskiy, Open quantum walks on graphs, *Phys. Lett. A* **376**, 1545 (2012).
- [148] S. Higashikawa, M. Bakagawa, and M. Ueda, Floquet Chiral Magnetic Effect, *Phys. Rev. Lett.* **123**, 066403(2019).
- [149] X.-Q. Sun, M. Xiao, T. Bzdušek, S.-C. Zhang, and S. Fan, Three-Dimensional Chiral Lattice Fermion in Floquet Systems, *Phys. Rev. Lett.* **121**, 196401(2018).
- [150] D. C. Brody, Biorthogonal quantum mechanics, *J. Phys. A: Math. Theor.* **47** 035305(2014).
- [151] J. C. Budich, Y. Hu, and P. Zoller, Helical Floquet Channels in 1D Lattices, *Phys. Rev. Lett.* **118**, 105302(2017).
- [152] T. Ozawa, H. M. Price, A. Amo, N. Goldman, M. Hafezi, L. Lu, M. Rechtsman, D. Schuster, J. Simon, O. Zilberberg, and I. Carusotto, Topological photonics, *Rev. Mod. Phys.* **91**, 015006 (2019).
- [153] F. Song, S. Yao, and Z. Wang, Non-Hermitian Topological Invariants in Real Space, *Phys. Rev. Lett.* **123**, 246801(2019).
- [154] F. Schindler and A. Prem, Dislocation non-Hermitian skin effect, *Phys. Rev. B* **104**, L161106(2021).
- [155] X.-Q. Sun, P. Zhu, and T. L. Hughes, Geometric Response and Disclination-Induced Skin Effects in Non-Hermitian Systems, *Phys. Rev. Lett.* **127**, 066401(2021).
- [156] J. Kruthoff, J. de Boer, J. van Wezel, C. L. Kane, and R.-J. Slager, Topological Classification of Crystalline Insulators through Band Structure Combinatorics, *Phys. Rev. X* **7**, 041069 (2017).